

Spatial Relationships among Hydroacoustic, Hydrographic and Top Predator Patterns:
Cetacean Distributions in the Mid-Atlantic Bight

by

Erin Ann LaBrecque

Marine Science and Conservation
Duke University

Date: _____

Approved:

Patrick N. Halpin, Supervisor

Andrew J. Read

James L. Hench

Steven J. Bograd

Dissertation submitted in partial fulfillment of
the requirements for the degree
of Doctor of Philosophy in
Marine Science and Conservation in the Graduate School
of Duke University

2016

ABSTRACT

Spatial Relationships among Hydroacoustic, Hydrographic and Top Predator Patterns:

Cetacean Distributions in the Mid-Atlantic Bight

by

Erin Ann LaBrecque

Marine Science and Conservation
Duke University

Date: _____

Approved:

Patrick N. Halpin, Supervisor

Andrew J. Read

James L. Hench

Steven J. Bograd

An abstract of a dissertation submitted in partial
fulfillment of the requirements for the degree
of Doctor of Philosophy in
Marine Science and Conservation in the Graduate School of
Duke University

2016

Copyright by
Erin Ann LaBrecque
2016

Abstract

Effective conservation and management of top predators requires a comprehensive understanding of their distributions and of the underlying biological and physical processes that affect these distributions. The Mid-Atlantic Bight shelf break system is a dynamic and productive region where at least 32 species of cetaceans have been recorded through various systematic and opportunistic marine mammal surveys from the 1970s through 2012. My dissertation characterizes the spatial distribution and habitat of cetaceans in the Mid-Atlantic Bight shelf break system by utilizing marine mammal line-transect survey data, synoptic multi-frequency active acoustic data, and fine-scale hydrographic data collected during the 2011 summer Atlantic Marine Assessment Program for Protected Species (AMAPPS) survey. Although studies describing cetacean habitat and distributions have been previously conducted in the Mid-Atlantic Bight, my research specifically focuses on the shelf break region to elucidate both the physical and biological processes that influence cetacean distribution patterns within this cetacean hotspot.

In Chapter One I review biologically important areas for cetaceans in the Atlantic waters of the United States. I describe the study area, the shelf break region of the Mid-Atlantic Bight, in terms of the general oceanography, productivity and biodiversity.

According to recent habitat-based cetacean density models, the shelf break region is an area of high cetacean abundance and density, yet little research is directed at understanding the mechanisms that establish this region as a cetacean hotspot.

In Chapter Two I present the basic physical principles of sound in water and describe the methodology used to categorize opportunistically collected multi-frequency active acoustic data using frequency responses techniques. Frequency response classification methods are usually employed in conjunction with net-tow data, but the logistics of the 2011 AMAPPS survey did not allow for appropriate net-tow data to be collected. Biologically meaningful information can be extracted from acoustic scattering regions by comparing the frequency response curves of acoustic regions to theoretical curves of known scattering models. Using the five frequencies on the EK60 system (18, 38, 70, 120, and 200 kHz), three categories of scatterers were defined: fish-like (with swim bladder), nekton-like (e.g., euphausiids), and plankton-like (e.g., copepods). I also employed a multi-frequency acoustic categorization method using three frequencies (18, 38, and 120 kHz) that has been used in the Gulf of Maine and Georges Bank which is based the presence or absence of volume backscatter above a threshold. This method is more objective than the comparison of frequency response curves because it uses an established backscatter value for the threshold. By removing all data below the threshold, only strong scattering information is retained.

In Chapter Three I analyze the distribution of the categorized acoustic regions of interest during the daytime cross shelf transects. Over all transects, plankton-like acoustic regions of interest were detected most frequently, followed by fish-like acoustic regions and then nekton-like acoustic regions. Plankton-like detections were the only significantly different acoustic detections per kilometer, although nekton-like detections were only slightly not significant. Using the threshold categorization method by Jech and Michaels (2006) provides a more conservative and discrete detection of acoustic scatterers and allows me to retrieve backscatter values along transects in areas that have been categorized. This provides continuous data values that can be integrated at discrete spatial increments for wavelet analysis. Wavelet analysis indicates significant spatial scales of interest for fish-like and nekton-like acoustic backscatter range from one to four kilometers and vary among transects.

In Chapter Four I analyze the fine scale distribution of cetaceans in the shelf break system of the Mid-Atlantic Bight using corrected sightings per trackline region, classification trees, multidimensional scaling, and random forest analysis. I describe habitat for common dolphins, Risso's dolphins and sperm whales. From the distribution of cetacean sightings, patterns of habitat start to emerge: within the shelf break region of the Mid-Atlantic Bight, common dolphins were sighted more prevalently over the shelf while sperm whales were more frequently found in the deep waters offshore and Risso's

dolphins were most prevalent at the shelf break. Multidimensional scaling presents clear environmental separation among common dolphins and Risso's dolphins and sperm whales. The sperm whale random forest habitat model had the lowest misclassification error (0.30) and the Risso's dolphin random forest habitat model had the greatest misclassification error (0.37). Shallow water depth (less than 148 meters) was the primary variable selected in the classification model for common dolphin habitat. Distance to surface density fronts and surface temperature fronts were the primary variables selected in the classification models to describe Risso's dolphin habitat and sperm whale habitat respectively. When mapped back into geographic space, these three cetacean species occupy different fine-scale habitats within the dynamic Mid-Atlantic Bight shelf break system.

In Chapter Five I present a summary of the previous chapters and present potential analytical steps to address ecological questions pertaining the dynamic shelf break region.

Taken together, the results of my dissertation demonstrate the use of opportunistically collected data in ecosystem studies; emphasize the need to incorporate middle trophic level data and oceanographic features into cetacean habitat models; and emphasize the importance of developing more mechanistic understanding of dynamic ecosystems.

Dedication

For Gram and Sadie.

Contents

Abstract	iv
Contents.....	ix
List of Tables.....	xiii
List of Figures	xiv
Acknowledgements	xxiii
1. Introduction	1
1.1 A Review of Biologically Important Areas for Cetaceans within US Waters – East Coast.....	2
1.2.1 Species-Specific Biologically Important Areas.....	8
1.2.1.1 Minke Whale (<i>Balaenoptera acutorostrata</i>).....	8
1.2.1.2 Sei Whale (<i>Balaenoptera borealis</i>).....	11
1.2.1.3 Fin Whale (<i>Balaenoptera physalus</i>).....	14
1.2.1.4 North Atlantic Right Whale (<i>Eubalaena glacialis</i>).....	18
1.2.1.5 Humpback Whale (<i>Megaptera novaeangliae</i>)	28
1.2.1.6 Harbor Porpoise (<i>Phocoena phocoena</i>).....	31
1.2.1.7 Bottlenose Dolphin (<i>Tursiops truncatus</i>).....	33
1.2.1.8 Summary	46
1.2 The Shelf Break Region in the Mid-Atlantic Bight.....	48
1.3 The Shelf Break as a Hotspot	52
1.4 Data Collection.....	58
1.5 Road Map	63

2. A Method to Categorize Opportunistically Collected Multi-frequency EK60 data	64
2.1 Introduction.....	64
2.2 Background: What are Marine Acoustics?	66
2.3 Acoustic Data Collection	78
2.4 Acoustic Data Processing	80
2.4.1 Removal of Intermittent Acoustic Interference.....	80
2.4.2 Background Noise Removal	83
2.4.3 Semi-automated Bottom Detection in a Steep Topography	88
2.5 Categorizing Acoustic Scattering Regions from Frequency Response Curves and Thresholding	89
2.6 Summary.....	101
3. Distribution and Spatial Scales of Biological Acoustic Scattering in the Shelf Break Region of the Mid-Atlantic Bight.....	103
3.1 Introduction.....	103
3.2 Methods	107
3.2.1 Study Area.....	107
3.2.2 Transect Region Classification.....	109
3.2.3 Physical Environment.....	111
3.2.4 Categorization of acoustic regions of interest	114
3.2.5 Analysis Methods.....	115
3.3 Results	119
3.3.1 Trackline effort.....	119

3.3.2 Physical Environment.....	122
3.3.3 Spatial Distribution of Categorized Acoustic Scattering Regions.....	125
3.3.4 Aggregations of Categorized Acoustic Scattering in Relation to Thermal Gradients	131
3.3.5 Identifying Scales of Spatial Patterns from Acoustic Scattering.....	139
3.4 Discussion.....	144
4. Fine-scale Distribution of Three Cetacean Species within the Mid-Atlantic Bight Shelf Break Region.....	148
4.1 Introduction.....	148
4.2 Methods	151
4.2.1 Study Area.....	151
4.2.2 Transect Region Classification.....	152
4.2.3 Physical Environment.....	155
4.2.4 Active Acoustic Data.....	156
4.2.5 Marine Mammal Sightings.....	160
4.2.6 Presence/Pseudo-Absence Points.....	160
4.2.7 Analysis Methods.....	161
4.3 Results	166
4.3.1 Cetacean Sightings	166
4.3.2 Distribution of Distances from Cetacean Sightings to Categorized Acoustic Regions.....	173
4.3.3 Multidimensional scaling, Classification Trees and Random Forests.....	175
4.3.3.1 Common dolphin results	178

4.3.3.2 Risso's dolphin results.....	182
4.3.3.3 Sperm whale results	186
4.4 Discussion.....	191
5. Summary and Future Directions	197
5.1 On-going research	201
References	202
Biography.....	227

List of Tables

Table 1: Frequencies and wavelengths.	68
Table 2: Acoustic transect effort by location and time of day. MAB = Mid-Atlantic Bight, GB = Georges Bank, SH = shelf region, SB = shelf break region, OSSB = offshore shelf break region.	121
Table 3: Detection of acoustic regions of interest by trackline effort. Asterisk (*) indicates significantly different from other values within the column.....	126
Table 4: Predictors variables for classification tree and random forest models. °C = degree Celsius. PSU = practical salinity units. P/A = presence/absence.....	165
Table 5: All cetacean species sighted during the 2011 summer AMAPPS ship-based survey in the Mid-Atlantic Bight.	168
Table 6: Cetacean species sighted on shelf break transects during the 2011 summer AMAPPS ship-based survey in the Mid-Atlantic Bight	170
Table 7: Combined confusion matrix based on random forest out-of-bag classification error for each model.	178

List of Figures

Figure 1: Two minke whale feeding BIAs from March – November in the northeast Atlantic substantiated through vessel based survey data and expert judgment.	11
Figure 2: Sei whale feeding BIA from May – November in the northeast Atlantic substantiated through vessel based survey data and expert judgment.	14
Figure 3: Fin whale feeding BIAs in the northeast Atlantic: (1) June to October in the northern Gulf of Maine; (2) year round in the southern Gulf of Maine; and (3) March to October east of Montauk Point, substantiated through vessel based survey data, photo identification data, and expert judgment. Also shown are the 15 m (solid line) and 50 m (dashed line) depth contours.	18
Figure 4: North Atlantic right whale feeding BIAs in the northeast Atlantic: (1) June and July, October – December on Jeffreys Ledge; (2) February to April on Cape Cod Bay and Massachusetts Bay; and (3) April to June in the Great South Channel and on the northern edge of Georges Bank substantiated through extensive vessel and aerial based survey data, photo identification data, radio tracking data, and expert judgment. NOAA Critical Habitat designation outlines are shown within areas 2 & 3.	21
Figure 5: North Atlantic right whale calving ground BIA in the southeast Atlantic from mid-November to late April substantiated through extensive vessel and aerial based survey data, photo identification data, radio tracking data, genetic analyses and expert judgment. NOAA Critical Habitat designation is outlined within the area.	24
Figure 6: North Atlantic right whale mating BIA in the central Gulf of Maine from November - January described from a demographic study of North Atlantic right whale habitats.	25
Figure 7: North Atlantic right whale migratory corridor BIA along the US east coast substantiated through vessel and aerial based survey data, photo identification data, radio tracking data, and expert judgment. Right whales migrate south to the calving grounds in November and December, and migrate north to the feeding areas, the Bay of Fundy and unknown areas in March and April.	27
Figure 8: Humpback whale feeding BIA, March through December, in the Gulf of Maine, Stellwagen Bank and the Great South Channel substantiated through vessel and aerial based survey data, photo identification data, radio tracking data and expert judgment	31

Figure 9: Harbor porpoise small and resident population in the Gulf of Maine, July to September, substantiated through vessel and aerial based survey data, genetic analyses and expert judgment. 33

Figure 10: Small and resident bottlenose dolphins in the Northern North Carolina Estuarine System substantiated through vessel based survey data, photo identification data, radio tracking data and expert judgment. Striped and solid area active July through October; solid area also active November through March. 35

Figure 11: Small and resident bottlenose dolphin BIA in the Southern North Carolina Estuarine System from July through October substantiated through vessel based survey data, photo identification data, radio tracking data and expert judgment..... 37

Figure 12: Small and resident bottlenose dolphin year round population from Prince Inlet, SC to the North Edisto River, centered on Charleston Harbor, substantiated through vessel based survey data, photo identification data and expert judgment. 38

Figure 13: Northern Georgia / Southern South Carolina Estuarine System year round bottlenose dolphin resident population BIA substantiated through vessel and aerial based survey data, photo identification data, radio tracking data and expert judgment. Area spans from St. Helena Sound, SC to Ossabaw Sound, GA..... 39

Figure 14: Southern Georgia year round bottlenose dolphin resident population BIA substantiated through vessel based survey data, genetic analyses and expert judgment. 40

Figure 15: Jacksonville, FL year round bottlenose dolphin resident population BIA substantiated through vessel based survey data, photo identification data and expert judgment. 42

Figure 16: Indian River Lagoon Estuarine System Population year round resident population BIA for bottlenose dolphins substantiated through vessel and aerial based survey data, photo identification data, radio tracking data and expert judgment..... 43

Figure 17: Bottlenose dolphin year round small and resident population BIA in Biscayne Bay, FL substantiated through vessel based survey data, photo identification data, genetic analyses and expert judgment. 44

Figure 18: Florida Bay bottlenose dolphin year round resident population BIA substantiated through vessel and aerial based survey data, photo identification data, genetic analyses and expert judgment.....	46
Figure 19: Schematic diagram of major features of the surface circulation in the western North Atlantic. The path of the shelf break jet is shown by blue arrows while the warmer Gulf Stream currents are shown as the red arrows. From Fratantoni and Pickart (2007).	49
Figure 20: A schematic diagram of important physical processes in the shelf break region of the Mid-Atlantic Bight. Figure used with permission from Gawarkiewicz and Plueddemann 2007.....	51
Figure 21: Stommel diagram recreated from Hazen et al. (2013). Spatial scale (y-axis) plotted against temporal scale (x-axis), focusing on persistence. Blue: bathymetric-driven hotspots; green: dynamic features that can move throughout the ocean. Grey outline: features that are persistent throughout time; dashed outline: features that are ephemeral. Red box: space and time scales examined in the Mid-Atlantic Bight shelf break system.	53
Figure 22: a) Generalized survey tracklines for 2011 summer AMAPPS survey. b) Labeled acoustic transects where cetacean sighting data, thermosalinograph data, and active acoustic data were concurrently collected (data sets not shown). Numbers are transect names. Leg I – black lines. Leg II – white lines. Leg III – red lines. Six transects were partially or completely sampled twice.....	62
Figure 23: Propagation of a sound wave. From Simmonds and MacLennan (2005).....	67
Figure 24: Echograms depicting intermittent noise and removal. The y-axis is depth in meters. The x-axis is time with vertical lines every 2000 meters the ship traveled. In panels a and c, color is S_v in dB. a - Vertical noise spikes in 120 kHz echogram. b – Noise spikes marked and removed. c – Data from adjacent samples averaged to fill areas where noise spikes were removed.....	82
Figure 25: Sensitivity of S_v in deep water (350 – 400 m) to signal-to-noise ratios for 120 and 200 kHz frequencies.	85
Figure 26: The effect of smoothing backscatter data when removing background noise. a) Raw data at 200 kHz. The TVG-noise ramp is between 250 and 500 meters. b) Noise-reduced echogram from unsmoothed data. c) Noise-reduced echogram from 3x3 cell averaged data above and below the bottom.	86

Figure 27: The effect of setting a minimum signal-to-noise ratio. a) Raw data at 200 kHz. The TVG-noise ramp is between 250 and 500 meters. b) Noise-reduced echogram from unsmoothed data and a minimum signal-to-noise ratio of 7. c) Noise-reduced echogram from 3x3 cell averaged data above and below the bottom and a signal-to-noise ratio of 7. 87

Figure 28: Volume backscatter as a function of frequency for major biological taxa assuming a numerical abundance of 1 organism/m³. From Lavery et al. 2007..... 91

Figure 29: a) 18 kHz and b) 200 kHz example echograms used to calculate the slope of the frequency response (c) over five frequencies. In c, positive slopes (greens) indicate areas with a frequency response curve similar in shape to copepods and euphausiids (red ovals). Negative slope (blues), indicate areas with a frequency response curve similar in shape to fish with swim bladders (yellow ovals). 94

Figure 30: Theoretical target strength scattering models of two types of fish, herring and myctophids (black), theoretical scattering curves of euphausiids from 1 to 6 cm (red), and copepods from 1 mm to 4 mm (blue). Dots along the x-axis indicate 18, 38, 70, 120 and 200 kHz..... 95

Figure 31: 18 kHz (left) and 200 kHz (right) (S_v) from a shelf break transect near Hudson Canyon. Ovals indicate areas selected to categorize backscatter. Magenta ovals were fish-like scattering. Black ovals were nekton-like scattering. Dark green ovals were plankton-like scattering. See figure 29 for comparison of frequency response curves..... 96

Figure 32: Comparison of frequency response curves from selected acoustic regions of interest to models of target strength by taxa. Selected regions are shown in figure 12. a) Herring and myctophid scattering models and two regions of fish-like scattering. b) Euphausiid scattering models for animals from 1 cm to 6 cm and two regions of nekton-like scattering. c) Copepod scattering models for organisms from 1 mm to 6 mm and two regions of plankton-like scattering regions. The dots along the x-axis indicate 18, 38, 70, 120 and 200 kHz. 97

Figure 33: Resampled and smoothed echograms at 18, 38, and 120 kHz for the shelf break transect near Hudson Canyon. Backscatter is S_v . White areas are where background noise was removed (no data). 99

Figure 34: Composite echogram of 18, 38, and 120 kHz data for the shelf break transect near Hudson Canyon. Volume backscatter cells are color-coded based on frequency

combinations where “1”, “2”, and “3” denote backscatter above the -66 dB threshold and “-” denotes the absence of a frequency. The black band across the surface is the upper 10 meters of the water column that was removed. 101

Figure 35: Labeled acoustic transect where thermo-salinograph data and active acoustic data were concurrently collected. Numbers are transect names. Leg I – black lines. Leg II – white lines. Leg III – red lines. Six transects were partially or completely sampled twice..... 108

Figure 36: Regions of a shelf break transect. Green dot is the position of greatest bathymetric gradient between 149.0 and 151.0 meters depth. SH = shelf region, SB = shelfbreak region, OSSB = offshore shelfbreak region. 110

Figure 37: Location of XBT deployments. Greyed out locations on XBT 11 transect were not included in this analysis. 114

Figure 38: Labeled acoustic transects where cetacean sighting data, thermosalinograph data, and active acoustic data were concurrently collected (data sets not shown). Numbers are transect names. Leg I – black lines. Leg II – white lines. Leg III – red lines. Six tr Six transects were partially or completely sampled twice..... 120

Figure 39: TS diagrams with density contours of near surface temperature and salinity from the flow-through thermo-salinograph. Grey dots are data points from all transect regions collected during the survey. Panel a, black dots are data from the shelf region. Panel b, black dots are data from the shelf break region. Panel c, black dots are data from the offshore of the shelf break region..... 122

Figure 40: Bathymetric, temperaure, salinity and density spatial gradients calcauted from the TSG along a transect (Leg 1, Line 01) in the Mid-Atlantic Bight. a) red indicates the shelf region, green indicates the shel break region, blue indicates the region offshore of the shelf break. The think blue line indicates the bathemetric spatial gradient (bathymetirc slope). b) Temperature (blue) and salinity (green) along the transect. c) Temperature gradient along the transect. d) Salinity gradient along the transect. e) Density gradient along the transect..... 124

Figure 41: Bathymetric, temperaure, salinity and density spatial gradients calcauted from the TSG along a transect (Leg 3, Line XBT07) in the Mid-Atlantic Bight. a) red indicates the shelf region, green indicates the shel break region, blue indicates the region offshore of the shelf break. The think blue line indicates the bathemetric spatial gradient

(bathymetric slope). b) Temperature (blue) and salinity (green) along the transect. c) Temperature gradient along the transect. d) Salinity gradient along the transect. e) Density gradient along the transect..... 125

Figure 42: Position of centroids of categorized acoustic scattering regions along a generalized transect. Red dots = centroid of plankton-like regions. Green dots = centroid nekton-like regions. Blue dots = centroid fish-like regions..... 128

Figure 43: Position of categorized acoustic scattering along a generalized transect. Pink dots = centroid of plankton-like layers. Red dots = centroid of plankton-like patches. Light green dots = centroid of nekton-like layers. Green dots = nekton-like patches. Light blue dots = centroid of fish-like layers. Blue dots = fish-like patches. 129

Figure 44: Boxplot of depths of categorized acoustic patches and layers by transect region. 131

Figure 45: Acoustic backscatter (S_v) at 18 kHz (a) and 200 kHz (b) along transect XBT03 and temperature contours. Asterisks are the centroids of fish-like acoustic regions. Circles are the centroids of nekton-like acoustic regions of interest. Diamonds are centroids of plankton-like acoustic regions of interest. 134

Figure 46: Acoustic backscatter (S_v) at 18 kHz (a) and 200 kHz (b) along transect XBT07 and temperature contours. Asterisks are the centroids of fish-like acoustic regions. Circles are the centroids of nekton-like acoustic regions. Diamonds are centroids of plankton-like acoustic regions. 136

Figure 47: Acoustic backscatter (S_v) at 18 kHz (a) and 200 kHz (b) along transect XBT11 and temperature contours. Asterisks are the centroids of fish-like acoustic regions of interest. Circles are the centroids of euphausiid-like acoustic regions of interest. Diamonds are centroids of copepod-like acoustic regions of interest..... 138

Figure 48: a) Lg1ln16, 18 kHz normalized S_v series used for the wavelet analysis. b) Lg1ln16, 38 kHz normalized S_v series used for the wavelet analysis. c and e) The local wavelet power spectrum using the Morelet wavelet. Warmer colors represent regions in scale-location space with large wavelet coefficients. The white line encloses regions greater than a 95% confidence level for a red-noise process. Black semi-circle is the cone of influence. Results below this line should not be trusted due to edge effects. d and f) Global wavelet spectrum averaged over the entire transect. The dashed blue line is the

95% confidence level for a red-noise process. g and h) Scale averaged wavelet power over the 1 – 4 km band. 142

Figure 49: a) Lg1ln19, 18 kHz normalized S_v series used for the wavelet analysis. b) Lg1ln19, 38 kHz normalized S_v series used for the wavelet analysis. c and e) The local wavelet power spectrum using the Morelet wavelet. Warmer colors represent regions in scale-location space with large wavelet coefficients. The white line encloses regions greater than a 95% confidence level for a red-noise process. Black semi-circle is the cone of influence. Results below this line should not be trusted due to edge effects. d and f) Global wavelet spectrum averaged over the entire transect. The dashed blue line is the 95% confidence level for a red-noise process. g and h) Scale averaged wavelet power over the 1 – 4 km band. 143

Figure 50: Labeled survey lines. Numbers are transect names (see Table 6). Black lines and numbers: Leg I. White lines and numbers: Leg II. Red lines and numbers: Leg III. Six tracklines were partially or completely sampled more than once. 152

Figure 51: Regions of a shelf break transect. Green dot is the position of greatest bathymetric gradient between 149.0 and 151.0 meters depth. SH = shelf region, SB = shelfbreak region, OSSB = offshore shelfbreak region. 154

Figure 52: General shapes of frequency response curves used to categorize scattering regions for fish-like scattering (black line), nekton-like scattering (red line) and plankton-like scattering (blue line). Dots are the frequencies from the EK60 (18, 38, 70, 120, and 200 kHz)..... 159

Figure 53: Geographic locations of all cetacean sightings during the 2011 summer, ship-based AMAPPS survey 169

Figure 54: Geographic locations of cetacean sightings along shelf break transects during the 2011 summer ship-based AMAPPS survey. Only shelf break transects with concurrent EK60 data were analyzed..... 171

Figure 55: Cetacean sightings per km of trackline. SH shelf region. SB - shelf break region. OSSB – offshore of the shelf break region. 173

Figure 56: Boxplots of closest distance (km) between marine mammal sightings and categorized acoustic regions. Red = plankton-like scattering regions (“P-like”). Green = nekton-like scattering regions (“N-like”). Blue = fish-like scattering regions (“F-like”). Bw = beaked whale (*Mesoplodon* sp. and *Ziphius*). Ba = minke whale, Bp = fin whale,

Mn = humpback whale, Gm = pilot whale, Sc = striped dolphin, Tt = bottlenose dolphin, Dd = common dolphin, Gg = Risso's dolphin, Pm = sperm whale. Y-axis, distance in kilometers with 0 at top of the panels. Horizontal lines within boxes are the medians. Dots are the means.....	174
Figure 57: Multidimensional scaling plot of model variables at cetacean sighting locations and at pseudo-absense locations.....	176
Figure 58: Classification tree output for common dolphin habitat. Pink nodes = not habitat. Blue nodes = habitat. The decimals (middle line in pink and blue nodes) are the probability of 'not habitat' and probability of 'habitat'. The bottom number is the percentage of data classified at that node.....	179
Figure 59: Random forest variable importance for common dolphin habitat.....	180
Figure 60: Partial dependence plots of random forest classification for common dolphin habitat. Partial dependence is the dependence of the probability of presence on one predictor variable after averaging out the effect of the other predictor variables in the model.	181
Figure 61: Common dolphin habitat (pink polygons) along transects with common dolphin sightings (red squares).	182
Figure 62: Classification tree output for Risso's dolphin habitat. Pink nodes = not habitat. Blue nodes = habitat. The decimals (middle line in pink and blue nodes) are the probability of 'not habitat' and probability of 'habitat'. The bottom number is the percentage of data classified at that node.....	183
Figure 63: Random forest variable importance for Risso's dolphin habitat.	184
Figure 64: Partial dependence plots of random forest classification for Risso's dolphin habitat. Partial dependence is the dependence of the probability of presence on one predictor variable after averaging out the effect of the other predictor variables in the model.	185
Figure 65: Risso's dolphin habitat (light green polygons) along transects with Risso's dolphin sightings (green circles).....	186
Figure 66: Classification tree output for sperm whale habitat. Pink nodes = not habitat. Blue nodes = habitat. The decimals (middle line in pink and blue nodes) are the	

probability of 'not habitat' and probability of 'habitat'. The bottom number is the percentage of data classified at that node.....	187
Figure 67: Random forest variable importance for sperm whale habitat.	188
Figure 68: Partial dependence plots of random forest classification for sperm whale habitat. Partial dependence is the dependence of the probability of presence on one predictor variable after averaging out the effect of the other predictor variables in the mode	190
Figure 69: Sperm whale habitat (blue polygons) along transects with sperm whale sightings (blue triangles).....	191

Acknowledgements

First and foremost, I must thank my family. I have made it this far in life because of their love, support, encouragement, and silliness.

My committee member: Drs. Patrick Halpin, Andrew Read, James Hench, and Steven Bograd, provided knowledge, advice, laughs and a wonderful opportunity to grow as a scientist. And a special thank you to my advisor, Pat Halpin, who is always more understanding than I am when life throws a curve ball. To have that kind of moral support while pursuing a graduate degree can be worth more than knowledge.

Data, bunk space, encouragement and all-around excitement about my research were provided by Drs. Debi Palka and Mike Jech from the Northeast Fisheries Science Center. The labs of Dr. Gareth Lawson and Dr. Peter Wiebe gave me and my dog office space, guidance, comradery, three wonderful summers in Woods Hole and some very tasty homebrew. Mike Lowe, Amy Maas, Alex Bergan, Nancy Copley and Jon Finke – thank you for welcoming Sadie and me into your lab.

Danielle Waples – I would not have made it without you. Allison Henry, Tonya Wimmer, Wu-Jung Lee, Shay Vieham, Maria Wise, MDD, Lynne Williams, Maria De Oca, Megan Ferguson, Christin Murphy, Leigh Torres, Gretchen Lovewell, Candice Emmons, Monica Zani, Joan and Tup Carris (my other parents)... there are so many more. It really does take a village to raise a graduate student. Thank you!

A note on funding and project deliverables.

The overall data collection and analyses for Atlantic Marine Assessment Program for Protected Species (AMAPPS) has been funded by the Bureau of Ocean Energy Management (BOEM), the U.S. Navy, the National Oceanic and Atmospheric Administration (NOAA) and the U.S. Fish and Wildlife Service (USFWS). No funding was given directly to me or Duke University for data collection or analysis used in this dissertation. Bunk space for the third leg of the 2011 Northeast Fisheries Science Center (NEFSC) summer AMAPPS research cruise and data were provided to me by the NEFSC. Expendable bathythermograph (XBT) probes were purchased with funds from the Oak Foundation. The analysis presented here was funded through the Nancy Foster Scholarship program, the Duke University Marine Lab Writing Fellowship, and research assistantships from my advisor, Dr. Patrick Halpin. As stipulated by the Nancy Foster Scholarship Program, section 2.2 is part of an active acoustics manual for marine mammal observers. It is my intension that the acoustic data analysis templates be used in further analysis of AMAPPS data where appropriate.

1. Introduction

As the targets of living marine resource conservation and management change from single species to ecosystem-based targets, more emphasis is being put on interdisciplinary studies. Many of the National Marine Fisheries Service (NMFS) marine mammal ship-based surveys now routinely collect oceanographic, plankton, nekton, and both passive and active acoustic data. By collecting and analyzing these data, scientists can gain a better understanding of the ecology of marine mammals and provide scientifically sound recommendations for their conservation and management. I begin by providing a description of biologically important areas for cetacean species along the Atlantic coast of the United States. Biologically important areas are spatially and temporally explicit areas for migrating, feeding, reproductive activities, and small and resident populations. These biologically important areas, delineated from published data and expert review, include a range of locations from coastal estuarine systems to the deep waters of the Gulf of Maine, and span all months of the year, but the review of biologically important areas omits an important area of interest – the continental shelf break. It is well known that the shelf break region is an important area for cetaceans, but most research only includes this area as part of larger studies focused on marine

mammal abundance because of logistics and the cost of getting to and working in the shelf break region. My research focuses on the Mid-Atlantic Bight continental shelf break region to expand the body of knowledge pertaining to marine mammals in this region.

1.1 A Review of Biologically Important Areas for Cetaceans within US Waters – East Coast

Sections of 1.1 are published as LaBrecque et al. (2015). Co-authors are Corrie Curtice, Jolie Harrison, Sofie Van Parijis, and Patrick Halpin, but the text presented here is my own.

Anthropogenic activities in the marine environment are increasing in number, geographic extent and often duration, potentially increasing the risk to marine ecosystems (Hooker and Gerber 2004, Halpern et al. 2008, Nowacek et al. 2015). Activities of concern with the US Atlantic waters included energy exploration (e.g. windfarm installation; oil and gas exploration, development, and production), shipping, fishing, and military testing and training (e.g. sonar exercises and equipment testing). Several components of these activities have the potential to directly and adversely affect marine mammals through ship-strikes, by-catch or entanglement, or alteration of habitat through physical or chemical changes. Indirect effects of these activities on marine

mammals include the spatial or temporal shifts of prey species or changes in prey species abundance.

In the United States, the Marine Mammal Protection Act (MMPA) (16 USC § 1361 et seq.) and the Endangered Species Act (ESA) (16 USC § 1531 et seq.) contain provisions for the protection and conservation of marine mammals, including sections that address federal or public activities that have the potential to disturb or harm marine mammals, their populations, or their habitat. If federal or public activities have the potential to disturb or harm marine mammals, the National Oceanic and Atmospheric Administration (NOAA) must reach conclusions, specific to each statute, regarding the scope and significance of the anticipated impacts of the proposed activity to individuals and their habitat, and how the impacts to individual marine mammals might affect populations. These analyses inform mitigation and monitoring measures, and the conclusions can affect whether the entities conducting the activity can proceed with their intended actions as planned or if the activity needs to be modified. The ability to characterize marine mammal behaviors or activities in a specific place and time is important in the assessment of potential impacts of a proposed activity and the development of appropriate mitigation measures (Ferguson et al. 2015).

In 2011, NOAA convened the Cetacean Density and Distribution Mapping (CetMap) Working Group to bring together experts with a diversity of experience in cetacean ecology, conservation, and management to map cetacean density and distribution within US waters. Their purpose was to understand the activities of cetaceans at a certain time and place, which is indicative of the area's biological importance, for the purposes of impact analysis and management (Ferguson et al. 2015). The primary goal of CetMap was to "create and compile comprehensive and easily accessible regional cetacean density and distribution maps that are time- and species-specific, ideally using survey data and models that estimate density using predictive environmental factors." (Ferguson et al. 2015). Habitat-based density models were considered the best tool to address spatially and temporally explicit questions on cetacean abundance, density, and distribution; however, habitat-based density models require a large amount of high-quality data. These types of data are only available to for limited number of cetacean species, regions, and time periods (Kot et al. 2010, Kaschner et al. 2012, Roberts et al. 2016). Additionally, habitat-based density models do not provide animal distribution information at relevant space and time scales that can be acquired from primary sources (e.g. acoustic data, sightings data, tagging data, genetic data, tagging data, and expert knowledge), nor provide information on an animal's

activity state. Therefore, the CetMap Working Group decided to augment habitat-density model information with additional information by identifying areas of biological importance to cetaceans (Ferguson et al. 2015).

To supplement CetMap's quantitative density and distribution mapping effort (see Roberts et al. 2016), and to provide additional context for cetacean impact analysis, CetMap undertook a process, through expert consultation, to identify Biologically Important Areas (BIAs) (Ferguson et al. 2015). This review coalesces existing published and unpublished information to define BIAs in U.S. East Coast waters (shoreward of the Exclusive Economic Zone [EEZ]) for cetacean species that meet the criteria for migratory areas, feeding areas, reproductive areas, and small and resident populations as defined by (Ferguson et al. 2015). Migratory areas (also presented as 'Migratory Corridor') is the area and time within which a substantial portion of a species is known to migrate (Ferguson et al. 2015). The migratory corridor is spatially restricted. Feeding areas are areas and times within which aggregations of the species preferentially feed. These areas may be persistent in space and time or associated with ephemeral features that are less predictable but are located within a larger area that can be delineated (Ferguson et al. 2015). Reproductive areas are areas and times within which a species selectively mates, gives birth, or is found with neonates or calves (Ferguson et al. 2015). Small and resident

populations are areas and times within which resident populations occupy a limited extent (Ferguson et al. 2015). A comprehensive overview of the BIA delineation process; its caveats, strengths, and limitations; and its relationship to international assessments also can be found in Ferguson et al. (2015). A summary can also be found at <http://cetsound.noaa.gov/important>. Metadata tables that concisely detail the type and quantity of information used to define each BIA are available as an online supplement. BIAs are delineated at the minimum spatial and temporal scales that available information can support.

Within the East Coast region, one species—North Atlantic right whale (*Eubalaena glacialis*)—was evaluated and found to meet the criteria for reproductive, feeding, and migratory corridor BIAs; four species—minke whale (*Balaenoptera acutorostrata*), sei whale (*B. borealis*), fin whale (*B. physalus*), and humpback whale (*Megaptera novaeangliae*)—met the criteria for feeding BIAs; and two species—bottlenose dolphin (*Tursiops truncatus*) and harbor porpoise (*Phocoena phocoena*)—met the criteria for small and resident populations. Several other cetacean species are found in this region but do not meet the BIA criteria. These species include sperm whale (*Physeter macrocephalus*), dwarf sperm whale (*Kogia sima*), pygmy sperm whale (*K. breviceps*), Cuvier’s beaked whale (*Ziphius cavirostris*), Blainville’s beaked whale (*Mesoplodon densirostris*), Gervais’

beaked whale (*M. europaeus*), Sowerby's beaked whale (*M. bidens*), True's beaked whale (*M. mirus*), Risso's dolphin (*Grampus griseus*), long-finned pilot whale (*Globicephala melas*), short-finned pilot whale (*G. macrorhynchus*), common dolphin (*Delphinus delphis*), white-sided dolphin (*Lagenorhynchus acutus*), Atlantic spotted dolphin (*Stenella frontalis*), and striped dolphin (*S. coeruleoalba*). Infrequently sighted cetacean species include blue whale (*B. musculus*), North Atlantic bottlenosed whale (*Hyperoodon ampullatus*), false killer whale (*Pseudorca crassidens*), killer whale (*Orcinus orca*), melon-headed whale (*Peponocephala electra*), rough-toothed dolphin (*Steno bredanensis*), Fraser's dolphin (*Lagenodelphis hosei*), white-beaked dolphin (*Lagenorhynchus albirostris*), pantropical spotted dolphin (*S. attenuata*), spinner dolphin (*S. longirostris*), and Clymene dolphin (*S. clymene*). Common dolphins, long and short-finned pilot whales, Risso's dolphin, Atlantic white-sided dolphin, and Atlantic spotted dolphin should be evaluated in future efforts to create BIAs for these species in this region as new information becomes available.

Information pertaining to East Coast BIAs was synthesized primarily from published data from systematic ship-based surveys, systematic aerial surveys, opportunistic whale-watching surveys, tagging studies, photo-identification studies, genetic analysis, acoustic recordings, and stranding and whaling records. The East Coast

BIA assessment benefitted from the inputs and insights of ten experts familiar with East Coast cetacean species.

1.2.1 Species-Specific Biologically Important Areas

1.2.1.1 Minke Whale (*Balaenoptera acutorostrata*)

General

Minke whales in the U.S. East Coast waters are recognized as part of the Canadian East Coast stock (Donovan 1991, Waring et al. 2014) and are found throughout the waters off the East Coast of the U.S., with the greatest number of sightings in northeastern waters (CeTAP 1982, Waring et al. 2013). Like other balaenopterids, there appears to be a strong seasonal division in minke whale distribution. They migrate between high latitudes in summer and low latitudes in winter. From May through September, minke whales are most abundant in New England waters, including the Gulf of Maine, Cape Cod Bay, the Great South Channel, and Georges Bank (Pittman et al. 2006, Waring et al. 2014). Year-round acoustic recordings from Stellwagen Bank detected minke whale vocalizations from August to November with a few detections from March to June (Risch et al. 2013). Minke whales are mostly absent from New England waters in winter. Although sighting data have not provided evidence of a migration corridor, year-round acoustic monitoring from the Gulf of St. Lawrence to Saba Bank in the

Caribbean suggest minke whales migrate in the deeper waters offshore of the U.S. continental shelf, and in winter they are spread out at low latitudes from the Mid-Atlantic Ridge to the U.S. continental shelf (Risch et al. 2014). No minke whale mating or calving grounds have been found in U.S. Atlantic waters. Mitchell (1991) speculated that offshore waters of the southeast U.S. and the West Indies might be important winter calving grounds. Recent records show minke whale mother/calf pairs offshore of the continental shelf near Florida and North Carolina (Nilsson et al. 2011) supporting possible winter calving grounds in the southeast U.S. Atlantic or further south.

Feeding

Minke whales have been observed feeding in the Great South Channel and adjacent waters from March through November. During vessel-based humpback whale surveys from 1988 to 2011, the Provincetown Center for Coastal Studies (PCCS) recorded 19 sightings of individual minke whales feeding along the northern edge of Georges Bank, Great South Channel, Stellwagen Bank, and off Race Point, Massachusetts (PCCS, unpub. data, 1988-2011) in waters less than 150 m. From 1998 to 2009, the Northeast Fisheries Science Center (NEFSC) aerial survey team recorded 15 sightings of minke whales feeding (NEFSC, unpub. data, 1998-2009) during all survey months (March to July, October) in waters less than 200 m. Twenty-one observations of surface or apparent surface feeding of minke whales were recorded from March through

September during the CeTAP (1982) surveys within the 100-m isobath in the Great South Channel, along Cape Anne, and at Jeffreys Ledge. Between 1979 and 1992, Murphy (1995) confirmed 27 sightings of minke whale feeding at the surface Cape Cod Bay, Massachusetts Bay, and on Stellwagen Bank. These sightings were recorded during dedicated marine mammal research cruises and on whale-watching vessels. Feeding group size was recorded in 24 of the 27 sightings; two sightings were of pairs of individuals, one sighting was of three individuals, and single individuals account for the rest of the 24 sightings recorded with group size. From these published and unpublished sightings of minke whale feeding activity, I define the minke whale feeding BIA in waters less than 200 m in the southern and southwestern section of the Gulf of Maine, including Georges Bank, the Great South Channel, Cape Cod Bay and Massachusetts Bay, Stellwagen Bank, Cape Anne, and Jeffreys Ledge (Figure 1). I include areas of the central Gulf of Maine to incorporate sightings of minke whale feeding in the shallow water around Parker Ridge and Cashes Ledge.

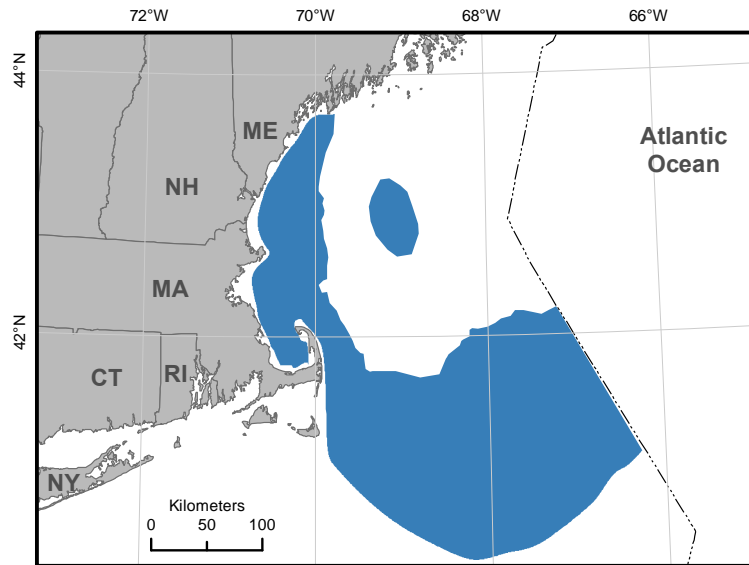


Figure 1: Two minke whale feeding BIAs from March – November in the northeast Atlantic substantiated through vessel based survey data and expert judgment.

1.2.1.2 Sei Whale (*Balaenoptera borealis*)

General

Sei whales in U.S. East Coast waters are recognized as part of the Nova Scotia Stock (Donovan 1991, Waring et al. 2014). Like other balaenopterids, sei whales migrate between high-latitude summer feeding areas and low-latitude winter breeding areas, but sei whales tend to occur in a more restricted range of latitudes in temperate waters (Mizroch et al. 1984a). Sightings from the 1978 to 1982 CeTAP surveys and data from the National Oceanic and Atmospheric Administration (NOAA) Fisheries shipboard

surveys (Waring et al. 2014) show peak abundance of sei whales in U.S. Atlantic waters occurs in spring, particularly along the shelf break of Georges Bank, into the Northeast Channel, and southwest to Hydrographer Canyon. However, they are also present in winter months and were the most common large whale sighted during aerial surveys conducted from January through March 2011 (Palka 2012). Sei whales are generally associated with the deeper waters off the shelf break edge (Hain et al. 1985); however, (Newhall et al. 2012a) provide new insights into sei whale presence in shallower waters (also see “Feeding” section for another exception). Sei whale conception occurs during a 5-month period centering on the winter months, with gestation approximately 12 months long (Mizroch et al. 1984a). No known mating or calving grounds have been found in U.S. Atlantic waters. Although a sei whale stranding in December 1972 on the coast of South Carolina (Mead 1977) lends some evidence to a migratory corridor, no migratory corridor for sei whales has been identified in U.S. Atlantic waters. Mitchell (1975) described a migration of sei whales from south of Cape Cod along the eastern coast of Canada in June and July with a return migration in September and October. This migration remains unverified and probably describes local seasonal movements.

Feeding

Known from whaling records (Jonsgard and Darling 1977) and observed feeding behavior, sei whales in the North Atlantic feed primarily on copepods and secondarily

on euphausiids (CeTAP 1982, Mizroch et al. 1984a, Kenney and Winn 1986, Baumgartner et al. 2011). During the CeTAP surveys, sei whales were observed feeding from April through July in the deeper waters off the southwestern and eastern edge of Georges Banks and into the southwestern section of the Gulf of Maine (CeTAP 1982, Kenney and Winn 1986). This has been shown to change in response to prey availability. In 1986, sei whales were reported feeding in the shallow waters of Stellwagen Bank from April through October in response to increased copepod availability (Payne et al. 1990, Schilling et al. 1992, Kenney et al. 1996). Waring et al. (2014) reported that sei whales feed at more inshore locations, such as the Great South Channel (in 1987 and 1989), when copepod abundance is elevated. During their vessel-based surveys from 1994 through 2011, PCCS recorded 58 instances of sei whale feeding activity from May through November around the shelf break areas of the southwestern section of Gulf of Maine and the eastern edges of Georges Bank (PCCS, unpub. data, 1994-2011). From these reports, publications, and unpublished PCCS data, the sei whale feeding BIA extends from the 25-m contour off coastal Maine and Massachusetts west to the 200-m contour in central Gulf of Maine, including the northern shelf break area of Georges Bank (Figure 2). The sei whale feeding BIA also includes the southern shelf break area of Georges Bank from 100 to 2,000 m and the Great South Channel. Their feeding activity in

the U.S. Atlantic waters is concentrated from May through November with a peak in July and August.

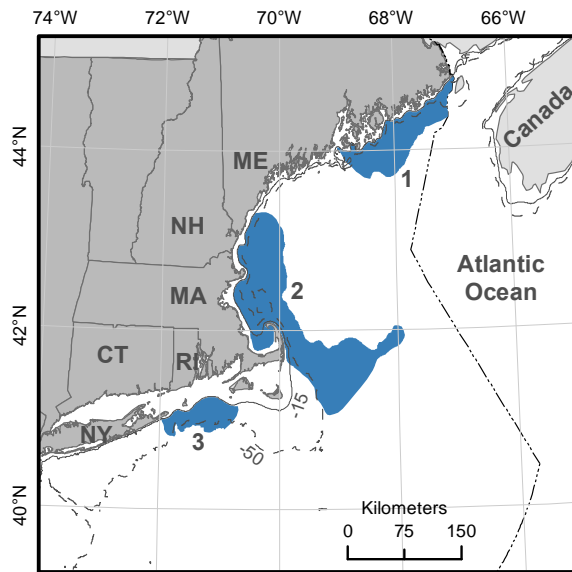


Figure 2: Sei whale feeding BIA from May – November in the northeast Atlantic substantiated through vessel based survey data and expert judgment.

1.2.1.3 Fin Whale (*Balaenoptera physalus*)

General

Fin whales in U.S. Atlantic waters were first recognized as part of the Nova Scotia Stock (Donovan 1991) but are now called the Western North Atlantic Stock (Waring et al. 2014). The Western North Atlantic Stock of fin whales are widely distributed over the U.S. continental shelf and shelf break from Cape Hatteras through

the Gulf of Maine (Geo-Marine Inc. (GMI) 2010a, Waring et al. 2014), although rarely sighted in the deep basin of the Gulf of Maine and the shallow banks of Georges Bank. Fin whales were the most frequently sighted large whale species in the nearshore waters off New Jersey during GMI's (2010) 24-month survey (37 sightings, mostly of individual whales). The majority of these sightings occurred during winter (18 December to 9 April) and spring (10 April to 21 June) months. The most abundant sightings of fin whales occur in New England waters during spring and summer (CeTAP 1982, Waring et al. 2014). Scattered sightings over the northeast shelf in winter and fall indicate that some fin whales are present during the non-feeding season (Hain et al. 1992). In addition, acoustic data from Massachusetts Bay (Morano et al. 2012) indicate fin whale presence throughout the winter months. Acoustic data from the U.S. Navy's Sound Surveillance System (SOSUS) arrays suggest that animals that do undertake southward migrations in the fall generally travel south past Bermuda and into the West Indies (Clark 1995); however, a migration corridor for fin whales in the U.S. Atlantic EEZ is not known. Based on stranding data of neonates and observations of mother-calf pairs, Hain et al. (1992) suggest fin whale calving occurs off the coast of the mid-Atlantic U.S. between October and January. Calving has not been verified in this area.

Feeding

Fin whales feed in higher latitude areas from March through October when primary production is high (Mizroch et al. 1984b). Fin whales feed primarily on euphausiids and small schooling fish such as capelin (*Mallotus villosus*) and sand lance (*Ammodytes* spp.) (Mizroch et al. 1984b, Pauly et al. 1998, Perry et al. 1999). Reporting from the CeTAP (1982) surveys and additional data from University of Rhode Island aerial and shipboard surveys, Manomet Bird Observatory surveys, and NOAA Fisheries shipboard surveys from 1980 through 1988, Hain et al. (1992) noted a particular spring and summer feeding concentration “in an arc that begins in the Great South Channel southeast of Nantucket, runs northwestward along the 40-50 m contour to the east of Chatham, continues from the Provincetown area north across Stellwagen Bank, passes east of Cape Ann and ends at the northeast tip of Jeffreys Ledge” (p. 657). This area composed the largest feeding area reported for fin whales in the CeTAP study area. A second major fin whale feeding area was reported directly east of Montauk Point between the 15- and 50-m contours (Hain et al., 1992). Fin whale feeding during spring and summer was also observed as far south as the Delmarva Peninsula and north to the Bay of Fundy (Hain et al., 1992) but not at concentrations comparable to the Great South Channel area (Figure 3).

Photo-identification records collected from 1974 to 1988 from the Gulf of Maine show that individual female fin whales exhibit feeding site fidelity in areas of the northern (lower Bay of Fundy, Seal Island, and Mt. Desert Rock, Maine) or the southern (Great South Channel, Jeffreys Ledge, and Stellwagen Bank) Gulf of Maine (Agler et al. 1993). From 1980 through 1987, 156 fin whales were individually identified through photo-identification techniques within the Massachusetts Bay area feeding grounds (Seipt et al. 1990). During this period, approximately 62% of the 156 individuals were observed in more than 1 year; and in some cases, individually known fin whales were observed within the Massachusetts Bay feeding grounds in as many as 8 year (Seipt et al. 1990). Clapham and Seipt (1991) (1991) suggest that these rates of return are evidence that site fidelity for the Western North Atlantic fin whale stock may be maternally determined. Fin whales were seen in the southern Gulf of Maine from March to October, while fin whales in the northern Gulf of Maine were seen only from June to October (Agler et al., 1993). Unpublished sighting data of feeding fin whales from the PCCS spatially coincide with previously published data. Temporally, PCCS sightings of feeding occurred in all months in southwestern Gulf of Maine, extending the seasonal feeding BIA period to year-round in areas of the Gulf of Maine (PCCS, unpub. data, 1984-2011).

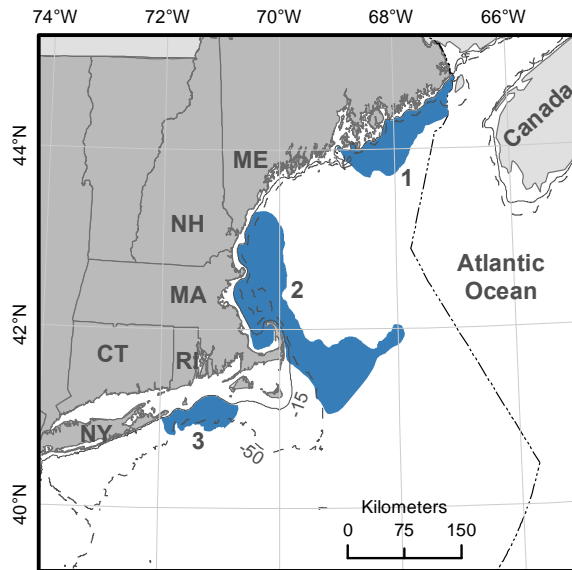


Figure 3: Fin whale feeding BIAs in the northeast Atlantic: (1) June to October in the northern Gulf of Maine; (2) year round in the southern Gulf of Maine; and (3) March to October east of Montauk Point, substantiated through vessel based survey data, photo identification data, and expert judgment. Also shown are the 15 m (solid line) and 50 m (dashed line) depth contours.

1.2.1.4 North Atlantic Right Whale (*Eubalaena glacialis*)

General

North Atlantic right whales are season-ally distributed throughout East Coast U.S. waters. They are listed as endangered under the U.S. Endangered Species Act (ESA) and are one of the most critically endangered large whale species in the world (Best et al. 2001). Research conducted by various groups, including the New England Aquarium,

NOAA Fisheries, PCCS, U.S. Fish and Wildlife Service, Georgia Department of Natural Resources, and Florida Fish and Wildlife Conservation Commission, suggest six major Atlantic right whale: (1) coastal waters of the southeastern U.S., (2) the Great South Channel, (3) Georges Bank/Gulf of Maine, (4) Cape Cod Bay and Massachusetts Bay, (5) the Bay of Fundy, and (6) the Scotian Shelf (Waring et al., 2014).

Critical Habitat for the North Atlantic right whale was federally designated by NOAA Fisheries in 1994 for the Great South Channel, Cape Cod Bay and a section of Stellwagen Bank, and the waters adjacent to the coast of Georgia and the east coast of Florida (*Federal Register* [FR] 59[226], 28805-28835). Although I include the federally mandated Critical Habitat areas as reference, calving, feeding, and mating BIAs for North Atlantic right whales expand beyond these areas.

Feeding

North Atlantic right whales primarily feed on copepods of the genus *Calanus* in New England, Bay of Fundy, and Scotian Shelf waters from late February through December (Kenney and Winn 1986, Weinrich et al. 2000, Baumgartner and Mate 2003, Baumgartner et al. 2003). Direct observations of feeding behavior from numerous boat-based and aerial surveys in New England and Canadian waters suggest four well-known, high-use feeding habitats in northern U.S. Atlantic waters: (1) Cape Cod Bay and Massachusetts Bay, (2) the Great South Channel, (3) Georges Bank/Gulf of Maine,

and (4) the lower Bay of Fundy (Kenney et al., 2001; Waring et al., 2014; Figure 4).

Locations of North Atlantic right whale feeding activity compiled from CeTAP (1982), commercial whale-watching trips, and the North Atlantic right whale sighting database also suggest that North Atlantic right whales feed at Jeffreys Ledge in the western Gulf of Maine (Weinrich et al., 2000).

Generally, North Atlantic right whales arrive and start feeding in Cape Cod Bay and Massachusetts Bay in late February with peak occurrence in March and April (Hamilton and Mayo 1990). The primary spring feeding ground for the majority of the population is the Great South Channel (Kenney et al. 1995), and to a lesser extent, the northern edge of Georges Bank (Waring et al., 2014), from April through June with a peak in May (CeTAP, 1982; Kenney et al., 1995). Individuals and mother-calf pairs leave the Great South Channel and head to the Bay of Fundy in June and July. During their travels to the Bay of Fundy, North Atlantic right whales have been observed feeding at Jeffreys Ledge (Weinrich et al., 2000). Although individuals move among the feeding grounds during summer and fall (Mate et al. 1997), many right whales feed outside of U.S. waters in the Bay of Fundy, including the lower Bay of Fundy, east of Grand Manan Island, from July through September (Kenney et al., 2001). Of the known North Atlantic

right whale feeding areas, only the Great South Channel and Cape Cod Bay have been designated Critical Habitat areas (FR 59[226], 28805-28835; Figure 4).

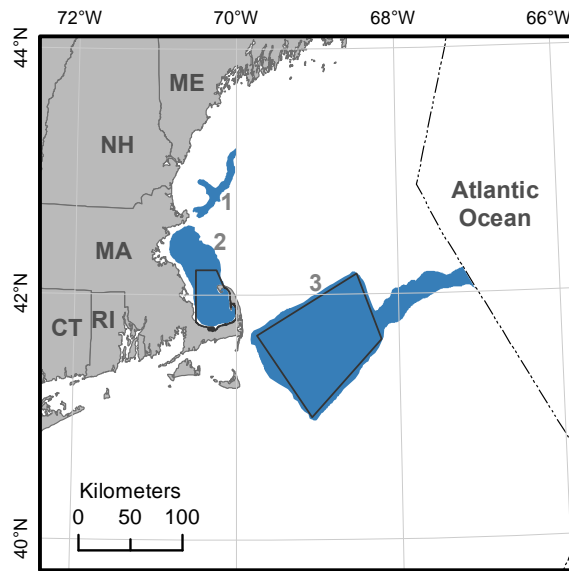


Figure 4: North Atlantic right whale feeding BIAs in the northeast Atlantic: (1) June and July, October – December on Jeffreys Ledge; (2) February to April on Cape Cod Bay and Massachusetts Bay; and (3) April to June in the Great South Channel and on the northern edge of Georges Bank substantiated through extensive vessel and aerial based survey data, photo identification data, radio tracking data, and expert judgment. NOAA Critical Habitat designation outlines are shown within areas 2 & 3.

Reproduction

North Atlantic right whales have a gestation period of approximately 1 year.

From mid-December through late March, pregnant North Atlantic right whales give

birth in the Critical Habitat calving grounds off Georgia and northeastern Florida (Knowlton et al. 1994). Although only one birth of a North Atlantic right whale has been observed in the Critical Habitat calving grounds (Zani et al. 2008), and one right whale birth was observed offshore of the defined shallow water calving habitat off northern Florida (Foley et al. 2011), most neonates and calves are first observed during dedicated North Atlantic right whale aerial surveys in the coastal waters of Georgia and northeast Florida during winter months. An outlier to these observations was the sighting of a newborn North Atlantic right whale mother-calf pair off Plymouth harbor, New England, in January 2013.

The currently designated Critical Habitat calving grounds encompass waters from the shore out to 15 nmi from Altamaha River, Georgia, to Jacksonville, Florida, and the shore out to 5 nmi from Jacksonville to Sebastian Inlet, Florida (FR 59[226], 28805-28835; Figure 5). This habitat boundary was based on annual observations of calving female North Atlantic right whales during the 1980s and early 1990s, and descriptions of local habitat features, including the presence of cooler water temperatures occurring in nearshore, shallow habitats (FR 59[226], 28805-28835). Spatial coverage of annual aerial surveys beyond the core Critical Habitat demonstrated that calving female North Atlantic right whales routinely use a broader habitat than that defined by the current

Critical Habitat designation. Habitat models indicated that peak calving North Atlantic right whale sighting rates occurred at sea surface temperatures between 13° to 15° C and in water depths between 10 to 20 m. Projecting these habitat features spatially indicated that calving habitats occur over continental shelf waters as far north as Cape Lookout, North Carolina (Good 2008, Keller et al. 2012). Calving North Atlantic right whales have been observed in waters off of South Carolina during aerial surveys conducted since 2004 (e.g., Schulte and Taylor 2012), and North Atlantic right whales have been observed in low numbers north off Cape Lookout, North Carolina, during winter aerial surveys, including at least one calving female (McLellan 2004). Calving North Atlantic right whales also occur as far south as Cape Canaveral, Florida, during winter with a restricted distribution in shallower waters close to shore (Keller et al. 2006). On their return from the winter calving grounds, the majority of mother-calf pairs use the lower section of the Bay of Fundy feeding grounds, north of U.S. waters, as a summer nursery; however, some females consistently take their calves to unknown nursery areas (Schaeff et al. 1993, Malik et al. 1999).

Based upon these habitat analyses and calving North Atlantic right whale aerial sightings data, I describe the reproductive calving BIA for North Atlantic right whales in the southeastern U.S. to encompass waters from the shoreline to 25-m water depth

between Cape Canaveral, Florida, and Cape Lookout, North Carolina (Figure 5). This definition of the calving BIA does not spatially include the sighting by Foley et al. (2011); however, I expect the definition of calving BIA to expand and include the southern U.S. continental shelf as more survey data become available. Calving North Atlantic right whales use these habitats each year between mid-November and mid-April.

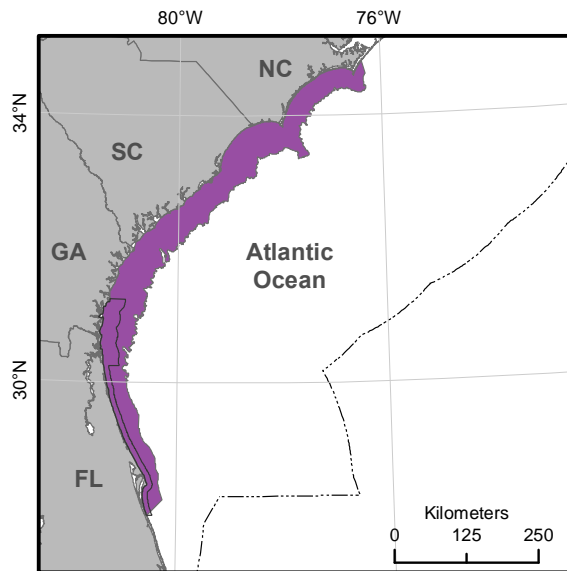


Figure 5: North Atlantic right whale calving ground BIA in the southeast Atlantic from mid-November to late April substantiated through extensive vessel and aerial based survey data, photo identification data, radio tracking data, genetic analyses and expert judgment. NOAA Critical Habitat designation is outlined within the area.

From November to January, non-calving North Atlantic right whales appear to use the central Gulf of Maine, including Outer Falls and Cashes Ledge, as a potential mating area (Cole et al. 2013; Figure 6). This area was part of a demographic comparison of North Atlantic right whale habitats. The mating BIA was drawn to incorporate the greatest amount of sightings in the central Gulf of Maine while following bathymetry contours to include Outer Falls and Cashes Ledge.

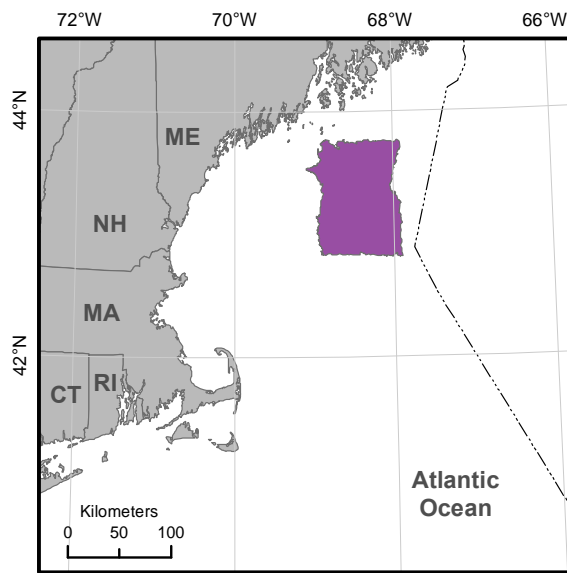


Figure 6: North Atlantic right whale mating BIA in the central Gulf of Maine from November - January described from a demographic study of North Atlantic right whale habitats.

Migration

Although individual North Atlantic right whales move among the feeding grounds during the summer and can travel hundreds of miles within a month (Mate et al. 1997, Baumgartner and Mate 2005), their true migration occurs in the late autumn and late winter. In November and December, North Atlantic right whales leave the feeding grounds of the Bay of Fundy and Scotian shelf (non-U.S. waters) and migrate along the U.S. continental shelf to either the calving grounds in the southeastern U.S. or to unknown winter areas (Brown et al. 2001, Kenney 2001, Whitt et al. 2013)(Brown et al., 2001; Kenney et al., 2001; Whitt et al., 2013; Figure 7). By late March, most right whales have left the calving grounds and traveled up the U.S. continental shelf to Cape Cod Bay (Kenney et al. 2001, Knowlton et al. 2002). Although North Atlantic right whales are known to travel along the continental shelf of the U.S. (Schick et al. 2009, Whitt et al. 2013), it is unknown if they use the entire shelf area during migration or restrict their movements to nearshore waters.

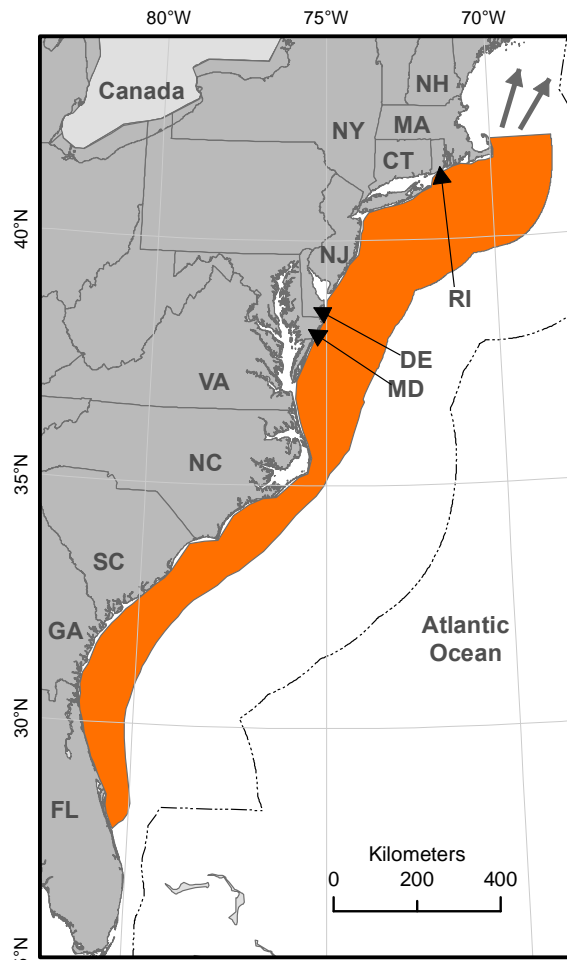


Figure 7: North Atlantic right whale migratory corridor BIA along the US east coast substantiated through vessel and aerial based survey data, photo identification data, radio tracking data, and expert judgment. Right whales migrate south to the calving grounds in November and December, and migrate north to the feeding areas, the Bay of Fundy and unknown areas in March and April.

1.2.1.5 Humpback Whale (*Megaptera novaeangliae*)

General

The Gulf of Maine feeding stock is the predominant subpopulation of humpback whales in U.S. Atlantic waters (Waring et al., 2014). Other areas of feeding subpopulations in the North Atlantic include Iceland, Denmark, Southwest Greenland, Southern Labrador and east of Newfoundland, and the Gulf of the St. Lawrence (Katona & Beard, 1990; Perry et al., 1999b). Humpbacks from all the North Atlantic feeding areas migrate to calving and breeding grounds off the West Indies in winter (Mattila et al., 1989, 1994). Most sightings in the Gulf of Maine occur between May and October, with peaks in July and August (Robbins, 2007). In late October, most humpbacks start leaving the Gulf of Maine feeding grounds for the West Indies calving grounds. However, small numbers of animals have been sighted throughout the winter months (Robbins, 2007), and acoustic data demonstrate that some animals remain through early winter (Mattila et al., 1987; Vu et al., 2012). Little is known about the actual migratory path. It is thought that most hump-backs migrate both north and south in the open ocean, but some have been seen on the continental shelf off the mid-Atlantic U.S. during migration periods (Swingle et al., 1993; Barco et al., 2002; GMI, 2010). Visual (Department of Navy, 2011) and acoustic (Hodge, 2011) surveys near Onslow Bay, North Carolina, and Jacksonville, Florida, provide evidence of humpbacks along or near the continental shelf. Winter

aerial surveys conducted by NOAA Fisheries have documented humpbacks off the coasts of North Carolina and Florida (Palka, 2012), and 17 sightings of humpback whales were recorded in all seasons during year-round visual surveys in the nearshore waters of New Jersey (GMI, 2010). Gulf of Maine humpbacks leave the calving grounds in early spring to return to the feeding grounds. Northbound migrants have been documented in the feeding areas as early as late March, though encounter rates during visual surveys begin to increase substantially by May (Robbins, 2007). Humpback mating and calving grounds are not within the continental U.S. Atlantic waters.

Feeding

Humpback whales show strong, maternally directed feeding site fidelity (Clapham & Mayo, 1987). Humpbacks feed in the Gulf of Maine from March through December, with most feeding activity observed in June and July (PCCS, unpub. data, 1984-2011; Figure 8). Studies of humpback whale ecology in the Gulf of Maine have been ongoing since the mid-1970s (Payne et al., 1986; Clapham & Mayo, 1987, 1990; Weinrich, 1991; Weinrich & Kuhlberg, 1991; Clapham et al., 1993; Weinrich et al., 1997; Friedlaender et al., 2009; Hazen et al., 2009) and have shown a link between the spatial and temporal distributions of humpbacks in the Gulf of Maine and their prey, Atlantic herring (*Clupea harengus*) and sand lance (*Ammodytes* spp.). Payne et al. (1986) showed that humpbacks shifted from their primary feeding grounds on Georges Bank and the

northern Gulf of Mexico to Stellwagen Bank and the Great South Channel in response to shifts in sand lance distribution.

Humpbacks have been observed in the waters off the U.S. mid-Atlantic (New Jersey to North Carolina) in all months of the year (Swingle et al., 1993; Wiley et al., 1995; Barco et al., 2002; GMI, 2010). Notably, most records are from January through March when whales are traditionally assumed to be in the breeding grounds (Barco et al., 2002). Swingle et al. (1993) and Wiley et al. (1995) suggest U.S. mid-Atlantic waters represent a supplemental winter feeding ground used by juvenile and mature humpback whales of U.S. and Canadian North Atlantic stocks.

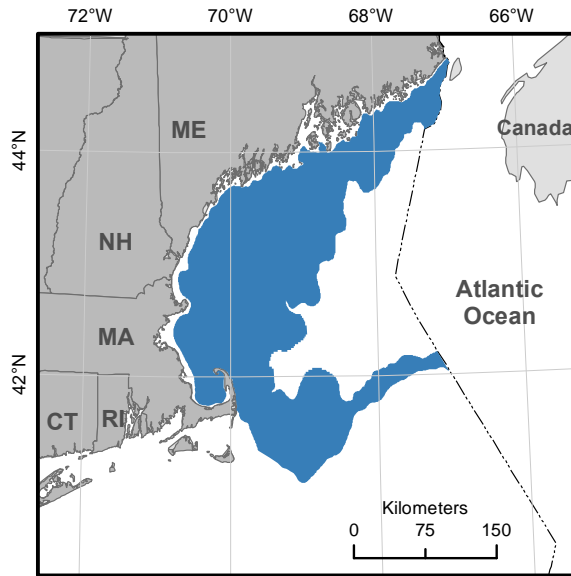


Figure 8: Humpback whale feeding BIA, March through December, in the Gulf of Maine, Stellwagen Bank and the Great South Channel substantiated through vessel and aerial based survey data, photo identification data, radio tracking data and expert judgment

1.2.1.6 Harbor Porpoise (*Phocoena phocoena*)

Small and Resident Population

Based on genetic analyses of summer breeding populations (Rosel et al., 1999), there are four known populations of harbor porpoises in the western North Atlantic: (1) the Gulf of Maine/Bay of Fundy, (2) Gulf of St. Lawrence, (3) Newfoundland, and (4) Greenland populations (Gaskin, 1984, 1992; Read & Hohn, 1995). Harbor porpoises in U.S. Atlantic waters are distributed from the Bay of Fundy to North Carolina (Waring et al., 2014). All harbor porpoises seen in the Gulf of Maine and Bay of Fundy are part of

the Gulf of Maine/Bay of Fundy population, but harbor porpoises sighted off the mid-Atlantic states during winter include porpoises from other western North Atlantic populations (Rosel et al., 1999).

Sightings have been documented by NOAA Fisheries ship and aerial surveys, strandings, and animals taken incidental to fishing reported by NOAA Fisheries observers. From July to September, harbor porpoises in U.S. waters (Gulf of Maine/Bay of Fundy) are concentrated in waters less than 150 m deep in the northern Gulf of Maine and southern Bay of Fundy (Gaskin, 1977; Kraus et al., 1983; Palka, 1995; Figure 9). Lower densities have been observed in the upper Bay of Fundy and northern edge of Georges Bank during this time frame (Palka, 2000).

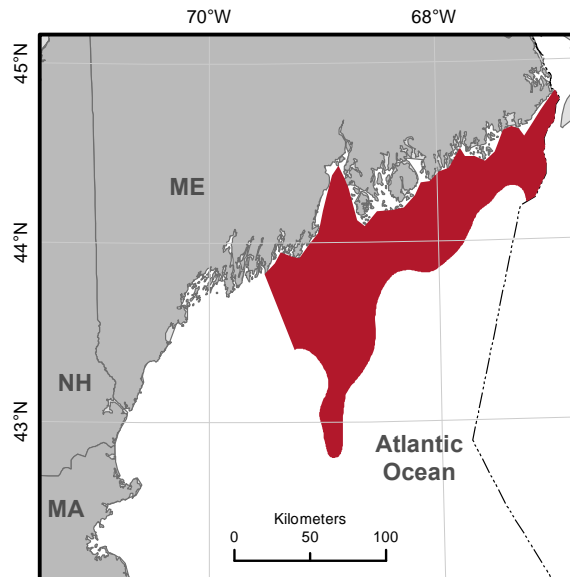


Figure 9: Harbor porpoise small and resident population in the Gulf of Maine, July to September, substantiated through vessel and aerial based survey data, genetic analyses and expert judgment.

1.2.1.7 Bottlenose Dolphin (*Tursiops truncatus*)

Small and Resident Populations

Bottlenose dolphins in the U.S. East Coast waters range from Long Island, New York, to the Florida peninsula and inhabit estuarine coastal, continental shelf, and continental slope waters. There are two genetically distinct ecotypes—nearshore (also referred to as *coastal*) and offshore (Mead & Potter, 1995; Hoelzel et al., 1998; Torres et al., 2003); however, studies support the existence of small and resident populations in several estuarine systems along the East Coast of the U.S. All of the small and resident

populations of bottlenose dolphins summarized here are described in the stock assessment reports produced by NOAA Fisheries. We do not present information on migratory populations even though some of the small and resident populations are migratory during parts of the year.

Northern North Carolina Estuarine System Population (NNCES)

Photo-identification studies, satellite telemetry data, and a stable isotope study suggest a small and resident population of bottlenose dolphins in the estuarine waters of North Carolina from Beaufort Inlet to the North Carolina/Virginia border (Urian et al., 1999; Cortese, 2000; Read et al., 2003). Satellite telemetry data (Waring et al., 2014) and photo-identification data indicate that the NNCES population occupies the waters of Pamlico Sound, North Carolina, and adjacent nearshore coastal waters (< 1 km from shore) from July through October (Figure 2.10). Since Beaufort Inlet is the southern boundary of NNCES dolphins and the northern boundary of Southern North Carolina Estuarine (SNCES) dolphins, individuals from these two groups likely overlap there in summer months. In the late fall and winter, November through March, the NNCES bottle-nose dolphins move out of Pamlico Sound and into the adjacent nearshore waters (Figure 10), likely overlapping with the Northern Migratory Stock of bottlenose dolphins (Waring et al., 2014). The geographical boundaries for this resident population are based

on ongoing photo-identification studies and are subject to change upon further study of dolphin residency patterns in North Carolina.

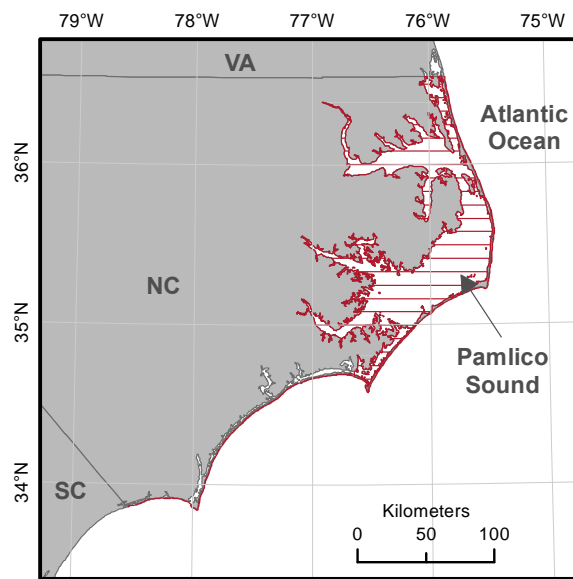


Figure 10: Small and resident bottlenose dolphins in the Northern North Carolina Estuarine System substantiated through vessel based survey data, photo identification data, radio tracking data and expert judgment. Striped and solid area active July through October; solid area also active November through March.

Southern North Carolina Estuarine System Population (SNCES)

Long-term photo-identification studies, satellite telemetry data, and recent genetic analysis suggest a small and resident population of bottlenose dolphins in estuarine and nearshore (< 3 km from shore) waters of North Carolina from Beaufort Inlet to the North Carolina/South Carolina border, including the Cape Fear River (Urian

et al., 1999; Read et al., 2003; Rosel et al., 2009; Waring et al., 2014). Limited data from satellite telemetry studies (Waring et al., 2014), along with photo-identification studies, suggest that bottlenose dolphins in the SNCES population occupy Bogue Sound and the estuarine and nearshore waters south to the Cape Fear River from July through October (Figure 2.11). Since Beaufort Inlet is the northern boundary of SNCES dolphins and the southern boundary of NNCES dolphins, individuals from these two groups likely overlap there during summer months. In late fall through spring, SNCES dolphins move to Cape Fear and its nearshore waters, likely overlapping with the Southern Migratory Stock (Waring et al., 2014). The geographical boundaries for this resident population are based on ongoing photo-identification studies and are subject to change upon further study of dolphin residency patterns in North Carolina.

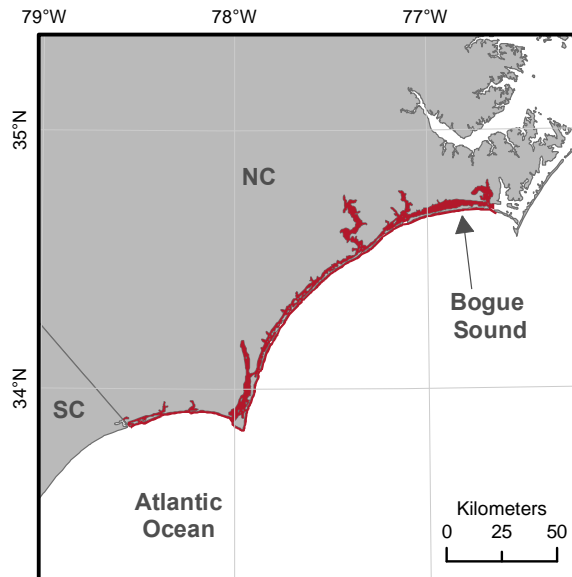


Figure 11: Small and resident bottlenose dolphin BIA in the Southern North Carolina Estuarine System from July through October substantiated through vessel based survey data, photo identification data, radio tracking data and expert judgment.

Charleston Estuarine System Population

High site fidelity of bottlenose dolphins suggests a year-round resident

population centered in Charleston Harbor, South Carolina, and ranging from Price Inlet to the North Edisto River, including the Ashley, Cooper, and Wando Rivers (Waring et al., 2014; Figure 12). Speakman et al. (2006) reviewed photo-identification, remote biopsy, capture-release, and radio-tracking data collected from 1994 through 2003 from these geographic areas. Eight-hundred and thirty-nine dolphins were individually identified, with 115 (14%) sighted more than 10 times. Of the 115 individuals who were

resighted on multiple occasions, 81% were sighted over a period greater than 5 years, and 44% were sighted over a period of 7.7 to 9.8 years.

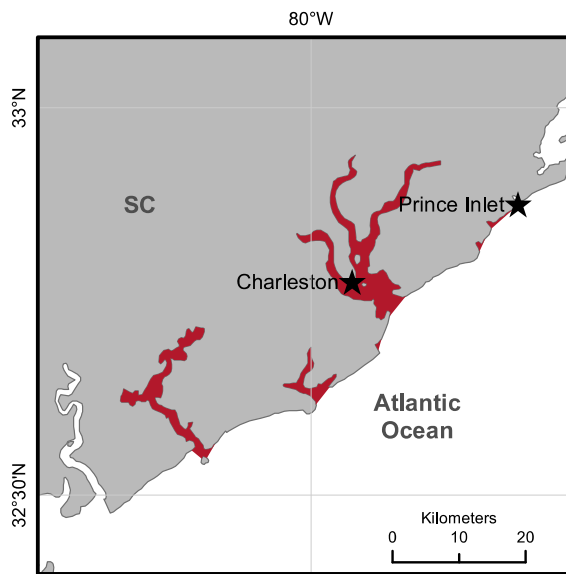


Figure 12: Small and resident bottlenose dolphin year round population from Prince Inlet, SC to the North Edisto River, centered on Charleston Harbor, substantiated through vessel based survey data, photo identification data and expert judgment.

Northern Georgia/Southern South Carolina Estuarine System Population

Photo-identification studies from 1994 to 1998 suggest a year-round resident population of bottlenose dolphins from St. Helena Sound, South Carolina, to Ossabaw Sound, Georgia, including the estuarine waters associated with the sounds and rivers of this area (Gubbins, 2002a, 2002b, 2002c; Figure 13). Resident dolphins were observed 10

to 116 times during this study. Although the northern area of this population abuts the Charleston Harbor population, no photo-identification matches have been made between the two populations (Urian et al., 1999). The geographical boundaries for this resident population are subject to change upon further study of dolphin residency patterns in South Carolina and Georgia.

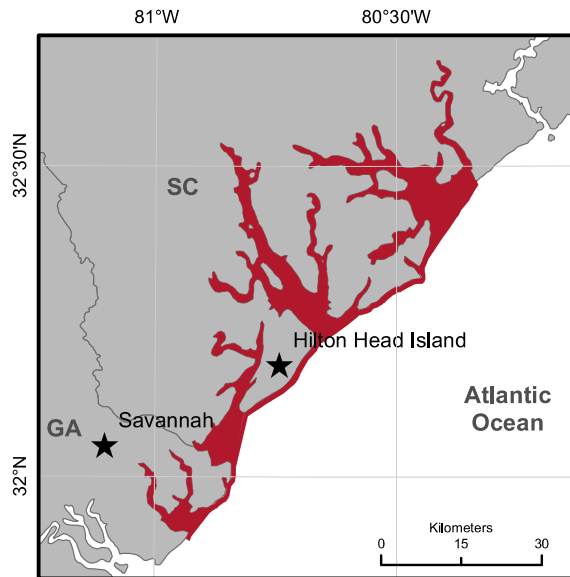


Figure 13: Northern Georgia / Southern South Carolina Estuarine System year round bottlenose dolphin resident population BIA substantiated through vessel and aerial based survey data, photo identification data, radio tracking data and expert judgment. Area spans from St. Helena Sound, SC to Ossabaw Sound, GA.

Southern Georgia Estuarine System Population

Genetic analysis of bottlenose dolphins biopsied from the estuarine and

intercoastal waterways from Altamaha Sound, Georgia, to the Cumberland River, and including the Turtle/Brunswick River estuarine system (Figure 14), shows a significant differentiation from animals biopsied in northern Georgia and southern South Carolina (Waring et al., 2014). Bottlenose dolphins from the Turtle/Brunswick River Estuarine System also exhibit contaminant loads consistent with long-term site fidelity (Pulster & Maruya, 2008).

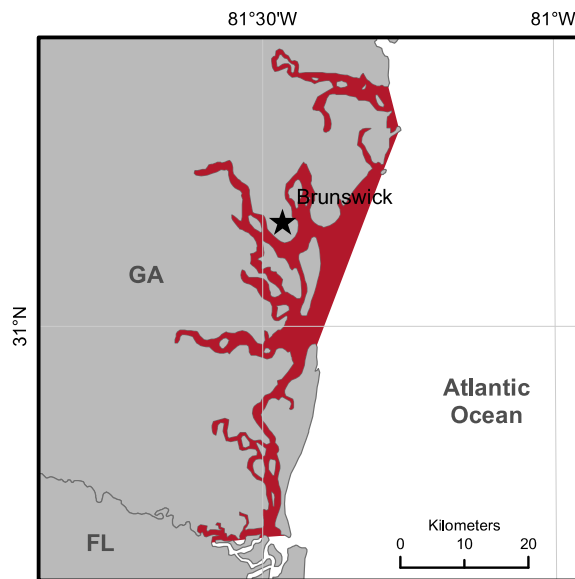


Figure 14: Southern Georgia year round bottlenose dolphin resident population BIA substantiated through vessel based survey data, genetic analyses and expert judgment.

Jacksonville Estuarine System Population

The Jacksonville Estuarine System bottlenose dolphin population has been defined as a resident population based on photo-identification and genetic studies conducted during 1994 through 1997 (Caldwell, 2001; Waring et al., 2014). The geographic boundaries from the Cumberland River, Georgia, to Jacksonville Beach, Florida (Figure 15), are based on the delineation of a photo-identification study area (Caldwell, 2001), which is also used by the NOAA Fisheries stock assessment report for this population (Waring et al., 2014). Within the Jacksonville Estuarine System, behavioral, photo-identification, and genetic analyses described two residency patterns of bottlenose dolphins, northern and southern (Caldwell, 2001). Dolphins in the northern and southern sections of the study area had significantly different mitochondrial DNA haplotype and microsatellite allele frequencies (Caldwell, 2001). Dolphins in both the northern and southern sections of the study area showed strong site fidelity; however, dolphins from both groups were photographed outside their preferred areas. Because the geographic boundaries of this resident population are based on a pre-defined study area, the boundaries are subject to change upon further studies.

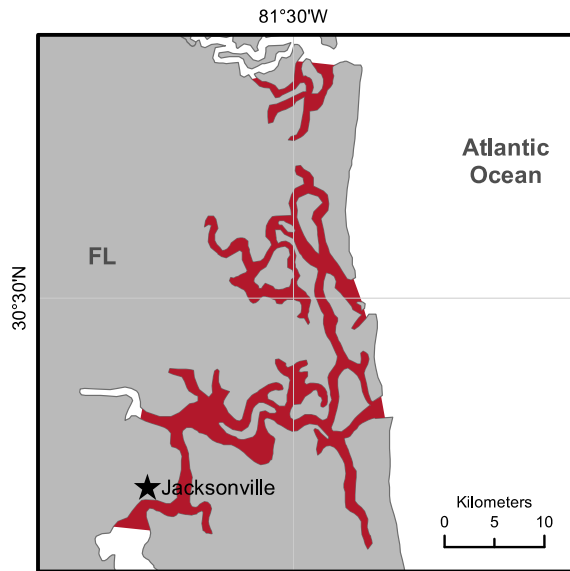


Figure 15: Jacksonville, FL year round bottlenose dolphin resident population BIA substantiated through vessel based survey data, photo identification data and expert judgment.

Indian River Lagoon Estuarine System Population

Bottlenose dolphins in the Indian River Lagoon estuarine system range from

Ponce de Leon Inlet to Jupiter Inlet, Florida (Waring et al., 2014; Figure 16). The geographic boundary is based on multiple studies of bottle-nose dolphins from 1979 to 2005. During a 4-year monitoring period from 1979 to 1982, none of 133 freeze-branded dolphins were observed outside of the Indian River Lagoon estuarine system (Odell & Asper, 1990). Photo-identification studies from 1996 to 2001 indicate long-term site fidelity within the Indian River Lagoon estuarine system (Mazzoil et al., 2005, 2008b).

Radio-tracks of two stranded and rehabilitated bottlenose dolphins from the Indian River Lagoon estuarine system indicate that neither dolphin left the system after their release (Mazzoil et al., 2008a).

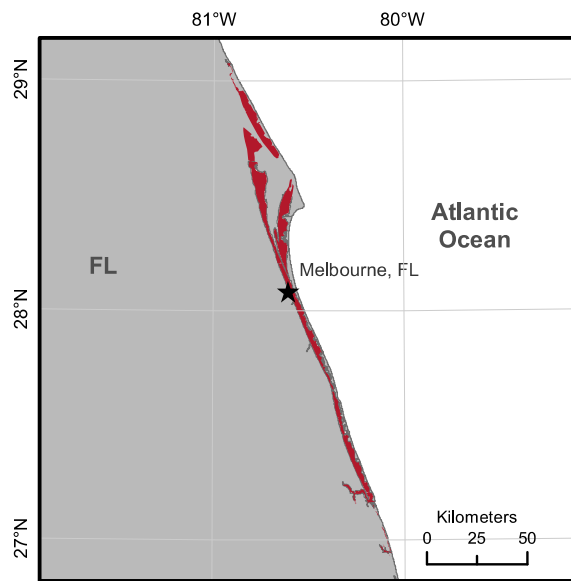


Figure 16: Indian River Lagoon Estuarine System Population year round resident population BIA for bottlenose dolphins substantiated through vessel and aerial based survey data, photo identification data, radio tracking data and expert judgment.

Biscayne Bay Population

Bottlenose dolphins in Biscayne Bay, Florida, have been the subject of an ongoing photo-identification study since 1990 (Waring et al., 2014). Approximately 80% of individual bottlenose dolphins sighted in Biscayne Bay are considered long-term residents with multiple sightings over the study period (Waring et al., 2014). Genetic

analysis and analysis of dolphin associations indicate two overlapping social groups within Biscayne Bay (Litz, 2007; Litz et al., 2012). The boundaries of the Biscayne Bay resident population, Hannover Inlet to the north and Card Sound Bridge to the south (Figure 17), are subject to change upon comparison of the Biscayne Bay photo-identification catalog to the photo-identification catalog for Florida Bay (Waring et al., 2014).

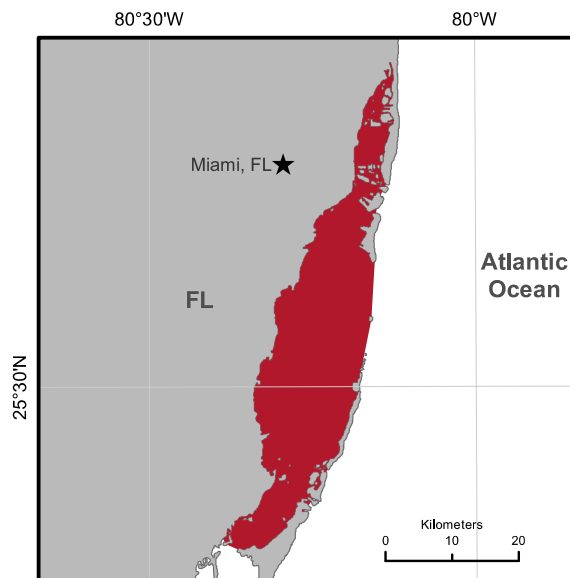


Figure 17: Bottlenose dolphin year round small and resident population BIA in Biscayne Bay, FL substantiated through vessel based survey data, photo identification data, genetic analyses and expert judgment.

Florida Bay Population

Dolphins in Florida Bay have been the subjects of an ongoing photo-identification study since 1999 by various groups, including the Dolphin Ecology Project, NOAA Fisheries, and Duke University (Engleby et al., 2002; Torres & Read, 2009; Waring et al., 2014). Approximately 577 unique individuals have been photographed in Florida Bay. These dolphins have been sighted throughout the Bay, are present year-round (Engleby et al., 2002), and demonstrate high site fidelity through the use of specialized foraging tactics (Torres & Read, 2009). Genetic analysis of bottlenose dolphins from Florida Bay and Biscayne Bay reveal a significant genetic differentiation between these locations (Litz et al., 2012). The boundaries of the Florida Bay resident population coincide with the geographic boundaries of Florida Bay and fall within the Gulf of Mexico-side portion of the Florida Keys National Marine Sanctuary (Figure 18).

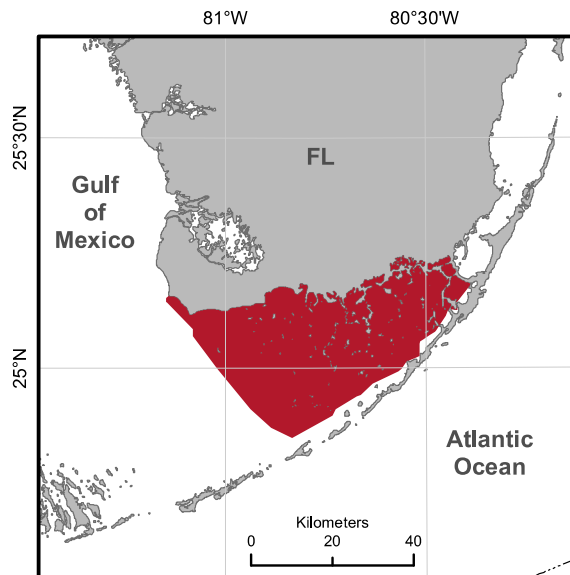


Figure 18: Florida Bay bottlenose dolphin year round resident population BIA substantiated through vessel and aerial based survey data, photo identification data, genetic analyses and expert judgment.

1.2.1.8 Summary

Eighteen BIAs were identified for seven cetacean species within the East Coast region based on extensive expert review and synthesis of published and unpublished information. Identified BIAs included feeding for humpback, minke, sei, fin, and North Atlantic right whales; migratory for North Atlantic right whales; reproductive for North Atlantic right whales; and small and resident populations for harbor porpoise and several stocks of bottlenose dolphins. The geographic extent of the BIAs in the East Coast region ranged from 152 to 270,000 km². The best estimates of abundance for the

small and resident populations identified here ranged from approximately 61,000 to 80,000 for harbor porpoise (Waring et al., 2014), and approximately 120 to 1,000 for the various stocks of bottlenose dolphins (Waring et al., 2014); however, some bottlenose dolphin stock abundance estimates are greater than 8-year old and deemed unreliable. The spatial extent of their overall ranges was on the order of 500 km², though the NNCES Stock occupied over 8,000 km². Although several cetacean species are known to have strong links to bathymetric features—for example, pilot whales and Risso’s dolphins aggregate at the shelf break in U.S. Atlantic waters, and Atlantic spotted dolphins occupy the shelf region from southern Virginia to Florida—there is currently insufficient information to identify these areas as specific BIAs. Passive acoustic recorders have provided baseline evidence that minke whales (Risch et al., 2014) possibly migrate through U.S. waters offshore of the shelf break, and that sei whales aggregate near meandering frontal eddies over the continental shelf in the Mid-Atlantic Bight (Newhall et al., 2012). These types of data, in addition to new information on other species, should be considered in future efforts to update and identify cetacean BIAs in the East Coast U.S. waters. BIAs are not a regulatory designation and have no direct implications for regulatory processes. These BIAs represent the best available information about the activities in which cetaceans are likely to be engaged at a certain time and

place. This information is essential to characterize, analyze, and minimize anthropogenic impacts on cetaceans. Furthermore, BIAs may be used to identify information gaps and prioritize future research to better understand cetaceans, their habitat, and ecosystem.

1.2 The Shelf Break Region in the Mid-Atlantic Bight

The study area for my dissertation is the Mid-Atlantic Bight shelf break region and the southwestern and northeastern edges of Georges Bank. The Mid-Atlantic Bight extends from the Georges Bank to Cape Hatteras. The most prominent surface feature in the Mid-Atlantic Bight is the northeastward flowing warm water of the Gulf Stream and the anticyclonic warm core rings that spin off the Gulf Stream. The second most prominent surface feature is the shelf break current that flows around the Grand Banks as part of the cooler Labrador Current then continues equatorward within the shelf break region as the Mid-Atlantic Bight shelf break front (Figure 19). The shelf break front terminates inshore of the Gulf Stream off Cape Hatteras.

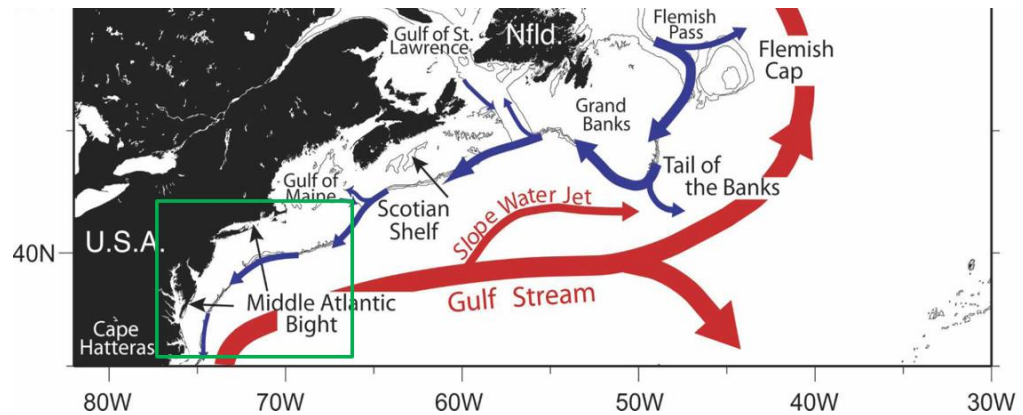


Figure 19: Schematic diagram of major features of the surface circulation in the western North Atlantic. The path of the shelf break jet is shown by blue arrows while the warmer Gulf Stream currents are shown as the red arrows. From Fratantoni and Pickart (2007).

The shelf break region, comprised of the outer continental shelf and upper continental slope, is a highly dynamic and productive area (Xu et al. 2011) that provides a wide range of habitat to many marine species over every trophic level. Several water masses with distinct temperature and salinity properties converge at the shelf break, creating one of the most oceanographically complex areas off the eastern United States (Stefansson et al. 1971, Chapman and Lentz 1994, Linder and Gawarkiewicz 1998, Lozier and Gawarkiewicz 2001, Gawarkiewicz et al. 2008, Zhang and Gawarkiewicz 2015). The shelf break front in the Mid-Atlantic Bight, first described by Bigelow (1933), separates the cooler, fresher water of the continental shelf from the warmer and more saline water

of the continental slope. This oceanographic feature is topographically trapped by the shelf break and is robust, reforming within several days after being disturbed by ocean or meteorological forcing (Gawarkiewicz and Chapman 1992). The shelf break front supports a persistent surface-intensified shelf break jet and large vertical and cross-shelf gradients in temperature, salinity, and nutrients (Figure 20) (Houghton and Marra 1983, Marra et al. 1990, Linder and Gawarkiewicz 1998, Fratantoni et al. 2001, Zhang et al. 2013).

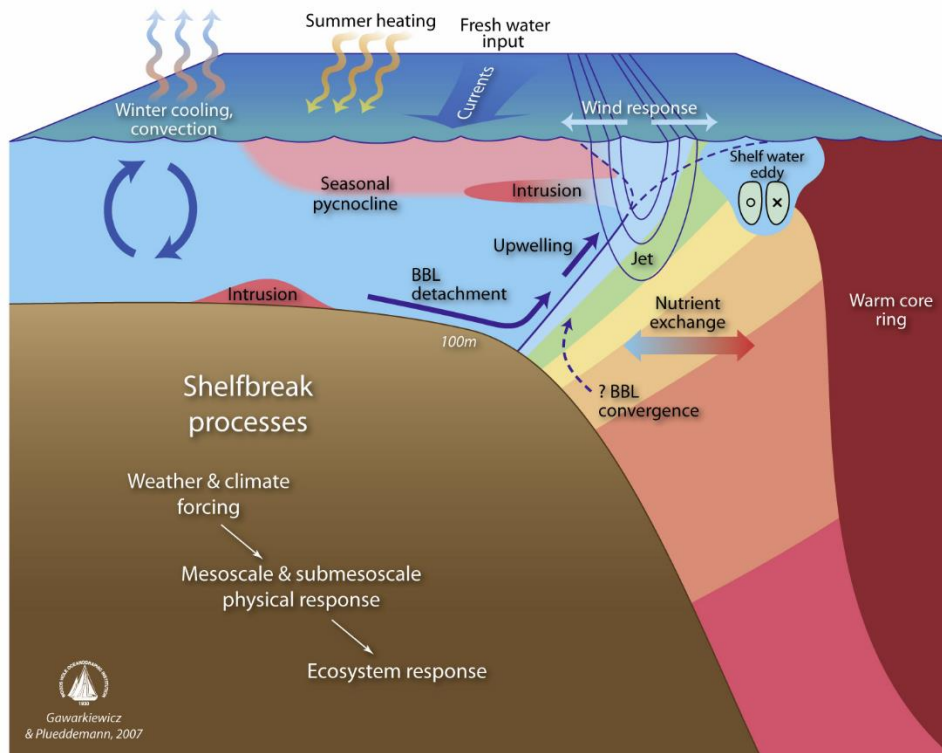


Figure 20: A schematic diagram of important physical processes in the shelf break region of the Mid-Atlantic Bight. Figure used with permission from Gawarkiewicz and Plueddemann 2007.

In winter and early spring, a surface chlorophyll bloom exists across the shelf and slope regions (Malone et al. 1983) with a localized maximum at the shelf break front (Marra et al. 1982). In late spring and summer the chlorophyll bloom becomes a subsurface feature due to the seasonal stratification that blocks the replenishment of the depleted nutrients at the surface (Marra et al. 1990). Recent work from Roberts et al.

(2016) indicates that the shelf break region is also an area of high cetacean diversity and density. For many of the species they modeled, the shelf break region was either the area of highest density within the US Exclusive Economic Zone, or the delineation between low densities and areas where a species was assumed to be absent. For example, the Mid-Atlantic Bight shelf break region exhibits the highest year-round densities of pilot whales (*Globicephala sp.*) and Risso's dolphins (*Grampus griseus*) with the greatest concentrations in summer months. Common dolphins (*Delphinus delphis*), known to occupy areas of the continental shelf, shelf break, and some areas offshore of Georges Bank, showed greatest densities within the shelf break region. Dwarf and pygmy sperm whale (*Kogia sp.*) are seen to have year-round densities between 0.01 and 0.15 animals per 100 km² offshore of the shelf break, and less than 0.01 animals per 100 km² over the shelf (Roberts et al. 2016).

1.3 The Shelf Break as a Hotspot

The term 'hotspot' is increasingly used in marine biology and conservation, but it has a longer history and more structured definition in terrestrial ecology. Myers (1988) was the first to define hotspots and later revised the definition as areas with both high endemism and risk to habitat (Myers et al. 2000). In terrestrial systems, this concept

works well because habitat boundaries are static over the many temporal scales (without anthropogenic influences). In marine systems, the concept translates well to coral reef systems and kelp forests because of their more static nature, but is more difficult apply to pelagic systems where boundaries are dynamic across multiple temporal and spatial scales (Figure 21, recreated from Hazen et al. (2013)).

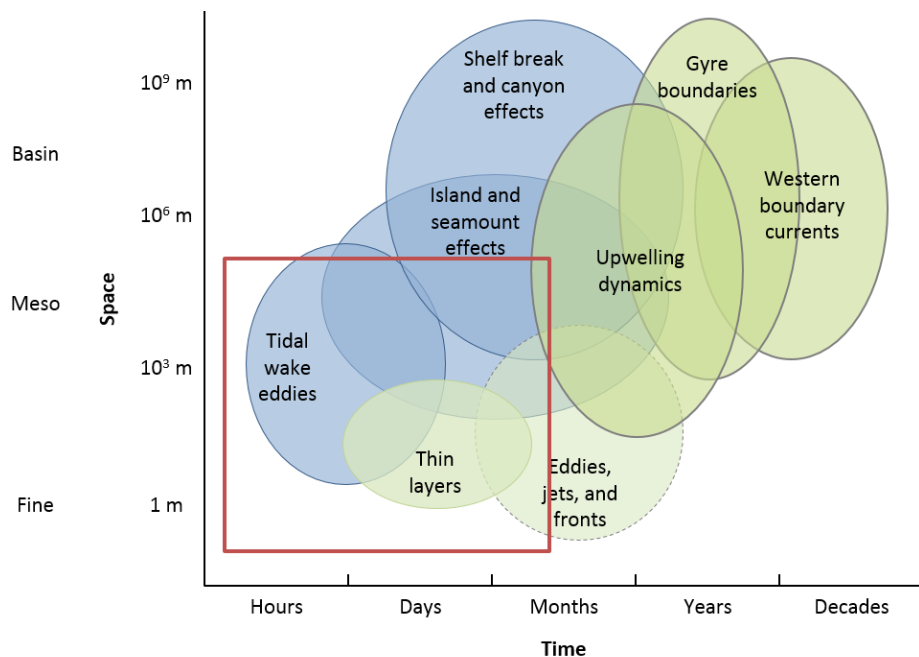


Figure 21: Stommel diagram recreated from Hazen et al. (2013). Spatial scale (y-axis) plotted against temporal scale (x-axis), focusing on persistence. Blue: bathymetric-driven hotspots; green: dynamic features that can move throughout the ocean. Grey outline: features that are persistent throughout time; dashed outline: features that are ephemeral. Red box: space and time scales examined in the Mid-Atlantic Bight shelf break system.

In addition to dynamic pelagic boundaries increasing the difficulty of spatially and temporally defining marine hotspots, marine organisms live at a variety of temporal and spatial scales that generally mirror their trophic levels (Mann and Lazier 1991). Small plankton usually have life spans of several months and travel relatively short distances, whereas large marine predators, such as cetaceans, have life spans of decades and travel vast distances. However, large marine predators tend to concentrate certain activities over localized regions and for short periods of time. For example, many marine mammals undertake long annual migrations, but return seasonally to confined foraging areas (Mate et al. 1995, Read and Westgate 1997, Baumgartner et al. 2003, Risch et al. 2014, LaBrecque et al. 2015). Albatrosses range over ocean basins, but forage in comparatively small areas for extended periods of time (Hyrenbach et al. 2002). It is assumed that these distribution patterns occur because highly mobile animals remain near a prey patch until the patch is no longer energetically beneficial to the animal (Stephens and Krebs 1986). Migration behaviors and feeding behaviors are examples of top predators using different spatiotemporal scales throughout their life history.

The problems of scale in ecology (understanding how observed patterns over multiple spatial and/or temporal scales elucidate ecological processes) has been one of

the central themes in ecological research (Haury et al. 1978, Wiens 1989, Levin 1992, Chave 2013) since the early 1990s, but scaling issues in other disciplines have been recognized for some time (Wiens 1989). Physical and biological oceanographers relate their findings in terms of local and global processes (Stommel 1963, Steele 1978, Legendre and Demers 1984). Stommel (1963) was the first to qualitatively portray typical physical ocean processes along space-time scales. Haury et al. (1978) expanded this concept to qualitatively show the importance of physical variability in determining the biological patterns observed. In the 1980s landscape ecologists started addressing the importance of scale in survey design and ecological inference (Dayton and Tegner 1984; Urban, O'Neill, and Shugart Jr 1987), and in the last few decades, marine ecologists have begun addressing issues of scale pertaining to top level marine predators and their interactions with their environment (Zamon et al. 1996, Fauchald et al. 2000, Fauchald and Erikstad 2002, Benoit-Bird and Au 2003, Torres et al. 2008, Redfern et al. 2008, Becker et al. 2010, Forney et al. 2012).

Research on the biological and physical scales of hotspots is usually constrained by sampling methodologies. Tagging/tracking studies of vertebrates often yields significant insights into behaviors, distributions, and use of marine ecosystems (Block et al. 2001, Stokesbury et al. 2004, Schick et al. 2008, Dragon et al. 2010, Hazen et al. 2012)

but are dependent on the resolution of the tag and initial tagging location. Satellite-based observations of the ocean provide broad temporal coverage and are relatively inexpensive data streams but are limited to only surface conditions, are currently limited to spatial resolutions that cannot define small scale patterns, and are only proxies for primary production (Palacios et al. 2006). Acoustic recorders allow for large scale and fine scale detection of animals, but are only useful if animals vocalize within range of the recorder (Clark 1995, Lammers et al. 2008, Newhall et al. 2012, Risch et al. 2014). Ship-based surveys have the capability, depending on survey design, to utilize a wide variety of sampling techniques that can quantify the horizontal and vertical dimensions of a marine ecosystem, offering detailed insights into the mechanisms that create a biological hotspot (Santora et al. 2011, Sigler et al. 2012).

Describing the relationships between patterns of species' distributions the physical and biological environment they inhabit can help us understand the mechanisms that control the distribution these species and consequently create marine hotspots. Taking into account the dynamism of pelagic boundaries and that marine organisms live at multiple spatial and temporal scales, characteristics of marine hotspots include important life history areas, areas of high biodiversity and abundance of individuals, and areas of high productivity, trophic transfer and biophysical coupling

(Hazen et al. 2013). The shelf break system in the Mid-Atlantic Bight has all of these characteristics.

Cetacean distributions in the Mid-Atlantic Bight have been studied for several decades through line transect surveys (CeTAP 1982, Geo-Marine Inc. (GMI) 2010b, Palka 2012), acoustic studies (Clark 1995, Risch et al. 2013, 2014), and photo-identifications studies (Clapham and Seipt 1991, Read et al. 2003). These studies are at regional scales (line transect) or at home range or species specific range (photo-id) scales and do not adequately capture the fine-scale and/or mesoscale variability within areas of high cetacean diversity and abundance. Collecting and analyzing fine-scale environmental and biological data that captures the variability in the shelf break region adds to our understanding of species distributions over multiple scales within this region by filling the data gap. This information can help forecast animal distributions if and when environmental conditions change, and can help discriminate between changes in marine mammal populations due to natural environmental variability and changes due to anthropogenic impacts.

1.4 Data Collection

Data for my dissertation were collected through the Atlantic Marine Assessment Program for Protected Species (AMAPPS) program. AMAPPS is a research program funded by the Bureau of Ocean Energy Management (BOEM), the U.S. Navy, the National Oceanic and Atmospheric Administration (NOAA) and the U.S. Fish and Wildlife Service (USFWS). NOAA's Northeast National Marine Fisheries Service (NEFSC) and Southeast National Marine Fisheries Service (SEFSC), and the USFWS Division of Migratory Birds have been collecting various data on marine mammals, sea turtles and seabirds since 2009 with the goals of quantifying their abundance and spatial distribution, and producing spatially explicit density distribution maps of these species in the U.S. waters of the western North Atlantic Ocean. AMAPPS data are being used in environmental assessments associated with BOEM and US Navy projects, to update marine mammal stock assessment reports required by the Marine Mammal Protection Act (MMPA), and to support programs that monitor the risk of extinction and recovery of species detected during AMAPPS surveys, including species not already covered under the MMPA (Palka 2012).

There are multiple components to the AMAPPS project including seasonal vessel and aerial surveys and tagging projects. Each component of AMAPPS has attempted to

collect and analyze several data streams in an effort to gain a better understanding of the processes that drive the distribution and abundance top predators. To this point, during the 2013 and 2014 summer ship-based surveys, mechanistic ecosystem studies were a priority once marine mammal survey effort ended for the day (due to survey logistics, mechanistic sampling could not be performed during day-time marine mammal effort). These studies included sampling the physical water column characteristics and sampling the distribution and densities of various fish and plankton trophic levels using conductivity, temperature, depth (CTD) sensors, a video plankton recorder, bongo nets, an Issac Kidd Midwater Trawl, a Multiple Opening/Closing Net Environmental Sensing System (MOCNESS), and active acoustics (Simrad multi-frequency EK60 echosounders). During the 2011 summer survey, trawl and net sampling were not performed, but the other methods of sampling the ecosystem listed were used. It is common for large-scale marine mammal line transect surveys to not collect trawl data because of time constraints. Gear logistics can affect the ability to conduct consistent survey tracks.

Data for these analyses were collected during the summer 2011 AMAPPS research survey on the NOAA ship *Henry B. Bigelow*. The survey was divided into three legs: 2-22 June, 27 June – 15 July, and 20 July – 1 August. The AMAPPS study area included waters south of Cape Cod (about 42° N latitude), north of North Carolina

(about 36° N latitude), east of the southern tip of Nova Scotia (about 64° 30'W longitude), and west of the U.S. coast (about 75° W longitude) (Figure 22a). Teams of scientists collected visual observations of marine mammals, sea turtles, and sea birds, cetacean vocalizations detected by a passive acoustic array, multi-frequency active acoustic data from a scientific echosounder, and hydrographic and plankton data. In total, 24 species or species groups of cetaceans and two turtle species were visually or acoustically detected, and 46 bird species were visually detected. Hydrographic and trophic data were collected from the continuous thermosalinograph (TSG), EK60 scientific echosounder, 21 vertical conductivity-temperature depth (CTD) profiles, 90 double oblique bongo net tows with a CTD, 81 deployments of the visual plankton recorder (VPR) with a CTD, and 44 expendable bathythermograph (XBT) profiles (Palka 2012). The study area was divided into three strata: continental shelf, shelf break, and offshore (Figure 22a).

The AMAPPS data used in my dissertation are: marine mammal sighting data, multi-frequency active acoustic data, continuous flow-through oceanographic data, and temperature profiles from expendable bathythermographs (XBT). All data were collected within the shelf break region (Figure 22b). These data are analyzed to describe the environment within the Mid-Atlantic Bight shelf break and ask questions pertaining

to the fine-scale distribution of marine mammals in relation to the dynamic shelf break region. This dissertation research provides a template to analyze opportunistic environmental information collected throughout the water column from both future and past ship-based surveys and will aid in examining distributions of marine mammal species. Opportunistically collected data are those data collected not directly related to the overall AMAPPS goal of providing spatially explicit marine mammal abundance estimates (e.g. active acoustic data, XBT data, hydrographic data).

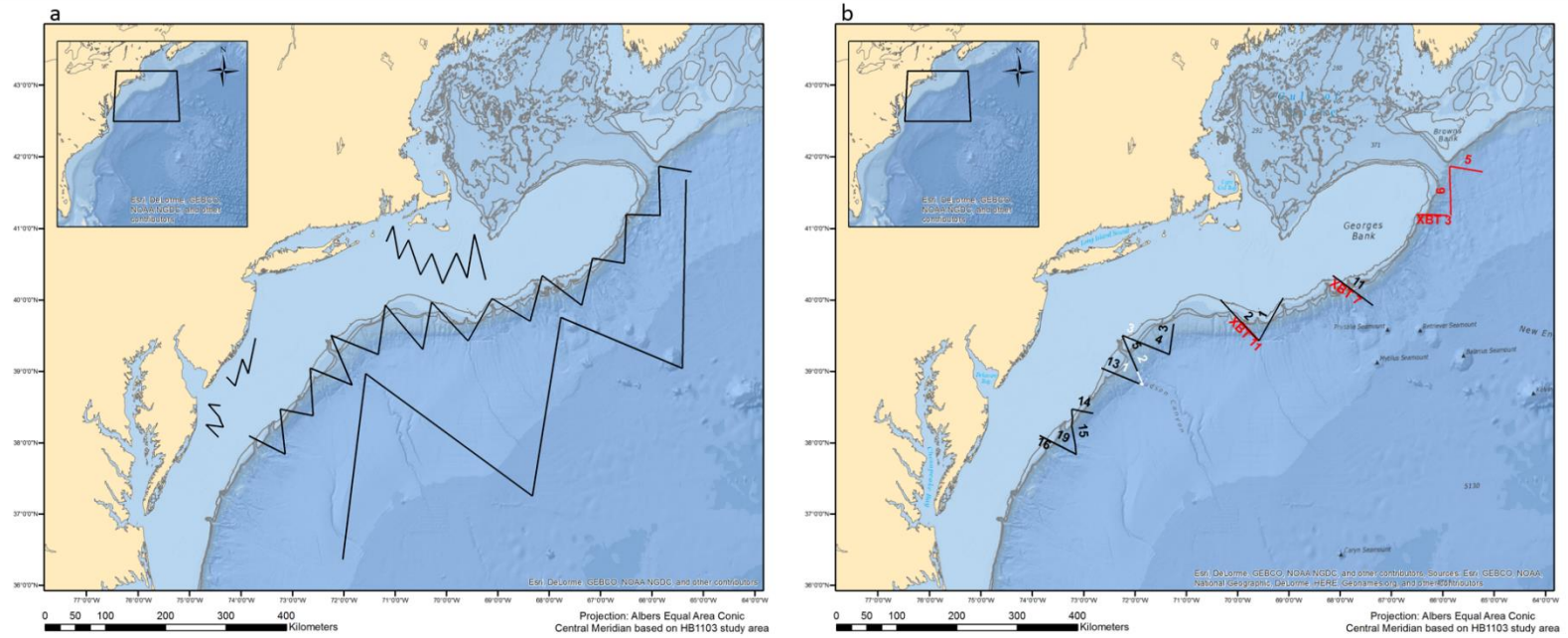


Figure 22: a) Generalized survey tracklines for 2011 summer AMAPPS survey. b) Labeled acoustic transects where cetacean sighting data, thermosalinograph data, and active acoustic data were concurrently collected (data sets not shown). Numbers are transect names. Leg I – black lines. Leg II – white lines. Leg III – red lines. Six transects were partially or completely sampled twice.

1.5 Road Map

In the next chapters of my dissertation I describe methodologies used to categorize multi-frequency active acoustic data into biological proxies and explore the distribution of the biological proxies, uncover significant scales of spatial patterns in acoustic scatterers along two transects, and investigate fine-scale habitat partitioning for three species of cetaceans within the shelf break region. The goal of Chapter 3 was to describe the spatial distribution of acoustic scatterers (fish-like, nekton-like, and plankton-like) within the Mid-Atlantic Bight Shelf Break region. I hypothesize that each of the shelf break regions will contain different counts of categorized acoustic regions because of the physical processes in the region. A further objective is to compare the scales of spatial patterns of fish-like scatterers and nekton-like scatterers along a transect that was sampled twice, with the aim of better understanding the important links between biological and physical processes. The goal of Chapter 4 was to determine habitat preferences for three species of cetaceans in the shelf break region by incorporating environmental and biological data. Sighting data suggested that common dolphins, Risso's dolphins, sperm whales were sighted more often in separate regions of the shelf break system. This is the first known study of fine-scale cetacean habitat and habitat delineation centered on the Mid-Atlantic Bight shelf break region.

2. A Method to Categorize Opportunistically Collected Multi-frequency EK60 data

2.1 Introduction

The development and use of acoustic technologies to remotely detect objects, biological and non-biological, in the marine environment is now commonplace and continues to rapidly evolve. Although references to underwater sound can be traced back to a notebook from 1490 in which Leonardo da Vinci observed that listening at one end of a long tube with the other end in the sea, allowed one to ‘hear ships at a great distance’ (Urick 1983), the first application of acoustics to detect an organism was in 1929 when sound was used to detect the presence of fish in a tank (Kimura 1929, Horne 2000). As ecologists, the goal of using active acoustic technologies is to extract biologically relevant quantities from measurements of backscatter. Since World War II, the use of echosounders has allowed ecologists to locate and visualize the distributions, abundance, and behavior of fish and zooplankton (Simmonds and MacLennan 2005), but the identification of acoustic backscatter to taxa is still considered a great challenge of fisheries and zooplankton acoustics (MacLennan and Holliday 1996, Horne 2000, Jech and Michaels 2006). Utilizing high frequency acoustic scattering techniques provides a

unique remote sensing tool to sample aquatic environments at finer temporal and spatial scales than other sampling techniques. However, two problems emerge when using acoustic data in marine ecology when one cannot compare backscatter data to net trawls or optical sampling: 1) identifying animals present and 2) estimating abundance and size of scatterers.

The traditional approach to species identification has been to combine information from trawls or optical instruments with acoustic measurements, and visually inspect echograms to interpret acoustic backscatter (McClatchie et al. 2000, Jech and Michaels 2006, De Robertis et al. 2010). This approach is useful if one can assume that all backscatter is from a single taxa, there are net-derived length measurements of the animals insonified, and a target strength model exists to both estimate mean target strength and to scale the measurements of volume backscatter for abundance estimation. In areas with single species aggregations, such as the walleye pollock (*Theragra chalcogramma*) fishery in Alaska (Burgos and Horne 2007, von Szalay et al. 2007) and the Atlantic herring (*Clupea harengus*) fishery on Georges Bank (Jech and Michaels 2006), this assumption is met. Multi-frequency acoustic scattering techniques expand the range of conditions in which it is possible to interpret backscatter in terms of biological relevance, such as animal size or abundance (Holliday and Pieper 1995).

In this chapter, I describe the basic physics of marine acoustics to provide background material for marine ecologists, present the techniques developed to preprocess multi-frequency acoustic data, and describe a method to categorize active acoustic data into categorized acoustic regions based on the frequency response curves of fish with swim bladders, euphausiids, and copepods. Additionally, I present a multi-frequency acoustic categorization method that has been used in the Gulf of Maine and Georges Bank (Jech and Michaels 2006) which is based the presence or absence of volume backscatter above a threshold.

2.2 Background: What are Marine Acoustics?

The idea behind active acoustic sampling is simple. Transmitted sound pulses propagate through a homogeneous, lossless medium (water) until they encounter a target that has a different density than the medium (e.g. fish, zooplankton, sea floor, pipes). The target scatters the sound, and some sound energy returns to the transducer (backscatter). The elapsed time between the transmission of the sound and the return echo determines the distance between the target and the transducer. In reality, sound in water is subject to scattering, reflection, and absorption.

Sound is a sequence of pressure waves which propagate through a compressible medium (Figure 23). The top section of the Figure 23 illustrates how pressure varies cyclically as a sine wave. The middle section shows the compression and rarefaction of the particles relative to the sine wave. The bottom section depicts the direction of the wave propagation as wave fronts.

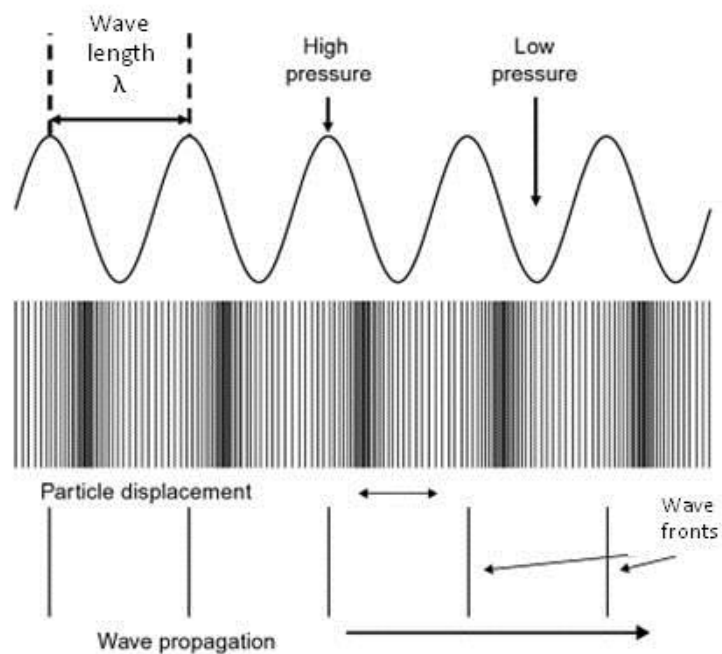


Figure 23: Propagation of a sound wave. From Simmonds and MacLennan (2005).

There are three fundamental parameters of a sound wave: wavelength, frequency, and amplitude. Wavelength (λ) is the distance over which the shape of a

sound wave repeats, measured in units of length (meters). Frequency (f) is the number of wavelengths per unit time, measured in Hertz (Hz = cycles/second). Wavelength and frequency are related by:

$$\lambda = \frac{c}{f}$$

with c = speed of sound (m/s)

Speed of sound in water (c) describes the movement of peak pressures (wave-fronts) and is a function of temperature, salinity and depth with generic units of length/time (meters/second). The speed of sound in the oceans is approximately 1500 m/s. Using this approximation and the relationships among the parameters, we can approximate wavelengths at specific frequencies.

Table 1: Frequencies and wavelengths.

Frequency (kHz)	Wavelength (m)
18	0.083
38	0.039
70	0.021
120	0.013
200	0.008

Amplitude is the degree of change in pressure caused by the sound wave and is directly related to sound intensity. Sound intensity (I) is the amount of energy passing through a unit area per second.

$$I = \frac{p^2}{\rho c}$$

I = intensity	W/m ²
p = pressure	Pa
ρ = water density	kg/m

There are three ways to express pressure amplitude: peak-to-peak, peak, and root-mean-square (RMS). Assume the sine wave in the top section of Figure 23 now has a horizontal axis of time. The absolute pressure $p(t)$ cycles between a pressure minimum (p_{\min}) and a maximum (p_{\max}). Peak-to-peak amplitude is $p_{\max} - p_{\min}$. The peak value is half the peak-to-peak amplitude, $p_{\max} - p_0$ or $p_0 - p_{\min}$. RMS value (p_{rms}) is the square root of the mean of $\{p(t) - p_0\}^2$. Values of peak-to-peak amplitudes are used when describing sounds from marine mammals because of the waves' highly variable shape, but RMS amplitude is the appropriate measure to use when dealing with energy, power (Watts),

or intensity (Watts/m²) expressed in decibels for continuous waves, bursts of waves, or pulses (e.g. from transducers).

Because acoustic impedance is constant within a few percent throughout the path sound travels, it is ignored when looking at the relationship between intensity and pressure. Intensity (I) is proportional to pressure (p) squared, and pressure squared is proportional to power (P).

$$I \propto p^2 \quad p^2 \propto P$$

The intensity of the sound wave decreases as it moves through the water column because the total energy of the transmission is fixed but the wave-fronts spread over area as they travel (beam spreading). Intensity varies with range (R) according to the inverse-square law:

$$I = \frac{I_0}{R^2}$$

I_0 = Initial intensity

The decibel (dB) is a logarithmic unit used to describe a ratio relative to a reference unit. Acoustic measurements are usually given in decibels rather than in units

of power, pressure, or intensity because the values involved can be very large, very small, or cover orders of magnitude. Power or intensity ratios are expressed in decibels as

$$I_{dB} = 10\log\left(\frac{I}{I_0}\right) \quad P_{dB} = 10\log\left(\frac{P}{P_0}\right)$$

where I_0 and P_0 are reference intensity and power respectively at 1 meter.

Pressure is converted to decibels as

$$p_{dB} = 20\log\left(\frac{p}{p_0}\right)$$

where p_0 is the reference pressure at 1 meter.

Echosounders transmit sound waves in pulses, usually called pings. Each ping is generated from multiple cycles at the transducer's frequency. The pulse duration (time from start to finish) is τ . For example, if 19 cycles were generated by a 38 kHz transducer, $\tau = (19 \text{ cycles}/38,000 \text{ cycles per second}) = 0.0005 \text{ seconds (or 0.5 ms)}$. The pulse length (L_p) is equal to the speed of sound (c) * τ .

$$L_p = c\tau$$

The distance (R) between the transducer and a target is measured by the time (t_e) it takes for a pulse to travel through the water column and the echo to return from the target. The two-way path is 2R:

$$R = \frac{ct_e}{2}$$

or

$$t_e = \frac{2R}{c}$$

In order to individually measure the echoes from two targets, the distance between them must be large enough that the two echoes do not overlap. This is target resolution. Therefore, to resolve the two targets,

$$R_2 - R_1 > \frac{c\tau}{2}$$

Acoustic energy is lost as sound waves travel through the water column and energy is converted to heat through the process of absorption. One mechanism that

contributes to absorption is friction. The amount of absorption due to friction is proportional to the square of the frequency. Higher frequencies involve greater velocities and thus higher frictional losses. The absorption coefficient, α , is the energy loss in decibels per unit distance and is estimated at a given frequency, temperature, salinity and depth. Because absorption increases rapidly with frequency, it is the limiting factor in determining the highest useful frequency for target detections at a given range.

Acoustic scattering occurs when a sound wave encounters a target and some of the energy is scattered creating a second sound wave that propagates away from the target. Reflection is a type of scattering in which the angle of incidence is equal to the angle of reflection. Scattering occurs because of a spatial change in acoustic impedance (Z), which is the product of the speed of sound and the density of the water.

$$Z = \rho c$$

Therefore, if a sound wave encounters an object with a different density than the surrounding water, the wave will be scattered. Any object that has a density close to the density of the water is difficult to detect with sound.

The target strength, a measurement of an individual target's acoustic reflectivity, is defined by the ratio of the intensity of the reflected sound at 1 meter from the target (I_2) to the intensity of the incident sound (I_1).

$$TS = 10\log\left(\frac{I_2}{I_1}\right)$$

An individual's target strength is related to its backscattering coefficient, σ_{bs} , which is measured in units of area and defined in terms of the intensities of the incident and backscatter waves by:

$$\sigma_{bs} = R^2 \frac{I_{bs}}{I_i}$$

$$\sigma_{bs} = \text{square meters}$$

where R is the distance from the target to where the intensity is measured, I_{bs} is the intensity of the backscatter and I_i is the intensity of the incident wave. Through the inverse-square law of energy, $R^2 I_{bs}$ is the same at any distance resulting in σ_{bs} being constant. Target strength is the decibel form of the backscattering coefficient:

$$TS = 10\log(\sigma_{bs})$$

$$\sigma_{bs} = 10^{\left(\frac{TS}{10}\right)}$$

When individual targets are very small or when there are enough in a sampled volume that their echoes combine to form a received signal, the received echo intensity is a measure of biomass in the water column. s_v is the volume backscatter coefficient obtained from integrating the acoustic returns:

$$s_v = \frac{\sum \sigma_{bs}}{V_0} [\text{m}^2 \text{m}^{-3}]$$

where V_0 is sampled volume and $\sum \sigma_{bs}$ is the sum of all the discrete backscattering cross-sections. The logarithmic equivalent of this is:

$$S_v = 10 \log(s_v)$$

units: dB re 1 m⁻¹

Mean volume backscattering strength (S_v) is the average of several pings of s_v over a volume larger than V_0 , and is common in studies of plankton and fish.

The signal received by the transducer includes backscatter from targets as well as noise from the water column. Noise is any unwanted signal independent of the transducer's transmission and can be classified as biological (animal sounds), physical (wind and waves), and artificial (propeller and other ship noises including other active acoustic systems on ships). The signal-to-noise ratio (SNR) is one way to measure the performance of an echo sounder.

$$\text{SNR} = \frac{\text{signal}}{\text{noise}}$$

In situations with high SNRs, thresholds can be set to exclude background noise and retain information on strong acoustic scatterers. When scatterers are weak or further away, the SNR is lower.

A backscatter signal decreases with time because of beam spreading and absorption. To compensate for beam spreading and absorption, the received signal is multiplied by a time-varied gain (TVG) function. The TVG removes range dependence (range is dependent on frequency and signal absorption is greater with increased frequency) but also amplifies noise in the received signal.

All of the components of acoustic theory presented pertain to sound in the far field (Fraunhofer zone). In the far field, wave-fronts are parallel, allowing the properties of the inverse square law to hold. In the near field (Fresnel zone), wave-fronts are not parallel and intensity varies with distance in an oscillatory manner. Distance to the far field (r) is frequency dependent through wavelength:

$$r = \frac{D^2}{\lambda}$$

where D is the diameter (m) of the active elements within the transducer.

Transducer calibrations are preformed to determine the combined transmit and received sensitivity of the transducer along the acoustic axis (direction in which the transmitted energy is greatest). The preferred calibration method is the 'standard target' method developed by Foote et al. (1987) in which a reference target (calibration sphere) with known scattering properties is placed below the transducer and the echosounder is operated at the same power level, time-varied gain, and pulse length as would be used during a survey. The optimum position of the calibration sphere is in the far field and estimated to be:

$$R_{\text{opt}} = \frac{2d^2f}{c} \quad \text{or} \quad R_{\text{opt}} = \frac{2d^2}{\lambda}$$

where d is the greatest width of the transducer face or the linear distance of the transducer face and f is frequency.

2.3 Acoustic Data Collection

Data were collected during the Northeast Fisheries Science Center's 2011 summer Atlantic Marine Assessment Program for Protected Marine Species (AMAPPS) on the NOAA ship *Henry B. Bigelow*. This was a dedicated marine mammal line transect abundance survey that consisted of systematic zig-zag transects in the Mid-Atlantic Bight over the continental shelf, the Mid-Atlantic Bight shelf break, and the offshore waters of the northeast U.S. Exclusive Economic Zone. Further details of the survey procedures can be found in the survey report (Palka 2012). Acoustic backscatter data were collected from the ship's Simrad EK60 scientific echosounder system with 5 split-beam transducers operating at 18, 38, 70, 120, and 200 kHz; the transducers are co-located on the ship's retractable centerboard. The beam widths are 7° for all transducers except the 18 kHz transducer, which has a beam width of 11° . When the centerboard is flush with the hull, the transducers are six meters below the waterline and when the

centerboard is in its intermediate position, the transducers are nine meters below the waterline. The ship's centerboard was not extended during the collection of data used in this research, therefore all transducers were six meters below the surface. Each frequency was transmitted simultaneously at a rate of one ping every two seconds when the vessel was in waters depths less than 1000 meters, and one ping every five seconds when the vessel was in water depths greater than 1000 meters. Pulse duration for each frequency was 1.024 ms. The ship's survey speed was 5.14 m/s (10 kts). Raw acoustic data were collected at 0.19 m vertical resolution (samples), and at approximately 10 m (ping every two seconds) and 25 m (ping every five seconds) horizontal resolution during survey effort. All five transducers in the EK60 system were successfully calibrated prior to the survey using the standard target method (Foote et al. 1987). Acoustic data were collected during nighttime hydrographic operations and every other day that mammal observers were on-effort. The purpose of only recording EK60 data every other day was to investigate the effects, if any, of active acoustic data collection on the encounter rates and reactions of marine mammals. That analysis is being conducted by NOAA scientists at the Northeast Fisheries Science Center and is not part of this dissertation.

2.4 Acoustic Data Processing

I initially processed all acoustic data in Echoview 6.1 (Myriax 2013) through the manual and automated inspection of volumetric backscatter (S_v) echograms. Discrete acoustic interference (noise spikes) and background noise amplified through time-varied gains at all five frequencies were removed by custom algorithms I built in Echoview (sections 2.4.1 and 2.4.2). Acoustic data from 0 to 10 meters of the water column were eliminated to remove noise from ping transmissions and cavitation. Acoustic returns from the seafloor and below the sea floor were also removed with an algorithm I specifically developed to deal with the steep topography of the shelf break region (section 2.4.3). Once noise spikes, background noise and the bottom/below bottom data were removed, each frequency was resampled to 1 meter vertical resolution and matched per ping. All acoustic analyses were performed on volume backscatter (S_v) data.

2.4.1 Removal of Intermittent Acoustic Interference

Before background noise can be removed from echograms, intermittent acoustic interference has to be removed from the raw data. Intermittent acoustic interference is usually the result of cross-talk from other instruments in operation on the ship. The

intermittent nature of the acoustic interference results in a sudden increase in S_v over all or some of the samples in a ping, and is referred to as noise spikes. During the 2011 AMAPPS survey, the ship's acoustic depth sounder and Acoustic Doppler Current Profiler (ADCP) were synchronized to the EK60 system; however these two systems still created unwanted noise spikes in the EK60 data at the 120 and 200 kHz frequencies.

To remove the noise spikes in the 120 and 200 kHz data, all samples of each ping were subtracted from samples of the ping directly before and directly after it. Samples where the S_v difference was greater than 12 dB were identified as spikes and removed from the echogram. Because S_v data are autocorrelated at the scale of the ping, the noise spikes were replaced with the mean of six good sample points on either side of the removed sample (Figure 24). This process for removing intermittent acoustic interference is robust for single spikes of noise, but will perform poorly when there are noise spikes over multiple adjacent pings. These data contained only single ping noise spikes.

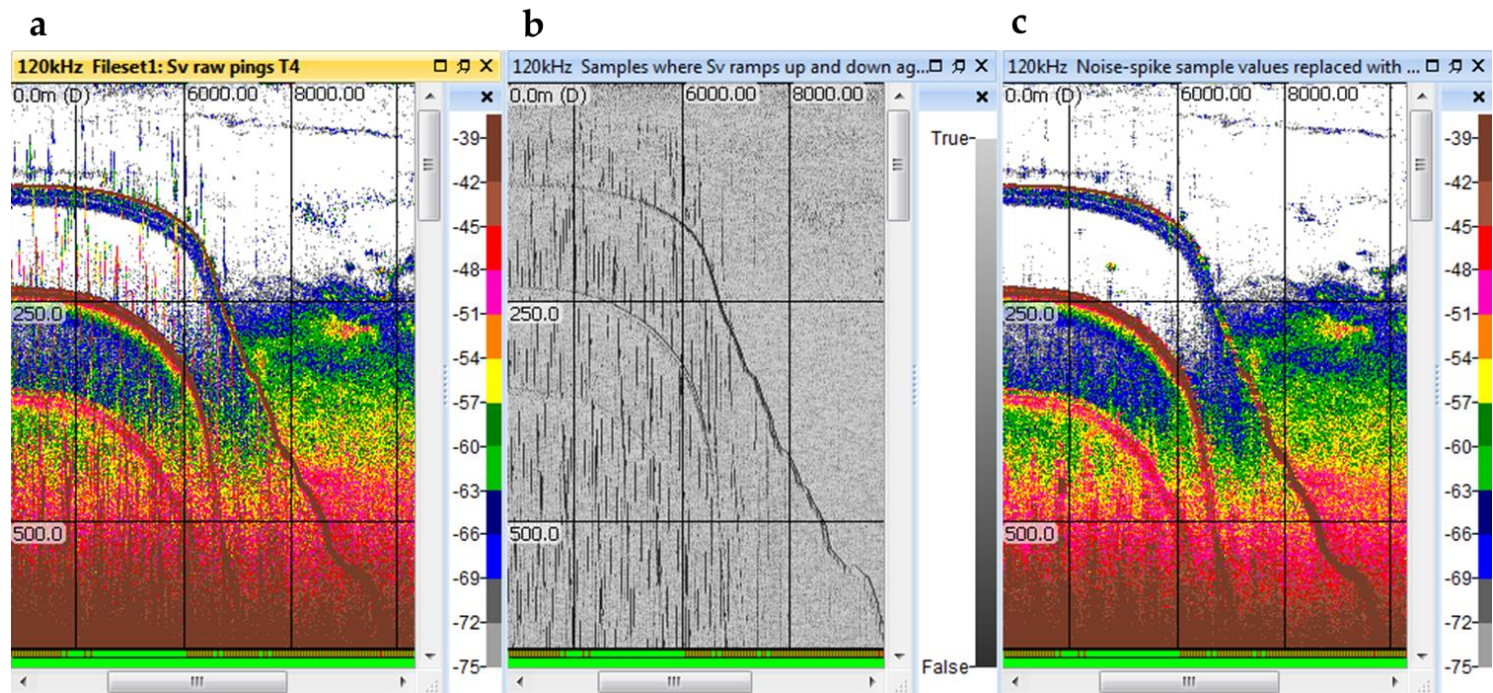


Figure 24: Echograms depicting intermittent noise and removal. The y-axis is depth in meters. The x-axis is time with vertical lines every 2000 meters the ship traveled. In panels a and c, color is S_v in dB. a - Vertical noise spikes in 120 kHz echogram. b - Noise spikes marked and removed. c - Data from adjacent samples averaged to fill areas where noise spikes were removed.

2.4.2 Background Noise Removal

Background noise in acoustic data can limit the range to which acoustic backscatter can be accurately measured. Background noise is any part of the received signal that is not from the returning backscatter (Simmonds and MacLennan 2005). Using this definition, background noise is defined as any signal measured when the transducer is disabled and the receiver enabled, and commonly includes rain, wind and animals (Urick 1983, Simmonds and MacLennan 2005). Background noise levels can change rapidly with changes in environmental conditions, vessel speed, bottom substrate and water depth (Urick 1983, Korneliussen 2000).

Backscatter signals decrease with time due to transmission loss (spherical spreading and absorption), which is frequency dependent. Higher frequencies travel at greater velocities, resulting in greater transmission loss due to friction. However, background noise remains constant over a ping. As previously stated, to compensate for absorption and spherical spreading of the signal, the received signal is multiplied by a time-varied gain (TVG) function (MacLennan 1986). The TVG function removes the range dependence in volume backscattering but at large ranges measurements of acoustic backscatter will be dominated by noise amplified by the TVG function and result in a low signal-to-noise ratio.

One method to estimate background noise is based on the assumption that noise is independent of a transmitted ping. With the transducer disabled, the echo sounder records all other received signals. Those signals are assumed to be representative of the background noise and are used to estimate and remove the noise (Takao and Furusawa 1995).

A second method, developed by De Robertis and Higginbottom (2007), estimates background noise level and signal-to-noise ratios during active pinging. This method assumes that some portion of the returned acoustic signal is dominated by background noise. For this analysis, data collected below the sea floor is completely composed of noise and the information in those portions of the ping are used to subtract the TVG-amplified background noise out of the biologically relevant data. To determine the portion of the ping that is noise, acoustic data from the water column and acoustic data from below the sea floor were separated and independently smoothed with a 3x3 window to decrease the variance in the data. After smoothing noise (below bottom) and signal (above bottom) separately and recombining them, TVG-amplified noise in the shelf break echograms from all five frequencies were calculated per ping and removed based on the sensitivity of the signal-to-noise ratio (Figure 25). S_v data over all frequencies were averaged over 20 pings horizontally and 10 meters vertically. From visual inspection of the echograms (compare Figure 26 and Figure 27), these spatial

parameters provided the best averaging to reduce noise and keep as much biological backscatter as possible when testing various signal-to-noise ratios.

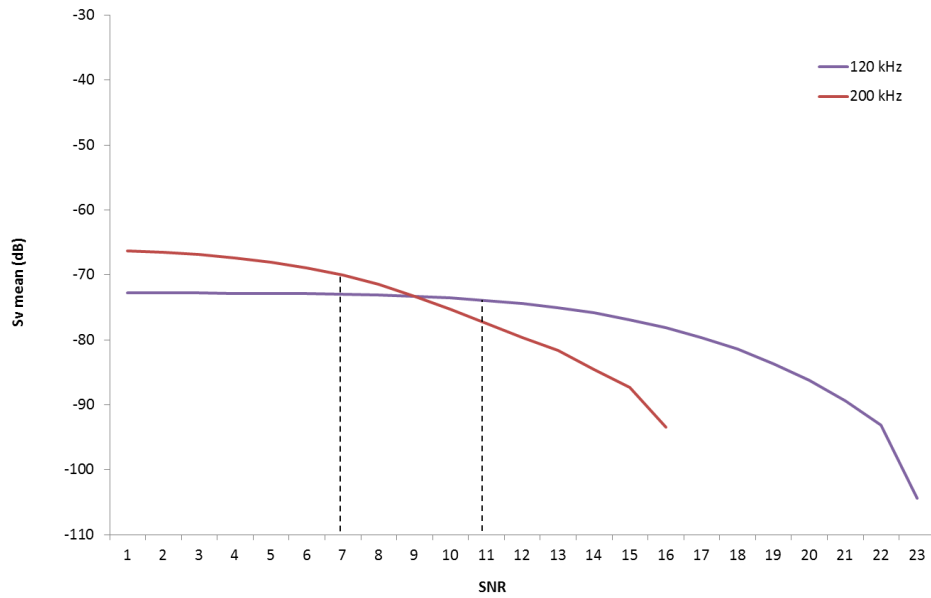


Figure 25: Sensitivity of S_v in deep water (350 – 400 m) to signal-to-noise ratios for 120 and 200 kHz frequencies.

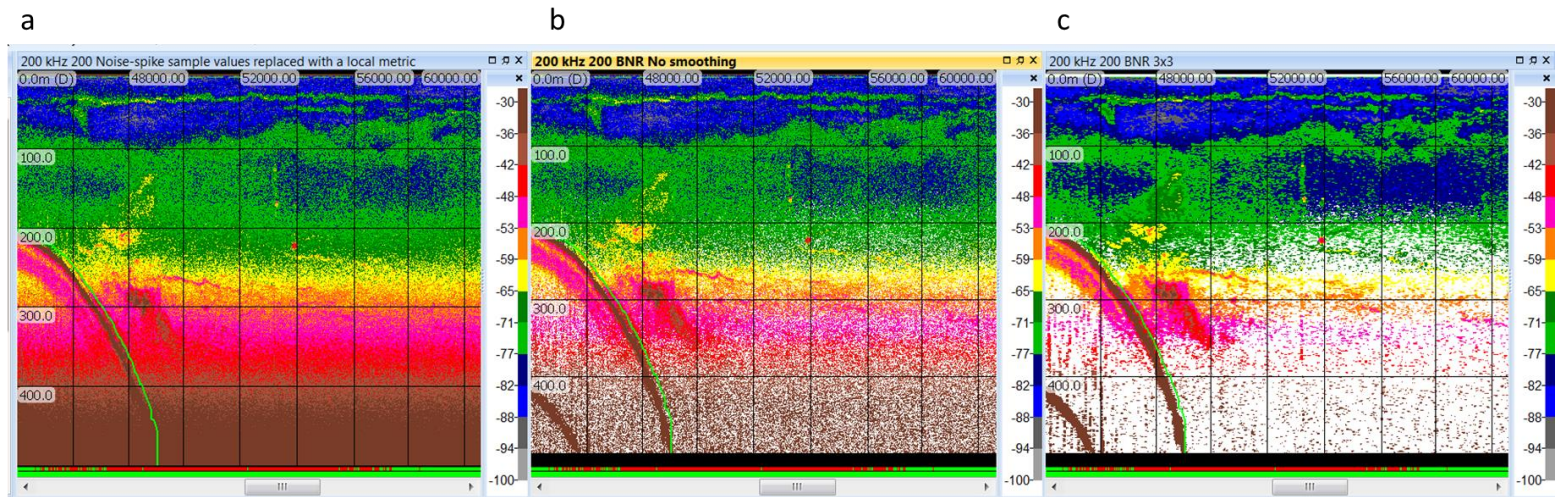


Figure 26: The effect of smoothing backscatter data when removing background noise. a) Raw data at 200 kHz. The TVG-noise ramp is between 250 and 500 meters. b) Noise-reduced echogram from unsmoothed data. c) Noise-reduced echogram from 3x3 cell averaged data above and below the bottom.

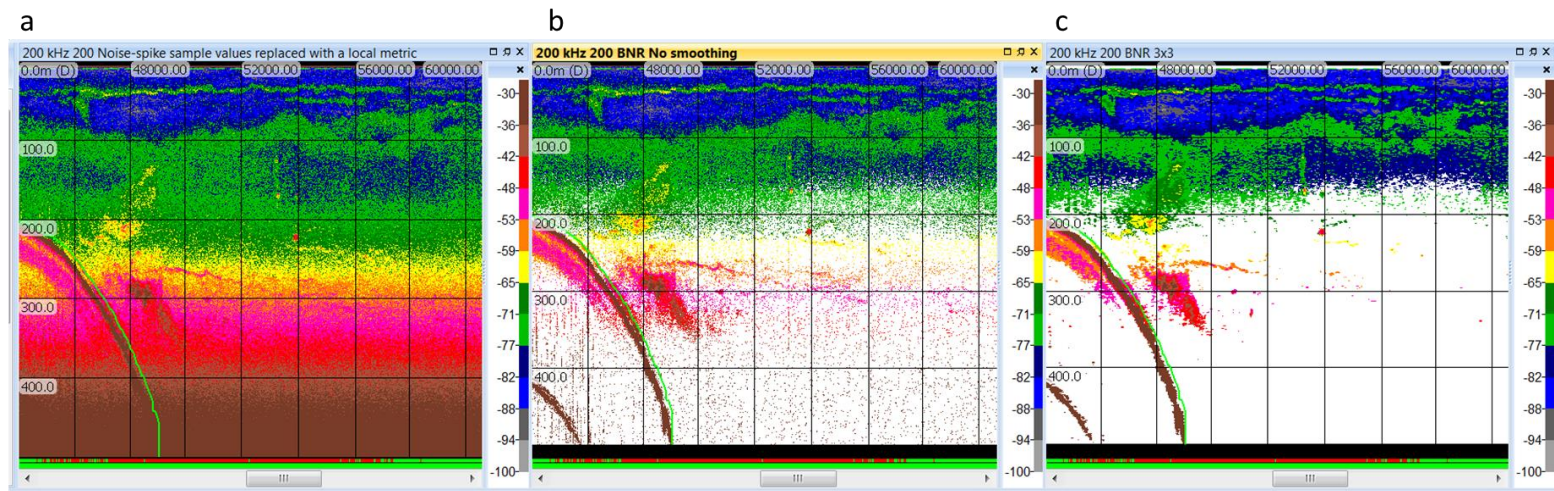


Figure 27: The effect of setting a minimum signal-to-noise ratio. a) Raw data at 200 kHz. The TVG-noise ramp is between 250 and 500 meters. b) Noise-reduced echogram from unsmoothed data and a minimum signal-to-noise ratio of 7. c) Noise-reduced echogram from 3x3 cell averaged data above and below the bottom and a signal-to-noise ratio of 7.

2.4.3 Semi-automated Bottom Detection in a Steep Topography

When the sea floor is within the operating range of an echosounder, it usually returns the most intense backscatter. This makes detecting the sea floor in echograms simple, except in areas of dynamic topography. Over steep bottom topography, such as the shelf break and seamounts, shadow zones are produced when the side lobes of the acoustic beam reverberate off the side of the topography (Kloser 1996). In the shadow zone it is difficult to differentiate between biological backscatter and the bottom signal.

For the AMAPPS survey I was not concerned with differentiating biological scatterers directly above the sea floor and chose to remove the sea floor, below the sea floor, and the shadow zone to increase processing speed. To determine the position of the sea floor I created a virtual bottom line and subtracted two meters from it to remove the shadow zone of the steep topography. The virtual bottom line was created by examining each ping from the 18 kHz transducer from 10 m to 3000 m (maximum depth of data collection) after smoothing with a 7x7 window to reduce ping-to-ping variability. The top 10 m of the water column were removed because of transducer interference and cavitation. For each ping, the sample (vertical position along the ping) with the maximum S_v was determined. The algorithm then searched up the ping to the first sample detected below a discrimination level set at -40 dB. A lower discrimination level

would select areas of the water column along shelf regions as the virtual bottom line and a greater discrimination value would not remove all the sea floor in areas of steep topography. The depth of the sea floor for that ping was set by vertically back stepping three meters from the position at the discrimination level. The bottom line was then drawn two meters above the virtual line, resulting in a bottom depth five meters above the depth of maximum S_v per ping. All echograms were manually inspected and the bottom line was corrected if there was an obvious error in the bottom detection (e.g. bubbles near the surface louder than the bottom).

2.5 Categorizing Acoustic Scattering Regions from Frequency Response Curves and Thresholding

A basic assumption in fisheries and zooplankton acoustics is that the backscatter from all animals in the insonified volume sum incoherently, and that the measured backscatter at a given frequency is the sum of the backscattering cross-section of each animal summed over all animals. If aggregations of animals in a region are monospecific and similar in size, then theoretical backscatter models can be used to estimate their distribution and abundance (Hewitt and Demer 2000). If backscatter is collected from more than one frequency then the range of conditions in which it is possible to interpret backscatter in terms of biological relevance, such as animal size or abundance, increases

(Holliday and Pieper 1995, Warren et al. 2003, Lawson et al. 2006). The rationale behind this idea is that backscatter varies with frequency (Figure 28).

Fish scatter sound with greater intensity at lower frequencies (here 18 kHz and 38 kHz) and euphausiids and copepods scatter sound with greater intensity at higher frequencies (120 kHz and 200 kHz). Although fish with swim bladders are in the geometric scattering range (intensity of backscatter changes little with changes in frequency) at 18 kHz, the frequency response is still that of a negative slope (Warren et al. 2003). In contrast, euphausiids and copepods are in the Rayleigh or resonant regions, where backscatter varies significantly with frequency, and they have a frequency response of a positive slope (Warren et al. 2003, Lavery et al. 2007) (Figure 28). The difference between the shape of the frequency response curves of copepods and euphausiids is the “rolling off” or transition point between 120 kHz and 200 kHz. The slope of the euphausiid frequency response curve changes, going towards 0, while the copepod frequency response curve stays constant (Figure 28).

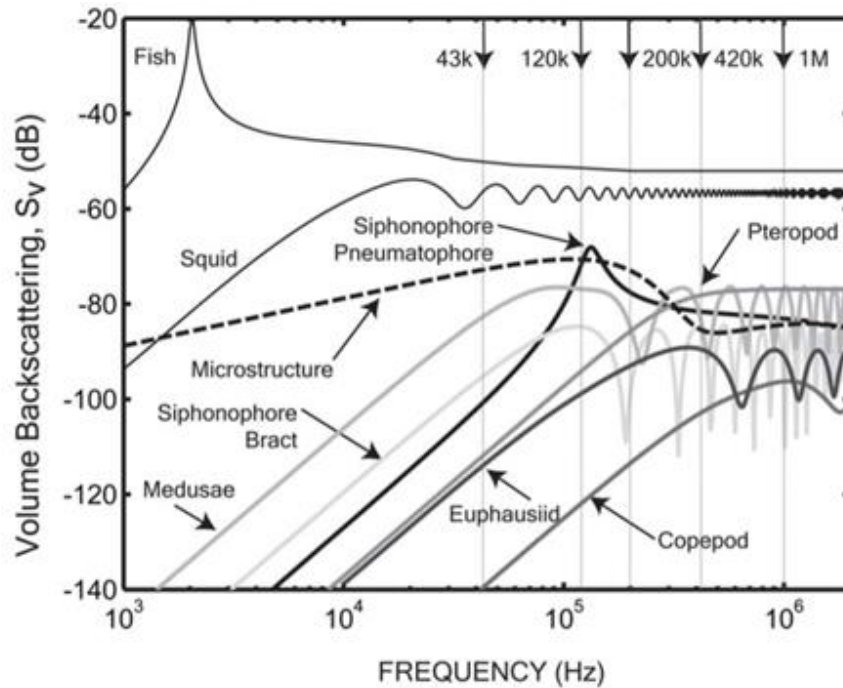


Figure 28: Volume backscatter as a function of frequency for major biological taxa assuming a numerical abundance of 1 organism/m³. From Lavery et al. 2007.

To select acoustic regions of interest for analysis, I visually scanned the 18 kHz and 200 kHz processed echograms of each transect in Echoview and selected regions of greatest intensity in both frequencies. Both frequencies were set to the same S_v scale to compare backscatter intensity between them. To verify the general shape of the frequency response curves in the selected regions I calculated slope of the frequency response per pixel over the entire echogram and calculated the average slope within the selected regions to compare to the slopes of known frequency response curves for several taxa (Figure 29). I was conservative when defining regions to categorize, only

selecting those regions with the most intense scattering in the 18 kHz and 200 kHz echograms.

The S_v of selected acoustic regions were then integrated and exported to MATLAB where the shape of each frequency response curve for the entire region was compared to the theoretical backscatter model of its taxa (Figure 30). Because concurrent net trawls were not conducted during the 2011 summer survey, size and length model parameters for fish, euphausiids, and copepods were determined from expert opinion and a literature search. Although fish with swim bladders usually create louder backscatter at lower frequencies due to the acoustic impedance of air bubbles (the swim bladder), a fish's body also contributes to backscatter (Jech and Horne 2002, Lee 2013). For the fish scattering model, I used a model that combined scattering properties from the swim bladder and the fish's body (Lee 2013). To model myctophid target strength, I chose a mean length of 70 mm because it is generally accepted that the length range for mature myctophids in the Mid-Atlantic Bight is 20 to 300 mm with *Benthosema glaciale* being one of the larger (50-107 mm) and most abundant species (Backus et al. 1968, Badcock and Merrett 1976, Mike Lowe WHOI personal communication 2014). To produce target strength curves for copepods and euphausiids, I used the distorted-wave Born approximation (DWBA) model (Stanton et al. 1998a, 1998b, Stanton and Chu 2000). Euphausiids were modeled as uniformity bent cylinders (Lawson et al. 2006) averaged

over a distribution of angles, and copepods were modeled as prolate spheroids averaged over a distribution of angles (Lavery et al. 2007). Because the categorizations of acoustic backscatter regions could not be verified with visual or trawl data, I conservatively labeled regions that matched euphausiid frequency response curves as “nekton-like”, regions that matched copepod frequency response curves as “plankton-like”, and regions that matched myctophid or herring frequency response curves as “fish-like”.

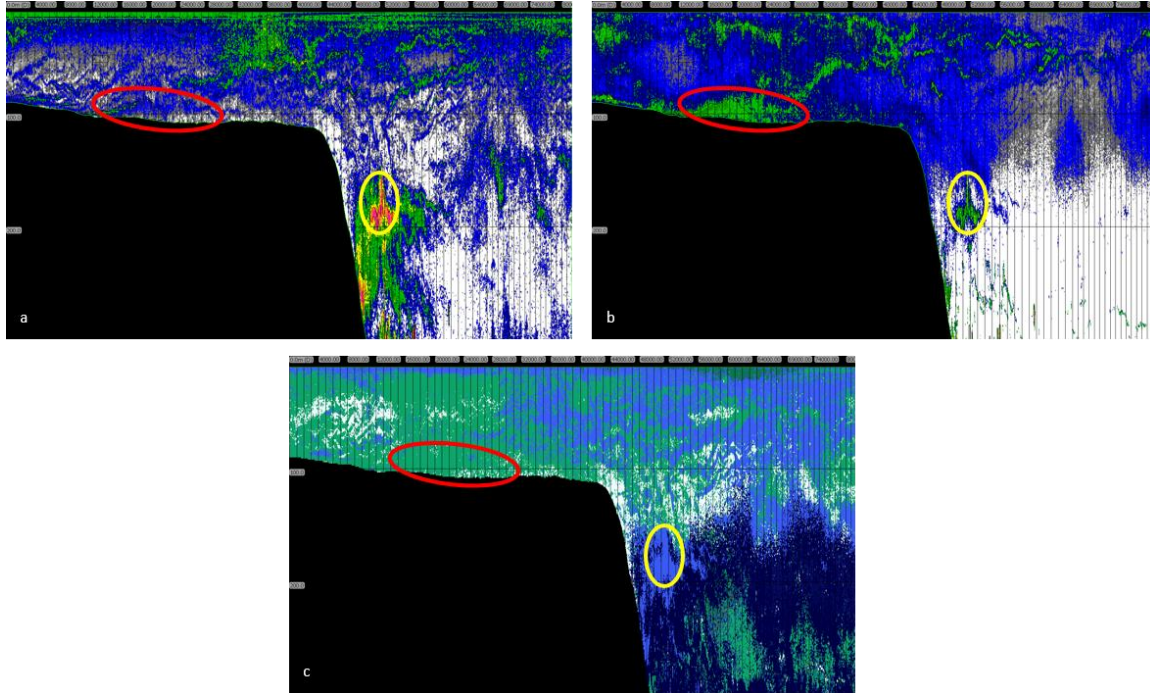


Figure 29: a) 18 kHz and b) 200 kHz example echograms used to calculate the slope of the frequency response (c) over five frequencies. In c, positive slopes (greens) indicate areas with a frequency response curve similar in shape to copepods and euphausiids (red ovals). Negative slope (blues), indicate areas with a frequency response curve similar in shape to fish with swim bladders (yellow ovals).

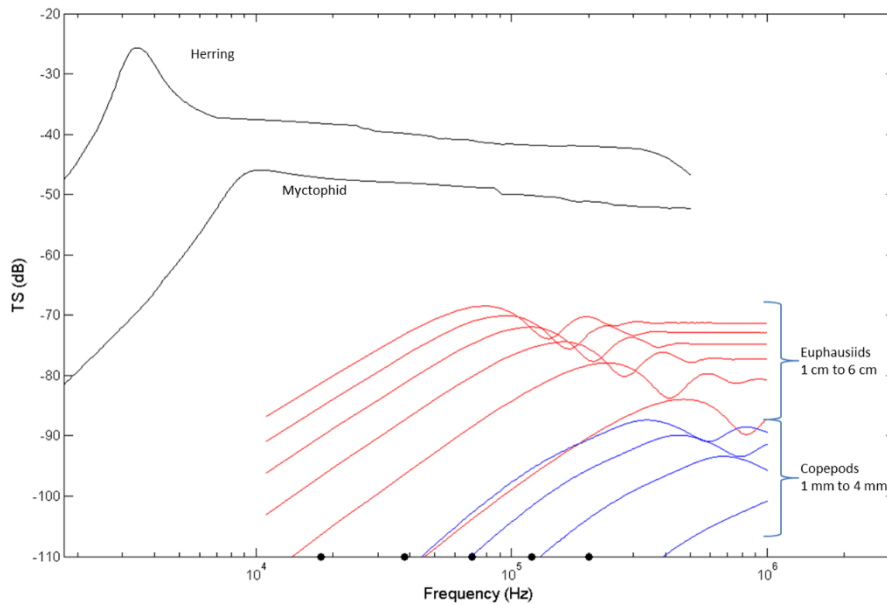


Figure 30: Theoretical target strength scattering models of two types of fish, herring and myctophids (black), theoretical scattering curves of euphausiids from 1 to 6 cm (red), and copepods from 1 mm to 4 mm (blue). Dots along the x-axis indicate 18, 38, 70, 120 and 200 kHz.

The key parameter used to determine the fit of the frequency response curve of a selected region to the modeled target strength was the position of the sharp transition point from the Rayleigh-scattering regime to the geometric-scattering regime. For scattering models of marine organisms, the size (or length) of the animal controls the location of the transition point. If multiple animals of the same size are within a given volume, then the modeled scattering curve for that volume will shift upward, predicting higher decibel levels, but the location of the transition point will not change. In Figure 31, the 18 and 200 kHz echograms from a transect that crossed the shelf break near

Hudson Canyon are given. Ovals indicate general areas of scattering that were categorized as fish-like (magenta ovals), nekton-like (black ovals), and plankton-like (blue ovals).

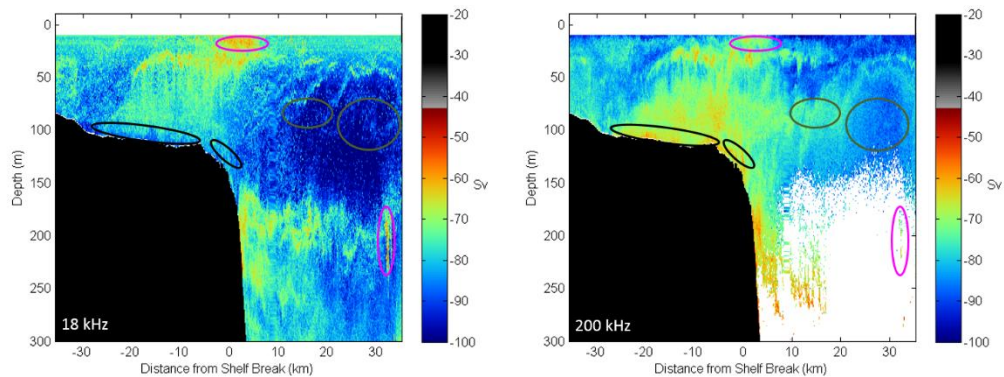


Figure 31: 18 kHz (left) and 200 kHz (right) (S_v) from a shelf break transect near Hudson Canyon. Ovals indicate areas selected to categorize backscatter. Magenta ovals were fish-like scattering. Black ovals were nekton-like scattering. Dark green ovals were plankton-like scattering. See figure 29 for comparison of frequency response curves.

Figure 32 shows the comparison between the frequency response of the selected regions and the theoretical scattering curves. For each selected region, the general shape of the curve matches the theoretical scattering curve, however, as mentioned previously, the transition point is shifted upwards for nekton-like and plankton-like scatterers. The transition point is shifted downwards for fish-like scatterers, most likely because the density of fish-like scatterers was less than predicted in the volume insonified.

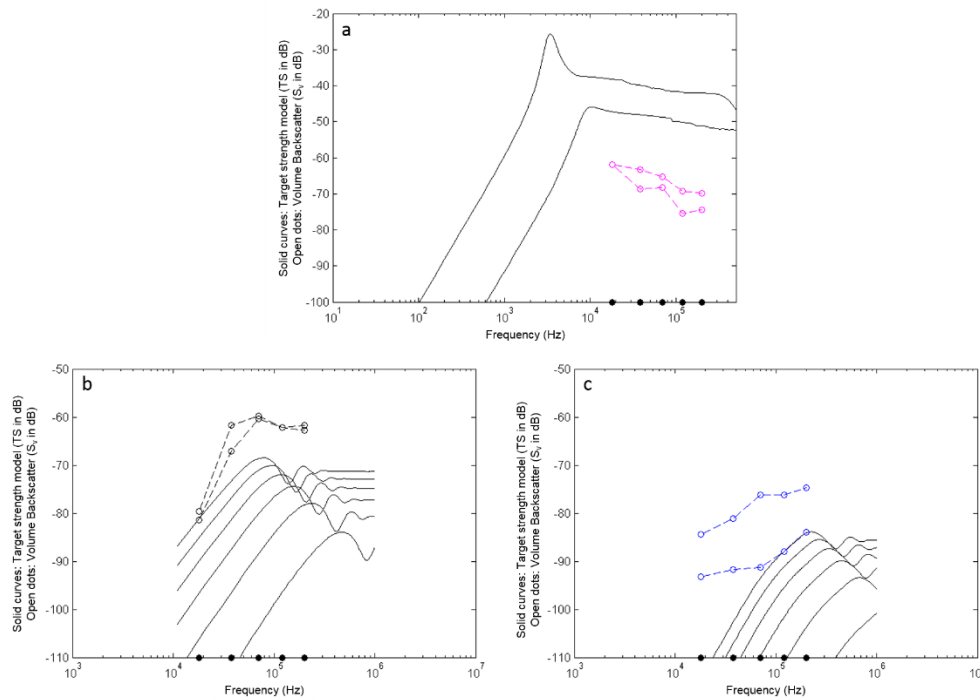


Figure 32: Comparison of frequency response curves from selected acoustic regions of interest to models of target strength by taxa. Selected regions are shown in figure 12. a) Herring and myctophid scattering models and two regions of fish-like scattering. b) Euphausiid scattering models for animals from 1 cm to 6 cm and two regions of nekton-like scattering. c) Copepod scattering models for organisms from 1 mm to 6 mm and two regions of plankton-like scattering regions. The dots along the x-axis indicate 18, 38, 70, 120 and 200 kHz.

Comparing the shape of the frequency response curves is an adequate starting point when categorizing the biological nature of multi-frequency acoustic scattering, but this technique is highly subjective when determining the edges of scattering regions. If areas adjacent to the selected region are included but do not contain scattering from a taxa of interest, the shape of the frequency response curve for the entire region might

change and the region not be selected. More objective classification techniques have been produced. One such method sets a volume backscatter threshold applied equivalently to all echograms and then a composite echogram is created based on which frequencies had volume backscatter greater than the threshold (Jech and Michaels 2006).

To categorize acoustic scattering regions using the Jech and Michaels (2006) method, volume backscatter for each frequency was averaged to a vertical resolution of 1 meter and smoothed with a 5x5 convolution kernel. Averaging and smoothing reduced pixilation in the data and decreased the variance of the backscatter. A threshold of -66 dB was applied to the 18, 38 and 120 kHz echograms which were the only echograms used in this classification scheme. I applied the -66 dB threshold used in Jech and Michaels (2006) to classify Atlantic herring because their study area encompassed the northern edge of Georges Bank and the Gulf of Maine, geographic areas adjacent to the Mid-Atlantic Bight where species overlap is likely. Figure 33 shows 18, 38, and 120 kHz data from the same daytime transect near Hudson Canyon as in Figure 31 after resampling and smoothing with the convolution filter.

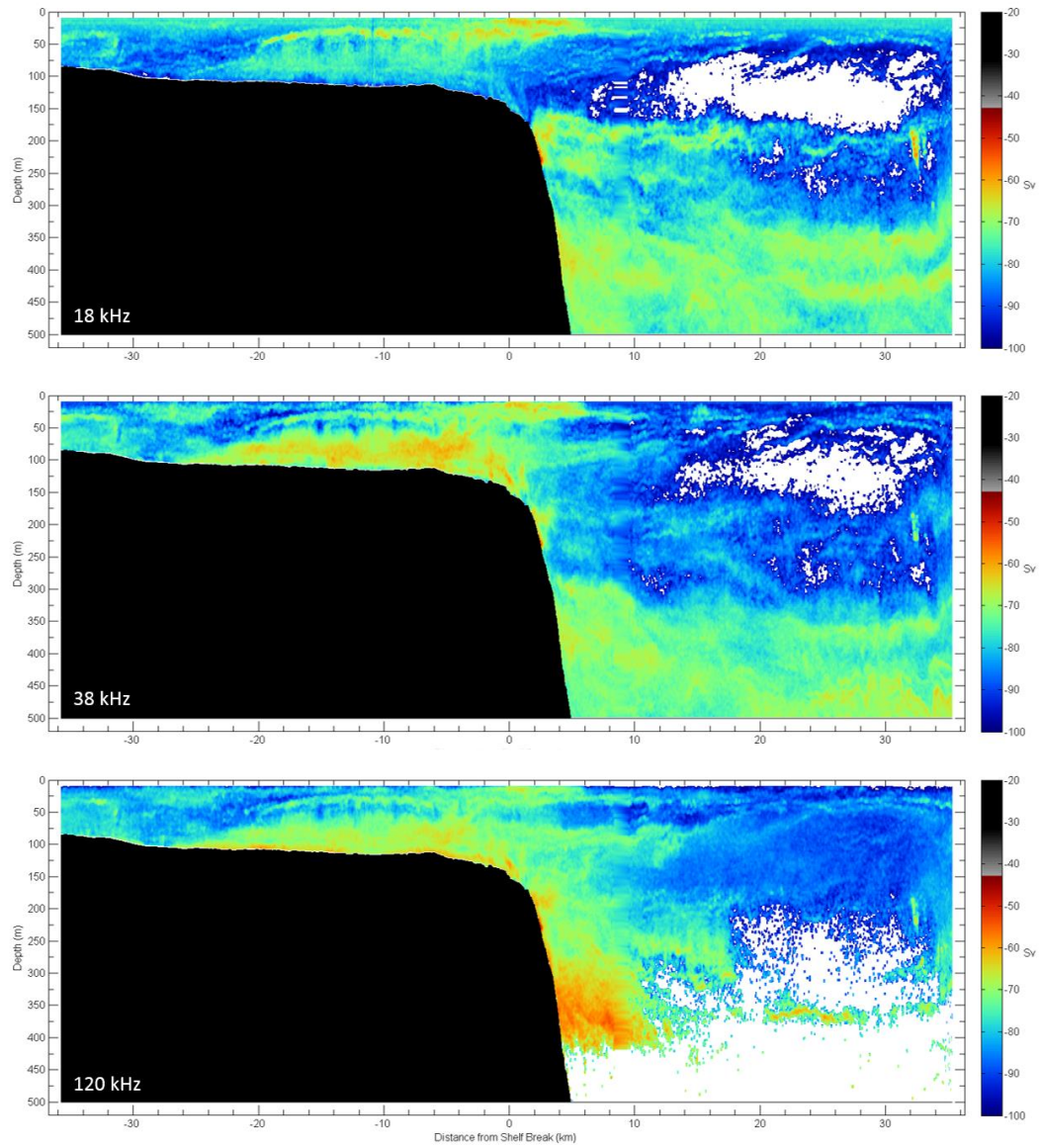


Figure 33: Resampled and smoothed echograms at 18, 38, and 120 kHz for the shelf break transect near Hudson Canyon. Backscatter is S_v . White areas are where background noise was removed (no data).

After the threshold was applied, I coded each cell in the echogram based on the presence or absence of the frequency and combined them into composite echograms. The number of presence or absent frequency combinations can be calculated with Pascal's triangle, resulting in eight possible outcomes from three frequencies: ---, 1--, 12-, 123, 1-3, -2-, -23, and --3, where "1", "2", "3", or "--" indicates the presence of 18, 38, or 120 kHz S_v values respectively, and "--" indicates the absence of a frequency. The composite echograms provide a color-coded version of the classification (Figure 34). Areas where all three frequencies are above the threshold are hypothesized to be Atlantic herring (Jech and Michaels 2006). Areas where the 120 kHz is above the threshold are assumed to be euphausiids, and areas where both the 38 kHz and 120 kHz dominate the backscatter are assumed to be euphausiids or shrimp. Because I did not use information from the 200 kHz echosounder in this classification scheme, small plankton-like scattering (e.g. copepods) were not included. Although this classification method still relies on contemporaneous ground-truthed data to identify species from acoustic scattering, this method was developed from ground-truthed data from 1999 to 2004 in an adjacent geographic area. This methodology also provides insights into the acoustic seascape by highlighting spatial distributions of backscatter patterns.

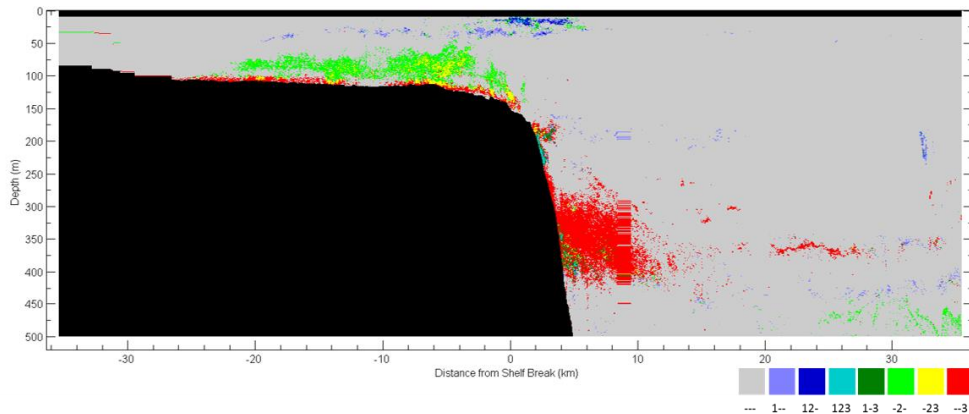


Figure 34: Composite echogram of 18, 38, and 120 kHz data for the shelf break transect near Hudson Canyon. Volume backscatter cells are color-coded based on frequency combinations where “1”, “2”, and “3” denote backscatter above the -66 dB threshold and “-” denotes the absence of a frequency. The black band across the surface is the upper 10 meters of the water column that was removed.

2.6 Summary

This chapter provides an introduction to the basic physical principles of sound in the marine environment, written for biologists who would like a better understanding of how and why EK60 data are collected on marine mammal surveys. Section 2.2 was presented to the Protected Species Branch of the Northeast Fisheries Science Center and to the Marine Mammal Program of the Protected Recourses Division of the Southeast Fisheries Science Center as a bioacoustics manual for marine mammal observers. This chapter provides two examples of how we can categorize opportunistically collected acoustic backscatter to infer biologically relevant information about the ecosystem. Also

presented are the descriptions of how the how multi-frequency data were processed before they were analyzed. These descriptions are specific to the active acoustic data collected on the AMAPPS surveys, but the templates I designed can be modified to process these types of data from other large scale ship-based surveys.

3. Distribution and Spatial Scales of Biological Acoustic Scattering in the Shelf Break Region of the Mid-Atlantic Bight

3.1 Introduction

Fish and plankton distributions in marine ecosystems are influenced by hydrologic features such as upwelling, thermal stratification, eddies and fronts (Olson and Backus 1985, Olson et al. 1994, Scales et al. 2014). As a result of these physical processes and animal behavior (Haury and Wiebe 1982, Mackas et al. 1985, Simard and Mackas 1989, Barange 1994), biological patchiness is considered a prominent feature of the marine environment (Steele and Henderson 1992) with the intensity of patchiness increasing in areas of upwelling, eddies and fronts (Mackas et al. 1985, Olson and Backus 1985, Nash et al. 1989, Nero et al. 1990). Patch structure in frontal regions may be the result of organisms orientating to density discontinuities, but until the advent of active acoustic technologies, biological sampling of front systems at adequate spatial and temporal scales was logistically unfeasible (Horne 2000, Koslow 2009). Acoustics methodologies have been used to observe and describe distributions of fish and zooplankton throughout the oceans (MacLennan and Holliday 1996) and within the last two and a half decades, advances in marine acoustic technology have made sampling biologically dynamic regions of the ocean possible (Simmonds and MacLennan 2005).

In marine systems, variables such as temperature, salinity, and density are not homogenous. Instead these variables usually vary gradually over horizontal distances and are bounded by narrow regions where the gradients are large. These narrow regions with large gradients are frontal regions (Mann and Lazier 1996). Although this is a standard description of an ocean front, it is vague at best, possibly owing to the diversity of front systems. Various physical processes from wind forcing to ocean currents can form a variety of fronts. Coastal and oceanic fronts vary in size and duration of existence. Tidal fronts are ephemeral, typically only a few kilometers long, and separate waters that may differ by only 1-2 °C (Mann and Lazier 1991). Fronts associated with western-boundary currents, such as the Gulf Stream, are thousands of kilometers long, persist over long periods of time, and exhibit temperature changes of 10°C in the upper water layers (Owen 1981, Mann and Lazier 1991). Mesoscale fronts (10s to 100s km) occur in regions where coastal water masses converge alongshelf and are an important conduit for onshore and offshore transport of nutrients and biota (Savidge and Austin 2007).

Fronts have been shown to contribute to several ecological effects including modifying vertical and horizontal migrations, influencing the distribution of populations or communities, and juxtaposing populations that would not normally co-occur (Owen 1981, Olson et al. 1994, Longhurst 2007). As an important influence on the

transport of nutrients and biota into or out of the euphotic zone, fronts are associated with high levels of productivity (Houghton and Marra 1983, Marra et al. 1990) and can drive the formation of prey patches (Legendre and Demers 1984, Mann and Lazier 1991, Franks 1992, Genin 2004). In the Mid-Atlantic Bight, the prominent mesoscale front is the Mid-Atlantic Bight shelf break front which flows equatorward along the shelf break from Georges Bank to Cape Hatters, NC (Chapman 1986, Chapman and Beardsley 1989, Gawarkiewicz and Chapman 1992, Gawarkiewicz et al. 2008).

Identification the scales of spatial process such as patch dynamics is an important topic in marine ecology. Non-random scales are those that are relevant to processes of interest that emerge from the data and are not an artifact of sampling design (Wiens 1989, Dungan et al. 2002). Determining spatial patterns within ecological data sets with multiple processes operating at multiple scales is challenging (Holling 1992), such as the dynamic shelf break system. Scale-specific information have demonstrated its usefulness in assessing wildlife habitat (Morris 2003), understanding the influence of natural disturbances on terrestrial ecosystems (Turner et al. 1993), examining spatial population dynamics (Levin 2000), and detecting scale-specific community dynamics (Keitt and Fischer 2006). Scale-specific analysis methods differ in terms of their concepts, but identification of meaningful and significant spatial scales depends that the method being used (Csillag and Kabos 2002, Saunders et al. 2002). One important element needed in

any method of analyzing non-stationary data is the capability to detect both local and global spatial patterns.

Although shelf break system in the Mid-Atlantic Bight is a highly productive region and has is the fishing grounds for several recreational and commercial fisheries (which use echosounders), there is a paucity of scientific acoustic data collection in this area. Stanton et al. (1987) and Nash et al. (1987) report one survey conducted in 1983 in which acoustics were used to investigate scattering by fish and zooplankton in relation to depth and temperature at the edge of the Gulf Stream. They found four, possibly five, horizontal “striations” of biological scattering across the Gulf Stream front, several crossing the front following the isotherms. Although this survey crossed the thermal front associated with the Gulf Stream, the survey was offshore of the Mid-Atlantic Bight shelf break front. The hydroacoustic group at the Northeast Fisheries Science Center in Woods Hole, MA, conducts seasonal fisheries acoustic surveys throughout Georges Bank and the Mid-Atlantic Bight, but their goal is fisheries specific and their surveys lines do not traverse the shelf break region.

This is the first study to examine the spatial distribution of acoustic scatterers within the complex and dynamic regions of the Mid-Atlantic Bight shelf break and shelf break front. Using the threshold categorization method by Jech and Michaels (2006) provides a conservative and discrete detection of acoustic scatterers and allows me to

retrieve backscatter values along entire transects. This provides continuous data values that can be integrated at discrete spatial increments for wavelet analysis.

The overall goal of this chapter is to describe the spatial distribution of the categorized acoustic scattering described in Chapter 2 (fish-like scatterers, nekton-like scatterers, plankton-like scatterers), within the context of the shelf break of the Mid-Atlantic Bight. Data were collected during daylight hours. The study area encompasses the continental shelf, shelf break, and pelagic areas of the Mid-Atlantic Bight shelf break region. I hypothesize that each section of the shelf break region will contain different counts of acoustic detections due to the dynamic nature of the physical processes in the region. A further objective of this chapter is describe the scales spatial acoustic backscatter patterns, with an aim to better understand the important links between fish-like scattering and nekton-like scattering. To achieve this objective, I use wavelet analysis to examine spatial scales of acoustic scatterers categorized by the Jech and Mischeals (2006) acoustic classification scheme.

3.2 Methods

3.2.1 Study Area

The study area encompasses the shelf break region of the Mid-Atlantic Bight from northeast corner of Georges Bank to the Delmarva Peninsula. Nineteen ship-based

daytime cross shelf transects were analyzed to assess the distribution of acoustic regions of interest categorized in Chapter 2 within the Mid-Atlantic Bight shelf break region. Six transects were spatially at least 48 hours after the initial transect was completed. Five transects were on Mid-Atlantic Bight side of Georges Bank (one transect duplicated) and the other 14 transects ranged from the shelf break off Cape Cod to the shelf break off the Delmarva Peninsula. Hydrographic data were collected with a surface flow-through thermo-salinograph (TSG) and expendable bathythermographs (XBTs) (Figure 35).

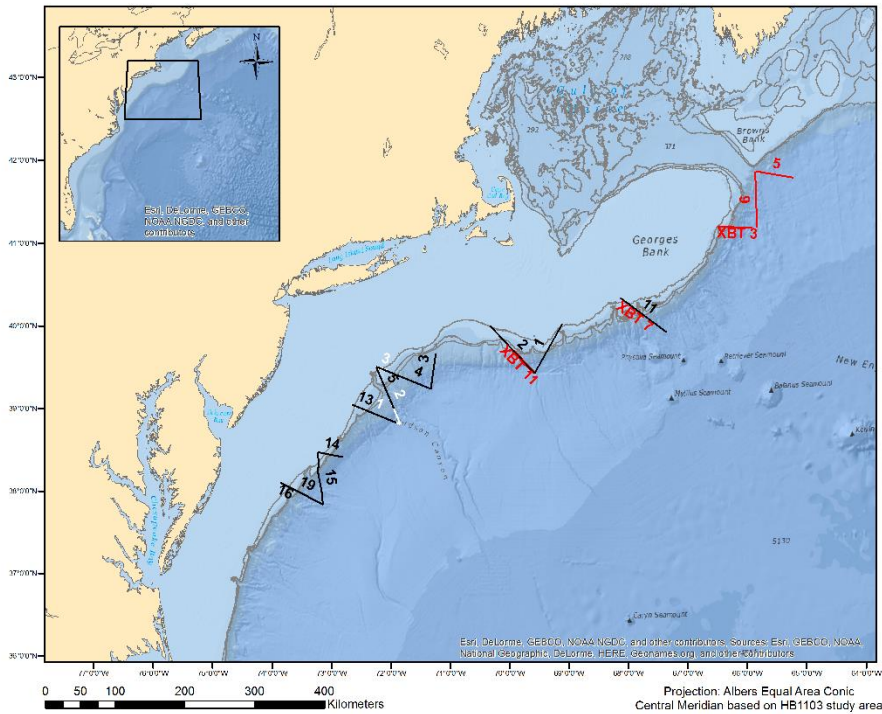


Figure 35: Labeled acoustic transect where thermo-salinograph data and active acoustic data were concurrently collected. Numbers are transect names. Leg I – black

lines. Leg II – white lines. Leg III – red lines. Six transects were partially or completely sampled twice.

3.2.2 Transect Region Classification

Each of the 19 shelf break transects were divided into three regions: shelf (SH), shelf break (SB), and offshore of the shelf break (OSSB). Data were collected in all regions of 14 transects while the five transects are missing data from either the SH or OSSB regions. Water depth along each cross shelf transect was determined using the bottom detection algorithm for the 18 kHz acoustic data described in Chapter 2 after all deviations from tracklines were removed. Deviations from the trackline occurred when the ship broke track to investigate marine mammal sightings or during CTD casts. Deviations from the trackline were marked in 18 kHz data in Echoview 6.1 (Myriax 2013) and removed in MATLAB (The MathWorks Inc. 2009) during acoustic processing. Once the deviations were removed, linear distance along the trackline was calculated in MATLAB and converted to distance from the shelf break. The greatest change in cross-shelf bathymetry in the Mid-Atlantic Bight varies from the 100 meter isobath to the 200 meter isobath. To provide a consistent definition of the shelf break I determined the position of the shelf break for each transect as the greatest bathymetric gradient around 150 meter isobath. The shelf break front, a persistent and prominent hydrographic feature in the Mid-Atlantic Bight, has a spatial correction scale for the upper 60 m of the

water column between 8 and 15 km (Gawarkiewicz et al. 2004). To encompass the horizontal scale of variability in water mass properties within the shelf break region, the shelf break region was defined as 15 km shoreward to 15 km offshore of the shelf break position (Todd et al. 2013). The shelf region was classified as the area along the transect shoreward of the shelf break region. The offshore shelf break region was classified as the area along the transect offshore of the shelf break region (Figure 36).

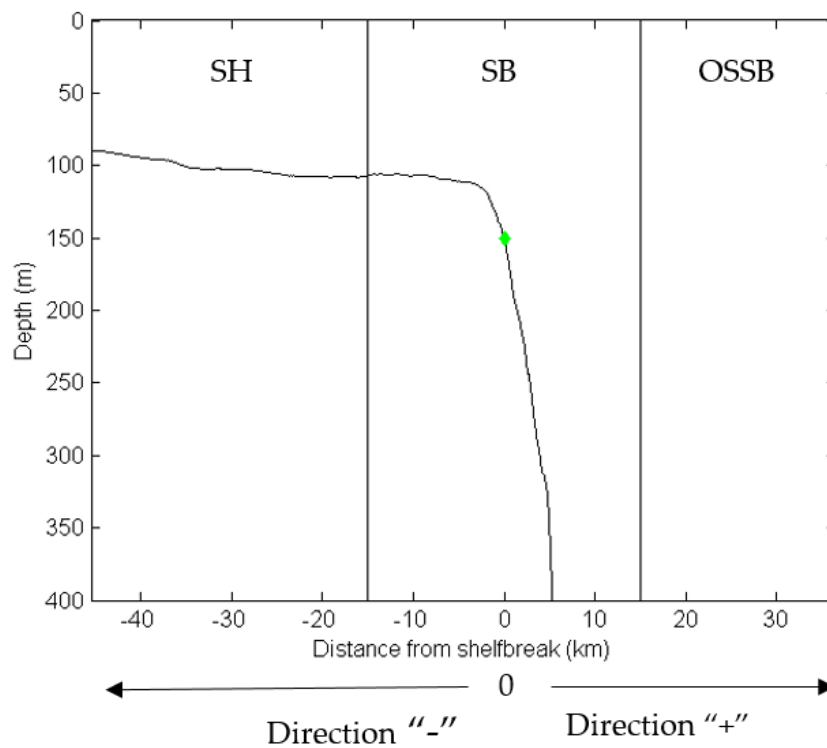


Figure 36: Regions of a shelf break transect. Green dot is the position of greatest bathymetric gradient between 149.0 and 151.0 meters depth. SH = shelf region, SB = shelfbreak region, OSSB = offshore shelfbreak region.

If the position of the shelf break could not be determined from the acoustic data (e.g. the shelf break was not crossed), the distance to the shelf break was calculated from the end of the transect to the 150 meter isobath in ArcGIS 10.2 (ESRI 2013). All data in ArcGIS were projected in an Albers Equal Area Conic projection with a modified central meridian specific to the AMAPPS study area. Bathymetric contours were derived from an 88 meter resolution bathymetric grid mosaicked from three data sources: Bathymetric Terrain Model of the Atlantic Margin for Marine Geological Investigations (Andrews et al. 2013), National Geophysical Data Center 3-arc second coastal relief model (NGDC 2012), and the USGS 15 arc second Gulf of Maine gridded dataset (Signell and Roworth 2013).

3.2.3 Physical Environment

Surface water temperature and salinity were sampled every 2 seconds by a Sea Bird Electronics model 45 thermo-salinograph (TSG) during the entire cruise. Post cruise, surface temperature and salinity data were synchronized to the Simard EK60 acoustic data and all deviations from the trackline were removed. For both temperature and salinity, outliers were determined by comparing the difference between a data point and its neighbors in MATLAB (The MathWorks Inc. 2009). If the difference was greater

than a threshold of 0.02 °C or 0.02 PSU, the data were marked and removed. To reduce noise in the TSG data, I smoothed the temperature and salinity data sets with a median filter, window size of 29 (approximately 1 minute of sampling). Density of the near surface water was then calculated using the SEAWATERv3.3 routines (Morgan 1994). To determine the spatial variability in surface temperature, salinity, and density along each transect, a one dimensional gradient was calculated for all variables on the smoothed data.

$$\frac{\sum_{i=1}^N \left| \frac{\Delta y_i}{\Delta x_i} \right| \Delta x_i}{\sum_{i=1}^N \Delta x_i}$$

where N is the number of transect segments, Δx is the change in distance along the transect, and Δy is the change in the hydrographic variable of interest. The mean and standard deviation of temperature, salinity, and density for each section (SH, SB, OSSB) were calculated to examine their variability within each section. The position of a front was determined at the point of the largest gradient along the transect and the distance from each front was calculated along each transect.

During the third leg of the cruise (20 July – 1 August, 2011), expendable bathythermographs (XBTs) were launched while underway along 3 daytime cross shelf transects every 3 nautical miles over the continental shelf and offshore of the shelf break

(Figure 37). Over the shelf break, XBTs were launched one per nautical mile. Due to weather restrictions, XBT line 11 was sampled in two parts on two consecutive days. However, more than 12 hours elapsed between last sample on the first day and the first sample on the second day. Because of this time difference and the dynamic nature of the shelf break area, I choose to analyze only the continuous OSSB to SB section of XBT line 11. XBT data were contoured and synchronized to the Simrad EK60 acoustic data in MATLAB to explore the distribution of acoustic regions of interest in relation to the shelf break and the spatial structure of the temperature field. To test the accuracy of the XBTs, an XBT was launched at the same time during a daytime CTD cast and compared to the upcast data collected by the CTD. XBT data were not compared to the CTD downcast data because the CTD downcast rate was greater than what was allowed for accurate measurements.

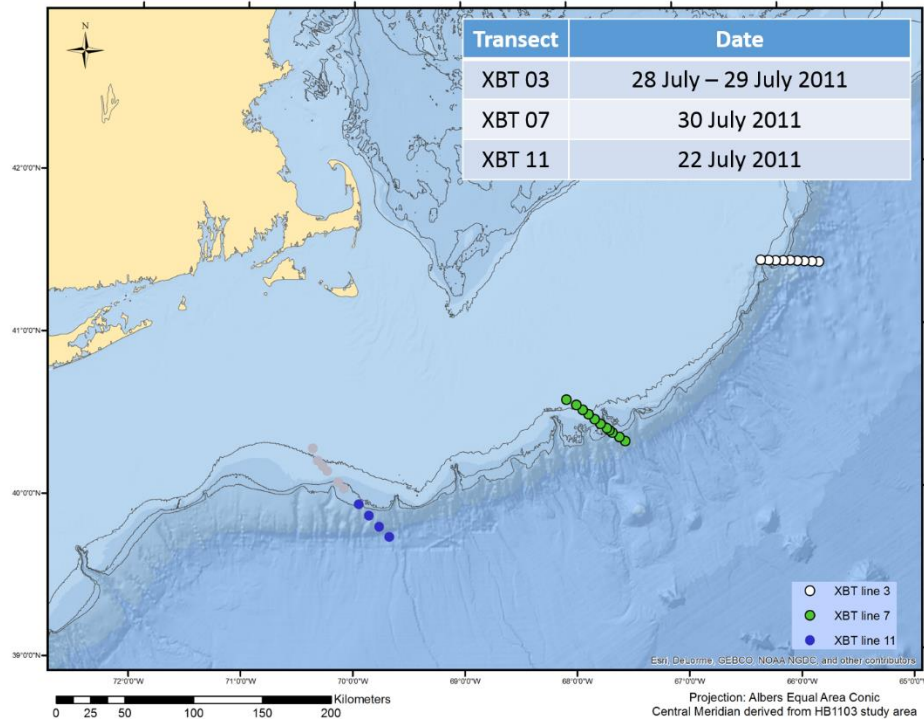


Figure 37: Location of XBT deployments. Greyed out locations on XBT 11 transect were not included in this analysis.

3.2.4 Categorization of acoustic regions of interest

Acoustic regions of interest were categorized into three groups based on the shape of their frequency response curve: fish-like (with swim bladder), nekton-like, and copepod-like and as patches or layers based on the shape of the 18 kHz (fish-like scattering) or 200 kHz (plankton-like scattering). A layer was horizontally exaggerated compared to its width, spanning several kilometers, with a thickness that was only a

percentage of its length. Patches were vertically roundish and concentrated within a few kilometers of the centroid of the region.

3.2.5 Analysis Methods

To investigate the distribution of categorized acoustic scattering along shelf break transects I used binomial linear regression models to explore the relationship between depth of a category, its morphology, and/or the region along the transect in which it was found. To test for differences in the number of acoustic categories of interest among the transect regions, I used a Kruskal-Wallis test and a nonparametric comparison for each pair using the Wilcoxon method with Bonferroni correction. Assuming that patches would be aggregated within the shelf break region because of the physical dynamics of the shelf break front, I hypothesized that the depth in which an acoustic region was found could be explained by its morphology, either a patch or a layer, and the region of the trackline in which it was found: SH, SB and OSSB. I measured the depth of an acoustic category at the centroid of the region. The assumptions of binomial regression were not violated. Residuals did not appear over or underestimated when plotted against raw values and residuals appeared to follow normality on a Q-Q plot. No outliers were detected with Cook's distance. Significance of the models was set at an alpha of 0.05 and models were compared using analysis of

variance and Akaike Information Criterion (AIC). Adjusted-R² values were calculated to assess how much variability was explained by the models. To compare the number of acoustic detections for each category (fish-like, nekton-like, and plankton-like) and across transect regions, I used a Kruskal-Wallis test with $\alpha = 0.05$ (Zar 1999). The number of acoustic categories detected was corrected by the amount trackline surveyed in that segment of the transect and each transect was considered an independent sample. I performed multiple comparison tests using Bonferroni correction on the significant results of the Kruskal-Wallis test to determine if effort-corrected detections of acoustic regions were significantly different in terms of the region of transect in which they were observed.

Global spatial pattern detection assumes that the process creating the global spatial pattern is stationary and can be summarized in a single scale determined from the size of the study area. These methods include spectral analysis (Keitt 2000, Csillag and Kabos 2002), and variograms (Cressie 1993). Multi-scale methods, in contrast, identify both global and local spatial scales at multiple scales and do not assume stationarity. Examples include lacunarity analysis (Plotnick et al. 1996), distance-based eigenvector methods (Borcard and Legendre 2002), and wavelet analysis (Dale and Mah 1998, Csillag and Kabos 2002, Mi et al. 2005, Cazelles et al. 2008). Wavelets are a useful tools for multi-scale analysis because they decomposes a data set into scale-specific

components and associate portions of the total signal variance with those scales (Torrence and Compo 1998, Csillag and Kabos 2002). Wavelets are similar to a localized Fourier analysis, but because they do not assume stationarity they are more flexible and are more accurate in identifying periodicity (Torrence and Compo 1998).

To analyze the spatial scales of pattern from acoustic scattering along a transect, I performed a wavelet analysis on volume backscatter (S_v) selected by the Jech and Michaels (2006) categorization method. After the S_v at 18 and 38 kHz were integrated from the surface to 300 meters and 250 meters horizontally in Echoview 6.1 (Myriax 2013). Both Morlet and Mexican Hat wavelets have been used in multi-scale pattern analysis of ecological data (Bradshaw and Spies 1992, Csillag and Kabos 2002, Mi et al. 2005). I chose the Morlet wavelet because it provides exact discrimination and location of scales of pattern while the Mexican Hat wavelet is better at detection and localization of gap events (Mi et al. 2005). The 250 meter horizontal resolution was chosen to reduce variation between pings. Data deeper than 300 meters were excluded from the analysis because of noise associated with the 120 kHz data below that depth. Because the Jech and Michaels (2006) method removes S_v below a threshold of -66 dB, I added a value of -100 dB to 'nodata' areas to obtain transects of continuous data. S_v was scaled to a mean of 0 normalized by standard deviation.

Wavelet analysis involves successive passes of a wavelet template of increasing size over a data set. The degree of similarity between the pattern of the data set and the shape of the template at each size and location are assessed on each pass (Torrence and Compo 1998, Cazelles et al. 2008). These values are wavelet coefficients and describe the degree of fit between the wavelet template and data set. For a give template size and a given location, a high wavelet coefficient indicated where the pattern of the data set matches the pattern of the wavelet. Coefficients close to 0 indicate no match between the data set and wavelet shape (Bradshaw and Spies 1992, Dale and Mah 1998). As this process is repeated at various template sizes, the wavelet transform decomposes the data set into multiple scales where a new series of wavelet coefficients at each level of decomposition are created. The set of coefficients at each scale reflects local variation in the original data set at that scale (Torrence and Compo 1998). Plotting the wavelet coefficients location by scale is referred to as a wavelet power spectrum. Scale-specific information independent of location is determined by examining the wavelet variance at each scale. Wavelet variance is the sum of the squared wavelet coefficients at a particular scale weighted by the number of coefficients (Bradshaw and Spies 1992, Torrence and Compo 1998). Scales of high wavelet variance are scales of interest. Plotting the wavelet variance versus scale provides a graphical view of the global wavelet spectrum. To test for significance, wavelet power spectra tested against red noise background level with a

lag-1 coefficient of the data. All data sets were padded to the a power of 2 and a cone of influence was applied to indicate areas where edge effect cause unreliable results (Torrence and Compo 1998, Cazelles et al. 2008).

Regression analyses were performed in R (R Core Team 2014) and wavelet analysis were performed in MATLAB with code from Torrence and Compo (1998) and Cazelles et al. (2014).

3.3 Results

3.3.1 Trackline effort

A total of 1,321 km of shelf break transects from the 2011 AMAPPS summer survey was analyzed (Figure 38 and Table 2). Table 2 lists the amount of effort by trackline, trackline region, and time of day (GMT) for all transects. All transects were completed during daylight hours. Of the 19 transects, four did not cover shelf regions and one did not cover the offshore region. Six of the transect lines were sampled twice, with more than 24 hours between sampling. Of the trackline regions, the greatest amount of effort was covered in the region offshore of the shelf break (633.1 km, mean = 33.3 km/transect), followed by the shelf break region (449.5, mean = 22.6 km/transect), and the shelf region (238.3 km, mean = 12.5 km/transect).

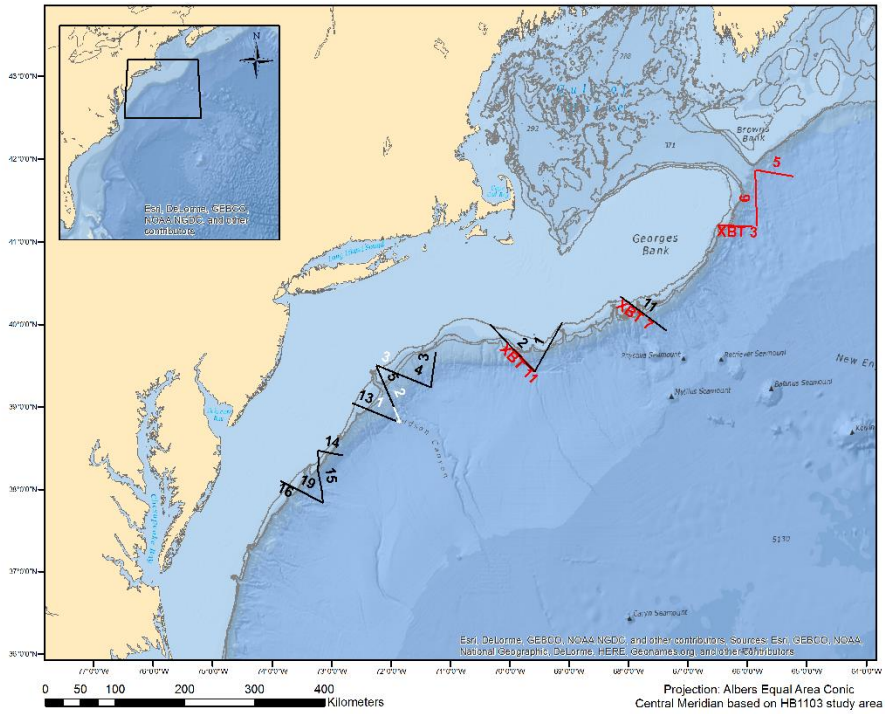


Figure 38: Labeled acoustic transects where cetacean sighting data, thermosalinograph data, and active acoustic data were concurrently collected (data sets not shown). Numbers are transect names. Leg I – black lines. Leg II – white lines. Leg III – red lines. Six tr Six transects were partially or completely sampled twice.

Table 2: Acoustic transect effort by location and time of day. MAB = Mid-Atlantic Bight, GB = Georges Bank, SH = shelf region, SB = shelf break region, OSSB = offshore shelf break region.

Transect (duplicated transects are grouped)	Location	Date (2011)	Time start/stop (GMT)	SH (km)	SB (km)	OSSB (km)	Total (km)
lg1Acln01	MAB	04-Jun	10:25 / 14:26	30.4	29.9	21.4	81.9
lg1Acln02	MAB	04-Jun	14:28 / 23:58	28.5	29.9	37.4	95.9
lg3AClnXBT11	MAB	22-Jul	10:09 / 12:22	0.0	6.9	33.9	40.8
lg1Acln03	MAB	06-Jun	09:43 / 12:29	0.0	1.1	47.5	48.6
lg1Acln04	MAB	06-Jun	12:34 / 17:54	13.7	29.9	49.2	92.9
lg2Acln03	MAB	29-Jun	20:48 / 22:20	16.7	8.0	0.0	24.8
lg1Acln05	MAB	06-Jun	17:56 / 22:11	20.7	29.9	20.3	71.0
lg2Acln02	MAB	29-Jun	14:40 / 20:48	15.7	29.9	47.2	92.9
lg1Acln11	GB	12-Jun	17:30 / 22:14	19.0	29.9	36.9	85.9
lg3AClnXBT07	GB	30-Jul	14:59 / 18:50	26.4	29.9	4.2	60.6
lg1Acln13	MAB	14-Jun	15:23 / 20:26	9.1	29.9	39.9	79.0
lg2Acln01	MAB	29-Jun	09:53 / 14:53	11.7	29.9	41.6	83.4
lg1Acln14	MAB	16-Jun	09:57 / 12:31	5.1	29.9	8.7	43.8
lg1Acln15	MAB	16-Jun	12:32 / 17:17	12.4	29.9	31.7	74.2
lg1Acln16	MAB	16-Jun	17:24 / 21:14	13.3	29.9	28.5	71.8
lg1Acln19	MAB	18-Jun	09:54 / 14:10	14.0	29.9	28.7	72.6
lg3ACln05	GB	28-Jul	09:33 / 13:25	0.0	8.3	58.1	66.4
lg3ACln06	GB	28-Jul	13:16 / 19:21	0.0	5.4	73.7	79.1
lg3AClnXBT03	GB	28-Jul/ 29-Jul	19:45 (28th) / 11:07 (29th)	1.1	29.9	23.5	54.6
Totals				238.3	449.5	633.1	1321.0
Mean				12.5	23.6	33.3	69.5
Standard Deviation				9.8	10.9	18.3	19.5

3.3.2 Physical Environment

Although temperature, salinity and density were highly variable along each transect, shelf waters had the coldest and least saline near surface water (Figure 39). Shelf waters were the most variable, and offshore waters were warmer and more saline than shelf waters near the surface. This pattern is typical of the Mid-Atlantic Bight where the cooler, less saline water from the Labrador Current is found over the shelf, slope water mixes with shelf water at the shelf break and offshore waters are influenced by the Gulf Stream or Gulf Stream eddies (Linder and Gawarkiewicz 1998, Fratantoni and Pickart 2007, Gawarkiewicz et al. 2008, Todd et al. 2013)

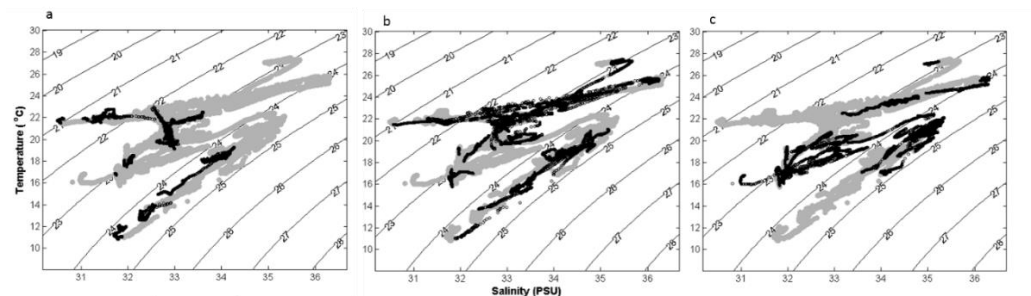


Figure 39: TS diagrams with density contours of near surface temperature and salinity from the flow-through thermo-salinograph. Grey dots are data points from all transect regions collected during the survey. Panel a, black dots are data from the shelf region. Panel b, black dots are data from the shelf break region. Panel c, black dots are data from the offshore of the shelf break region.

Temperature, salinity and density fronts were detected on every full cross shelf transect. In general, the greatest gradient for each variable was detected in the shelf region of each transect. Figure 40 depicts the temperature, salinity, and density gradients for Leg 1, line 01 in the Mid-Atlantic Bight. The top panel of the figure indicates the region of the transect: red = shelf region, green = shelf break region, blue = offshore of the shelf break region. The thin blue line is the bathymetric slope. Figure 41 shows the gradients of the hydrographic variables for Leg 3, XBT07 off the southern edge of Georges Bank. This figure only shows the variability in surface temperature, salinity, and density. It does not include the XBT data from this transect. In both transects, the greatest change in each of the hydrographic variables per kilometer of transect occurs in the vicinity of the shelf break. Although there is a great deal of variability among the transects in near surface temperature, salinity, and density, Figure 40 and Figure 41 are characteristic of the spatial changes in the hydrographic variables.

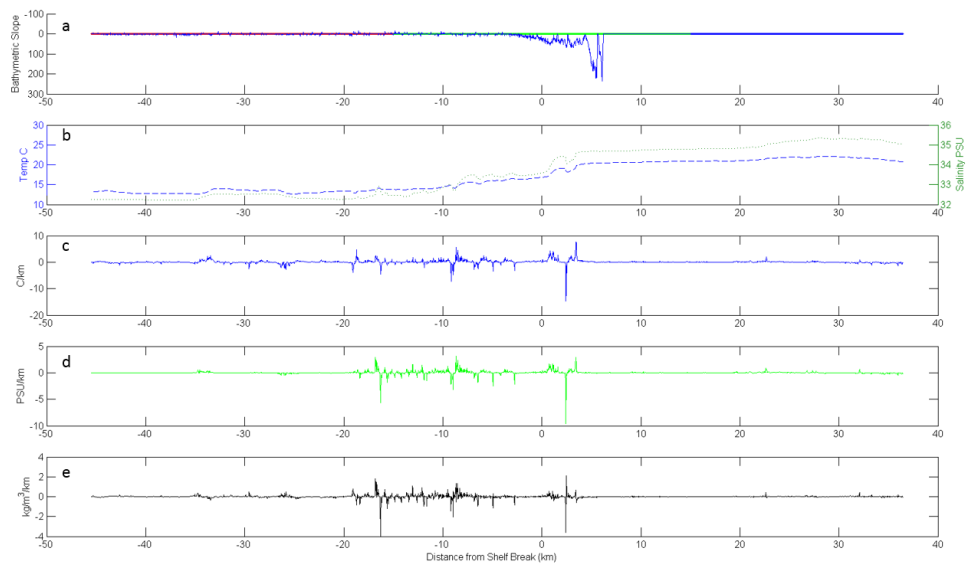


Figure 40: Bathymetric, temperature, salinity and density spatial gradients calculated from the TSG along a transect (Leg 1, Line 01) in the Mid-Atlantic Bight. a) red indicates the shelf region, green indicates the shelf break region, blue indicates the region offshore of the shelf break. The thick blue line indicates the bathymetric spatial gradient (bathymetric slope). b) Temperature (blue) and salinity (green) along the transect. c) Temperature gradient along the transect. d) Salinity gradient along the transect. e) Density gradient along the transect.

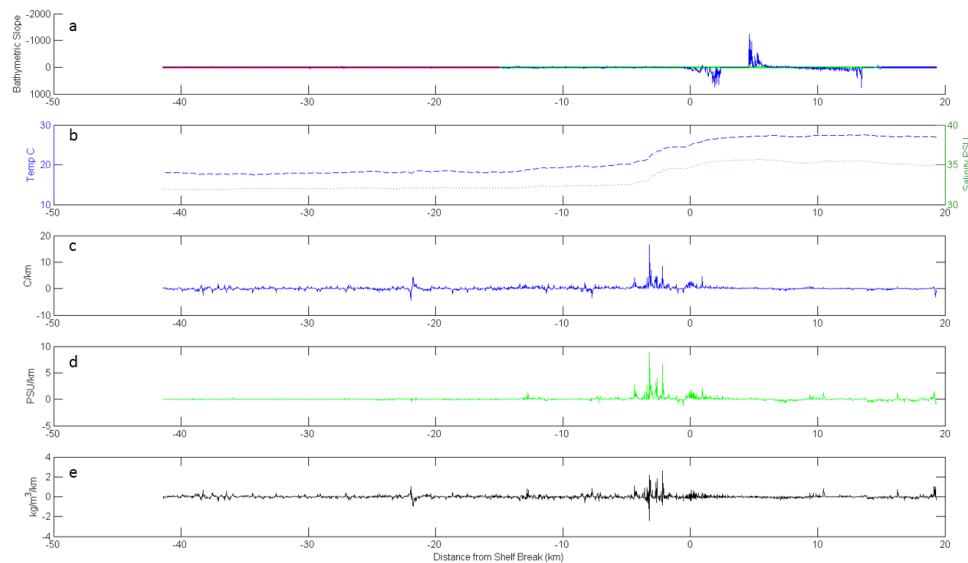


Figure 41: Bathymetric, temperature, salinity and density spatial gradients calculated from the TSG along a transect (Leg 3, Line XBT07) in the Mid-Atlantic Bight. a) red indicates the shelf region, green indicates the shelf break region, blue indicates the region offshore of the shelf break. The thick blue line indicates the bathymetric spatial gradient (bathymetric slope). b) Temperature (blue) and salinity (green) along the transect. c) Temperature gradient along the transect. d) Salinity gradient along the transect. e) Density gradient along the transect.

3.3.3 Spatial Distribution of Categorized Acoustic Scattering Regions

All categories of acoustic regions of interest were observed on all transects. Over all transects, plankton-like acoustic regions of interest were detected most frequently, followed by fish-like acoustic regions of interest and nekton-like acoustic regions (Table 3). Plankton-like detections per transect were the only significantly different acoustic

detections per kilometer (Kruskal-Wallis, $\chi^2 = 11.1475$, $p = 0.0038$), although nekton-like acoustic scattering was only slightly not significant (Kruskal-Wallis, $\chi^2 = 5.4996$, $p = 0.0630$).

In the shelf region and shelf break regions of the transects, fish-like regions of interest were most frequently detected, while plankton-like scattering was the most frequently detected in offshore regions (Table 3). Pair-wise comparison with Bonferroni correction of plankton-like scattering among regions of the transects was significant between detections of plankton-like scattering in the shelf region and in the region offshore of the shelf break ($Z = -2.49618$, $p = 0.0126$), and between detections of the plankton-like scattering in the shelf region and in the shelf break region ($Z = -3.21813$, $p = 0.0013$).

Table 3: Detection of acoustic regions of interest by trackline effort. Asterisk (*) indicates significantly different from other values within the column.

Acoustic Categorization	SH detections / km	SB detections / km	OSSB detections / km	All transect detections / km
Fish-like	0.0965	0.2247	0.1516	0.1665
Nekton-like	0.0168	0.0890	0.0300	0.0477
Plankton-like	0.0671	0.1935	0.2290	0.1877*

Fish-like scattering were predominately in the top 75 m of the water column along the entire generalized transect and between 100 m and 450 m, concentrated within the 25 km of the shelf break (Figure 42). Nekton-like scattering regions (green dots) were more concentrated along the area of the sea floor over the shelf and throughout the water column from the shelf break to approximately 25 km offshore of the shelf break (Figure 42). Plankton-like scattering regions were predominately over the shelf and offshore of the shelf break (Figure 42).

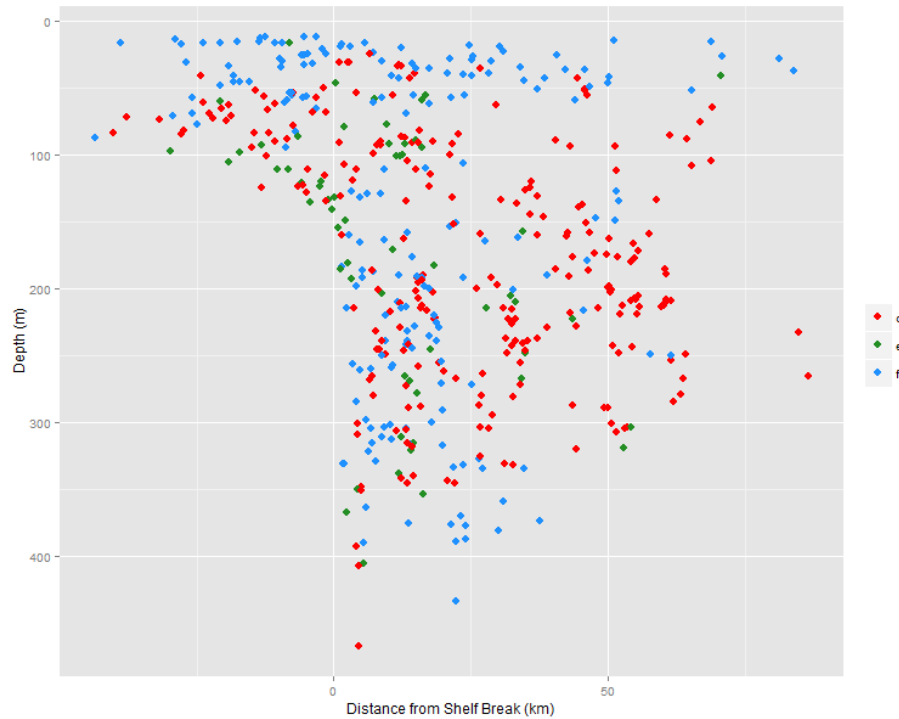


Figure 42: Position of centroids of categorized acoustic scattering regions along a generalized transect. Red dots = centroid of plankton-like regions. Green dots = centroid nekton-like regions. Blue dots = centroid fish-like regions.

Fish-like layers were predominately found in the top 75 m of the water column along the entire generalized transect while fish-like patches were mostly between 100 and 450 m, concentrated within 25 km of the shelf break (Figure 43).

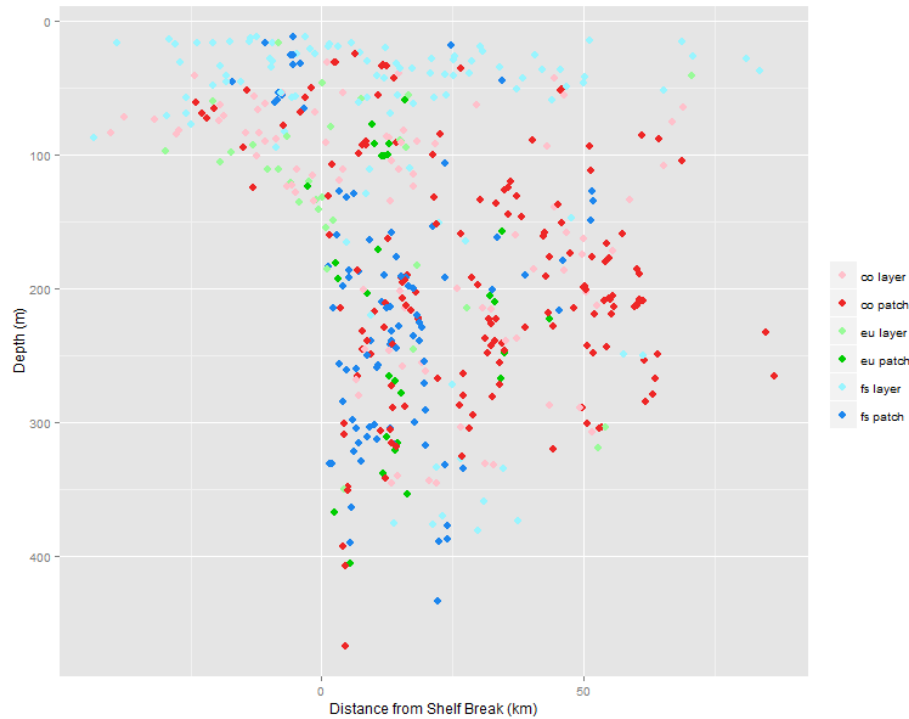


Figure 43: Position of categorized acoustic scattering along a generalized transect. Pink dots = centroid of plankton-like layers. Red dots = centroid of plankton-like patches. Light green dots = centroid of nekton-like layers. Green dots = nekton-like patches. Light blue dots = centroid of fish-like layers. Blue dots = fish-like patches.

I hypothesized that there is a relationship between the depth of an acoustic scattering region, its morphology (either a patch or a layer), and the region of the transect in which it was found: SH, SB and OSSB. The results of the simple binomial linear regression suggest that patches are generally 85 m deeper than layers (F: 93.94 on 1 and 487 DF, $p < 0.001$); however the r^2 value (0.16) is low, indicating that this model,

although highly significant, does not explain a large proportion of the variation in the depth of acoustic regions of interest.

The results of adding transect region as a coefficient to the binomial model, suggests that patches are generally 75 m deeper than layers; layers are 25 m shallower in the shelf break region compared to the offshore region; and layers are 94 m shallower in the shelf region than in the offshore region (F: 44.28 on 3 and 485 DF), $p < 0.001$ for all coefficients). However, the r^2 value increased only slightly to $r^2 = 0.22$, indicating that the variation in depth of the acoustic scattering region is not fully explained by either its morphology or region in which it was detected (Figure 44).

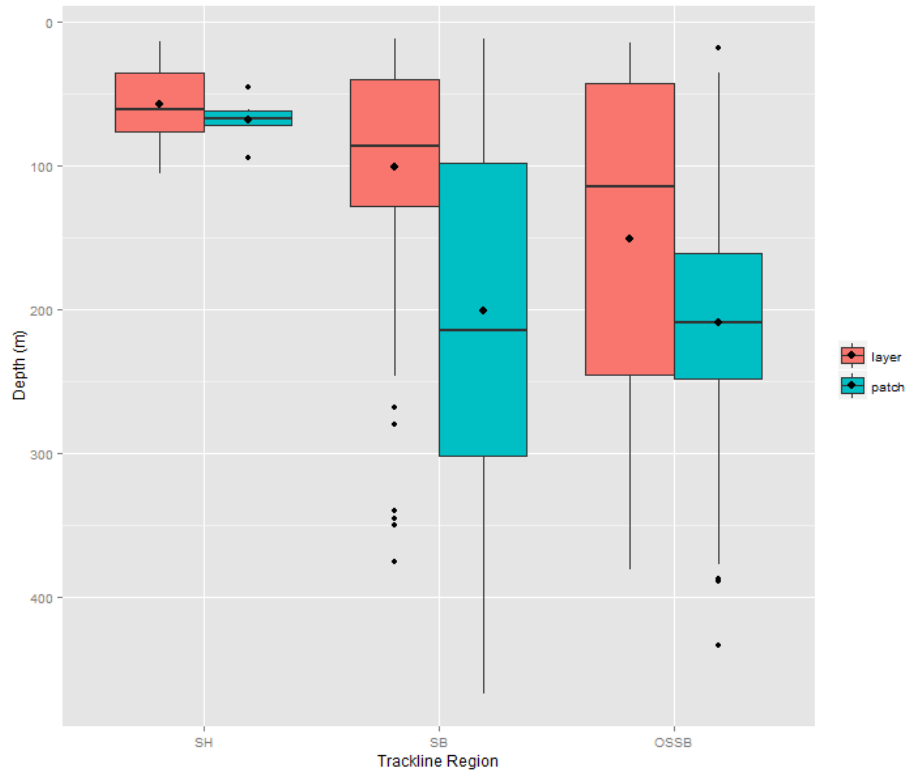


Figure 44: Boxplot of depths of categorized acoustic patches and layers by transect region.

3.3.4 Aggregations of Categorized Acoustic Scattering in Relation to Thermal Gradients

Temperature data from the XBT test probe and the concurrent CTD upcast had a significant $R^2 = 0.98$ ($p \sim 0$).

An objective of this chapter was to describe the distribution of categorized acoustic regions of interest within the shelf break region of the Mid-Atlantic Bight and to compare the spatial differences between water masses. Echograms of the three transects where XBT were deployed and thermal contours plotted are presented here to describe acoustic scattering in the context of the shelf break frontal system.

In the Mid-Atlantic Bight, the shelf break front is delineated as the 34.5 PSU isohaline (Linder and Gawarkiewicz 1998). Unfortunately, CTD sampling along the shelf break transects was not conducted at a spatial resolution that could resolve the shelf break frontal structure and position because of the survey logistics to collect marine mammal abundance data. However, during the summer months, the frontal boundary can also be defined as the 10 °C isotherm (Linder and Gawarkiewicz 1998).

In transect XBT03 (Figure 45) the cold pool, formed from the winter remnant of shelf water trapped by the summer warming of surface waters (Beardsley and Flagg 1976, Houghton et al. 1982) and also defined by the 10 °C isotherm (Linder and Gawarkiewicz 1998), is seen over the shelf and extends about 20 km offshore of the shelf break. The shelf break front can clearly be seen in the 18 kHz and 200 kHz backscatter, as areas of greater scattering intensity (yellow and red areas in Figure 45) at both frequencies that coincide with the 10 °C isotherm. Eight plankton-like regions were detected within the cold pool over the shelf, one nekton-like region was detected where

the cold pool abuts the edge of a warm-core ring (~ +18 km to +30 km, in the top 50 m), and 24 fish-like acoustic regions were detected in the slope waters near the shelf break. Two fish-like regions were also detected at the edge of the warm-core ring. In this transect there is a clear spatial delineation between the plankton-like scattering regions in the cold pool and fish-like scattering regions offshore of the shelf break front and at the edge of the warm-core ring.

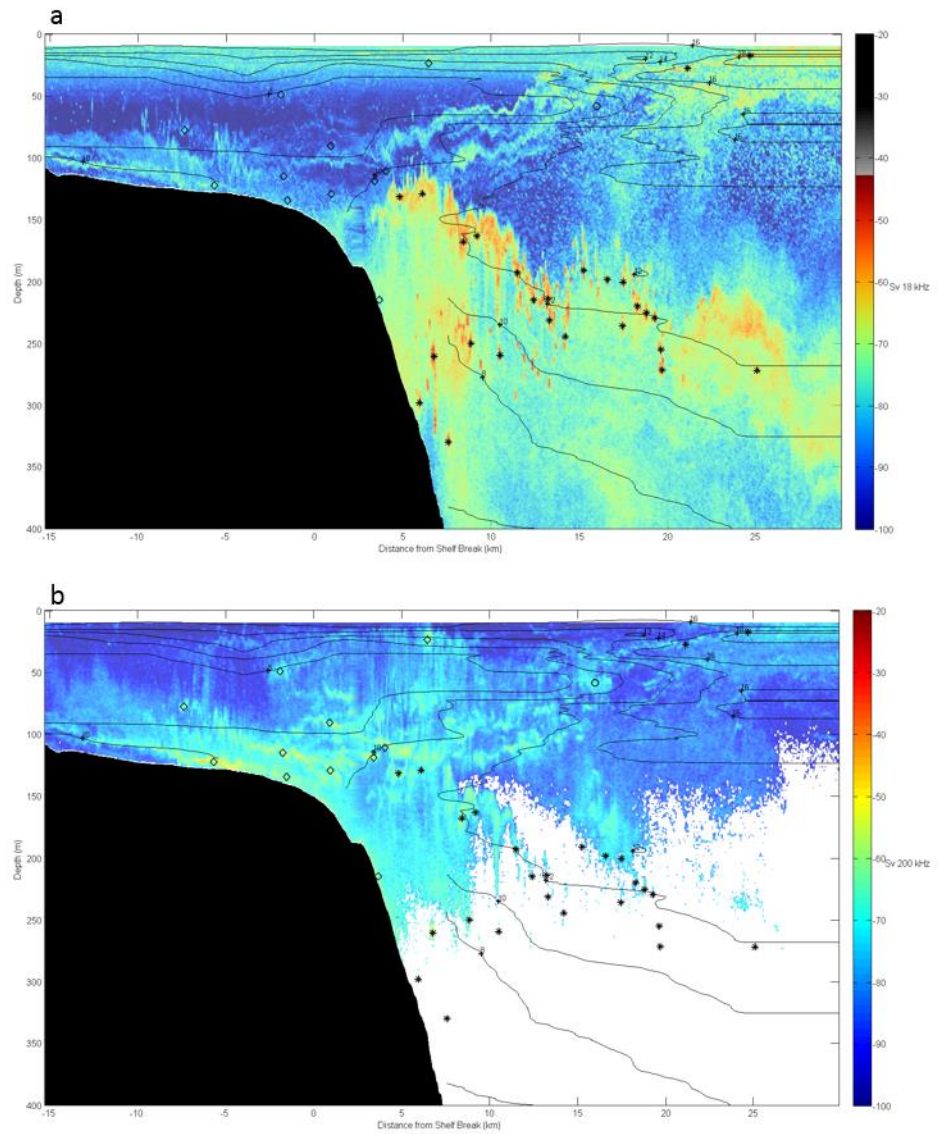


Figure 45: Acoustic backscatter (S_v) at 18 kHz (a) and 200 kHz (b) along transect XBT03 and temperature contours. Asterisks are the centroids of fish-like acoustic regions. Circles are the centroids of nekton-like acoustic regions of interest. Diamonds are centroids of plankton-like acoustic regions of interest.

In transect XBT07 (Figure 46) the cold pool is also clearly defined over the shelf but the edge of a warm-core ring has intruded over the shelf and pushed the front (10 °C isotherm) shoreward in the top 30 m of the water column. Both plankton-like and fish-like acoustic categories were detected in the cold pool; however, only fish-like acoustic categories were detected at the intruding edge of the warm-core ring. Plankton-like scattering was also detected at the shelf break and within the canyon (Lydonia Canyon). A fish-like scattering was detected above the canyon wall (+8 km, ~100 m depth). The shelf break front is apparent in the 18 kHz and 200 kHz echograms as areas of greater intensity of scattering at both frequencies that coincide with the 10 °C isotherm. In this transect there is a spatial delineation between the categorized acoustic regions detected in the cold pool and in the warm-core ring; however, with the intrusion of the warm-core ring over the shelf, fish-like scattering was also detected in the cold pool.

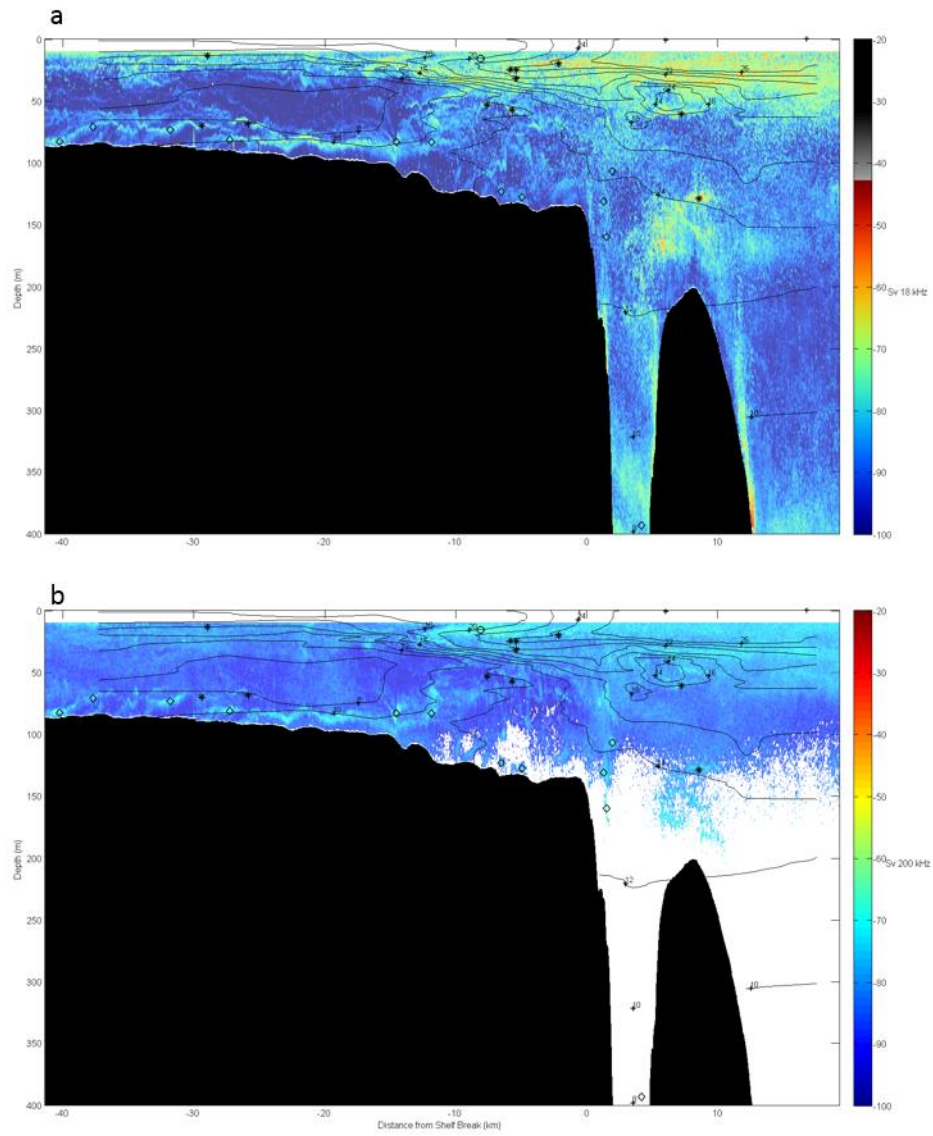


Figure 46: Acoustic backscatter (S_v) at 18 kHz (a) and 200 kHz (b) along transect XBT07 and temperature contours. Asterisks are the centroids of fish-like acoustic regions. Circles are the centroids of nekton-like acoustic regions. Diamonds are centroids of plankton-like acoustic regions.

Transect XTB11 (Figure 47) covers more offshore area and less shelf/shelf break area than transects XBT03 and XBT07. There was no intrusion of a warm-core ring on this transect and the cold pool extends offshore. The foot of the cold pool was not detected and the frontal boundary could not be delineated. Acoustic regions of interest are mostly plankton-like and not aggregated as in transects XBT03 and XBT07. Two fish-like scattering regions were detected in the thermocline offshore and a clustering of plankton-like scattering detections near the lower lip of the shelf break.

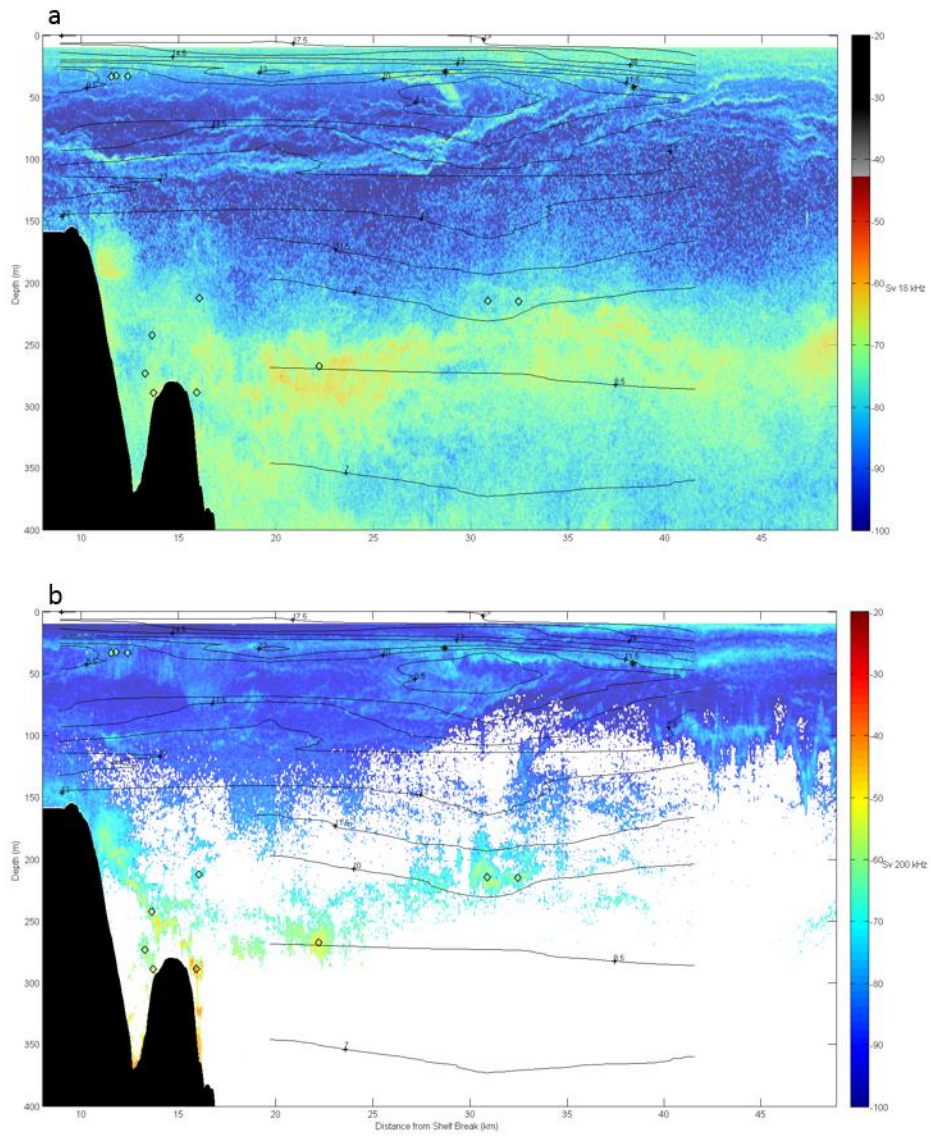


Figure 47: Acoustic backscatter (Sv) at 18 kHz (a) and 200 kHz (b) along transect XBT11 and temperature contours. Asterisks are the centroids of fish-like acoustic regions of interest. Circles are the centroids of euphausiid-like acoustic regions of interest. Diamonds are centroids of copepod-like acoustic regions of interest.

3.3.5 Identifying Scales of Spatial Patterns from Acoustic Scattering

Scales of spatial patterns in 18 and 38 kHz backscatter were analyzed with wavelet analysis for transects lg1ln16 (16-June) and lg1ln19 (18-June). Acoustic backscatter at these frequencies, after applying the Jech and Michaels (2006) categorization method, are proxies for fish-like scattering (18 kHz) and nekton-like scattering (38 kHz). Plankton-like scattering was selected from the 120 kHz S_v data, but its distribution did not lend itself to wavelet analysis. Geographically, lg1ln19 is the same transect as lg1ln16, but data from lg1ln19 were collected 48 hours after lg1ln16.

The significant scales of spatial pattern varied between transects. Within transects, patterns of spatial scales varied between fish-like scattering and nekton-like scattering. One to 4 kilometer scales were significant for both fish-like and nekton-like scattering and both transects, although the variability of the pattern varied along the transects.

Over the entire transect of lg1ln16, fish-like scattering indicated a spatial pattern at scales 0.75, 1.25, 4 and 8 km (peaks above the dashed line in Figure 48d). Nekton-like scattering indicated a spatial pattern at scales 1, 2.25, and 4 km (peaks above the dashed line in Figure 48f). The location of the fish-like and nekton-like scales of spatial pattern also varied in relation to the shelf break. For fish-like scattering, the 4 km and 8 km scales crossed the transect from the 10 km shelf-side of the shelf break to approximately

17 km offshore of the shelf break (Figure 48c), whereas the 4 km scale for nekton-like scattering was located only over the shelf region (Figure 48e). Nekton-like scattering also indicated less intense and discrete scales of spatial pattern at the shelf break, and between 15 – 20 km and 27 km offshore of the shelf break. To examine the variability within the 1 to 4 kilometer scales I calculated the scale-average wavelet variance for both fish-like scattering (Figure 48g) and nekton-like scattering (Figure 48h). The scale-averaged wavelet variance differed between fish-like scattering and nekton-like scattering. More peaks and stronger peaks were present in nekton-like scattering, but were located over the shelf region and between 25 and 30 km offshore of the shelf break (Figure 48h). The 1-4 km scale averaged wavelet variance for fish-like scattering was strongest centered around 10 km offshore of the shelf break with additional peaks at approximately 15 and 5 km shelf-side of the shelf break (Figure 48g).

Over the entire transect of lg1ln19, fish-like scattering indicated a spatial pattern at scales 0.25, 1, and 2 km (peaks above the dashed line in Figure 49d). Nekton-like scattering indicated a spatial pattern at scales 1, 2, and 4 km (peaks above the dashed line in Figure 49f). The location of the fish-like and nekton-like scales of spatial pattern also varied in relation to the shelf break. For fish-like scattering, the 1 to 4 km scales crossed the entire transect and the 8 km scale was noticeably absent (Figure 49c), whereas the 1 to 4 km scales for nekton-like scattering was located over the shelf region

and approximately 8 to 20 km offshore of the shelf break (Figure 49e). I calculated the 1 – 4 km scale-average wavelet variance for both fish-like scattering (Figure 48g) and nekton-like scattering (Figure 48h) for $\lg1n19$ as well. The scale-averaged wavelet variance for fish-like scattering and nekton-like scattering had similar numbers of peaks, but the peaks for the nekton-like scattering were stronger (Figure 49 g and h). The strongest peak for the scale-averaged variance fish-like scattering moved well offshore – 30 to 40 km offshore of the shelf break (Figure 49g), while the strongest peak for the nekton-like scattering remained over the shelf region but narrowed in location (10 to 20 km shelf-side of the shelf break) and intensified (Figure 49h).

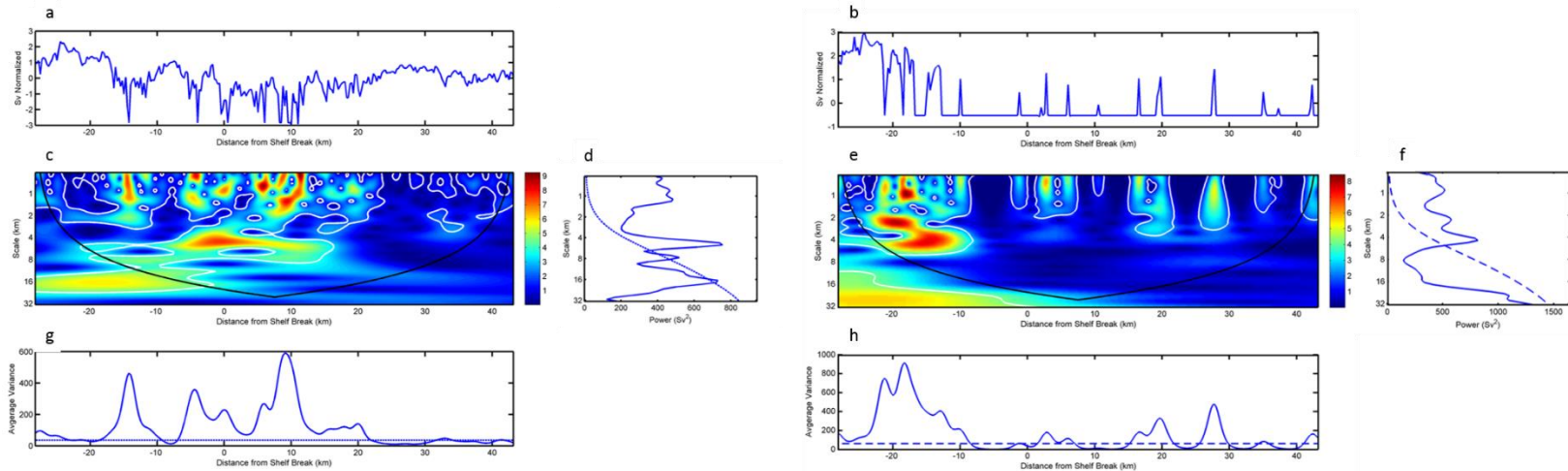


Figure 48: a) Lg1ln16, 18 kHz normalized S_v series used for the wavelet analysis. b) Lg1ln16, 38 kHz normalized S_v series used for the wavelet analysis. c and e) The local wavelet power spectrum using the Morelet wavelet. Warmer colors represent regions in scale-location space with large wavelet coefficients. The white line encloses regions greater than a 95% confidence level for a red-noise process. Black semi-circle is the cone of influence. Results below this line should not be trusted due to edge effects. d and f) Global wavelet spectrum averaged over the entire transect. The dashed blue line is the 95% confidence level for a red-noise process. g and h) Scale averaged wavelet power over the 1 – 4 km band.

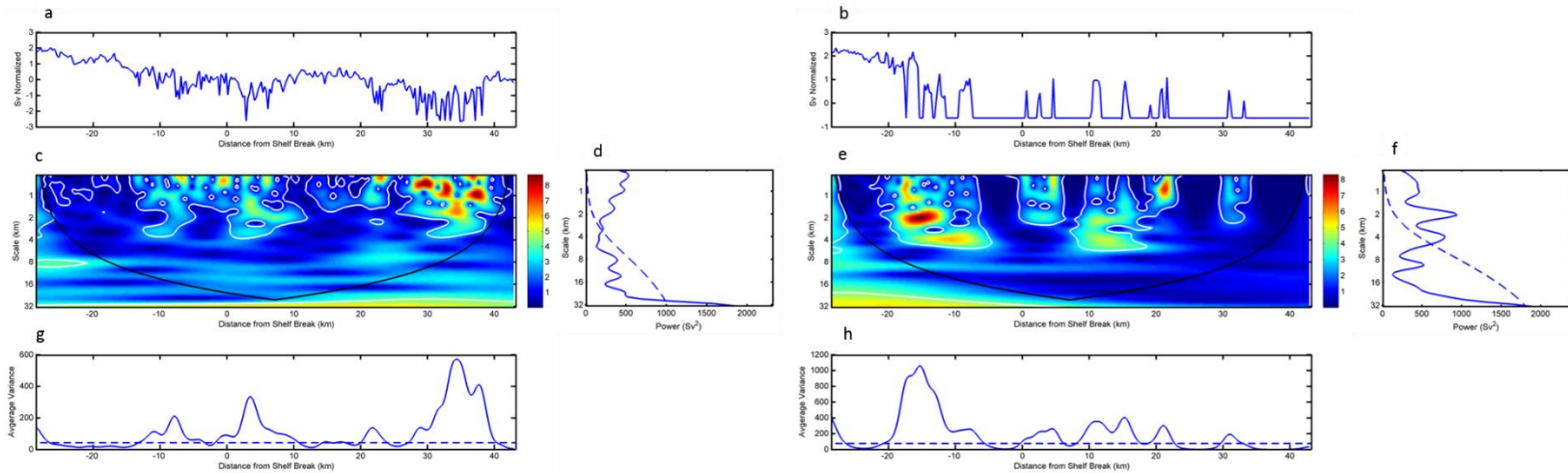


Figure 49: a) Lg11n19, 18 kHz normalized S_v series used for the wavelet analysis. b) Lg11n19, 38 kHz normalized S_v series used for the wavelet analysis. c and e) The local wavelet power spectrum using the Morelet wavelet. Warmer colors represent regions in scale-location space with large wavelet coefficients. The white line encloses regions greater than a 95% confidence level for a red-noise process. Black semi-circle is the cone of influence. Results below this line should not be trusted due to edge effects. d and f) Global wavelet spectrum averaged over the entire transect. The dashed blue line is the 95% confidence level for a red-noise process. g and h) Scale averaged wavelet power over the 1 – 4 km band.

3.4 Discussion

The Mid-Atlantic Bight shelf break front is one of the main forcing mechanisms of water structure in the shelf break region of the Mid-Atlantic Bight. The jet of this mesoscale front follows the edge of the continental shelf (between 100 and 200 m) from Georges Bank to Cape Hatteras and has been detected on the continental shelf as shallow as 50 meters (usually forced by the Gulf Stream or a Gulf Stream eddy) (Churchill and Gawarkiewicz 2009). Because the primary design of the 2011 summer AMAPPS survey was to collect standardized marine mammal abundance data, the survey lines were stratified in such a way to be comparable to previous marine mammal abundance surveys. This resulted in less survey effort over the shelf compared to the shelf break and offshore of the shelf break and resulted in an inability to resolve the position of the shelf break front on line XBT11, biasing the results of the overall distribution of acoustic regions of interest. A potential mechanism influencing the distribution of acoustic scatterers is likely the upwelling associated with bottom boundary layer detachment of the shelf break front, but because the survey did not encompass the full spatial distribution of the front, the region of upwelling cannot be discerned and questions of pertaining to biological distribution in a physically dynamic are only partially answered. It was difficult to get a clear picture of the distribution of categorized

acoustic scattering regions within the shelf break; however, it is clear in two of the XBT transects that categorized acoustic backscatter separate in areas around the shelf break front and at the edge of the warm-core ring.

Although not utilized in this analysis, other descriptive characteristics of the categorized acoustic regions were calculated, including corrected region length, corrected region width, kurtosis, skewness, horizontal and vertical acoustic roughness, and corrected area. These characteristics could be used in clustering analyses to provide information on the internal structure of patches (Lawson et al. 2004) related to the hydrographic features. Nero et al. (1990) and Barange (1994) both identified acoustic roughness as the factor that provided the most information on the structure of acoustic patches but was not applied here because of the uncertainty surrounding the categorization of the acoustic data. Another approach to describe the spatial patterns of mid-trophic level taxa is to look at the correlation length scales of plankton and fish patches in relation to the physical structure (Wiebe et al. 1996). This cannot be accomplished with the daytime transects because CTD profile data were collected at a large spatial scale that would not create a meaningful interpolation of the data – in some cases there are only two CTD stations along an 80 km transect.

Multi-frequency S_v echograms highlight a variety of acoustic backscattering patterns that are indicative of the spatial and temporal distributions of mid-trophic

levels. Some of the patterns are unique to specific species, times, and locations.

Biophysical interaction of small gas-bearing organisms entrained in internal waves are known to occur in the Mid-Atlantic Bight and can be seen in multi-frequency data, as well as “speckles” of individual gas-bearing fish usually found just beneath the internal wave (Jech 2014, personal communication). Mesopelagic fish dominate acoustic backscatter at/near the shelf break where certain species (primarily myctophid species) migrate from 400-600 m depths to near the surface at night and other species stay at depth (Bergstad et al. 2008, 2012). Wavelet approaches to analyses these types of multi-frequency acoustic scattering can lead to a richer understanding of the biological structure within this dynamic region.

Even without the ability to classify the acoustic backscatter data collected on this cruise, wavelet analysis showed how patterns of spatial scales along the same transect, sampled 48 hours apart, can change over that time period. Fish-like scattering (represented by the 18 kHz) presented significant patterns at small spatial scales (1-2 km) along the entire transect and between 4 and 8 km scales around the shelf break on 11/16. Forty-eight hours later, fish-like scattering was only significant at scales of 1 to 2 km along the entire transect – as the shelf break front moved offshore, the spatial scales of interest around the shelf break dissipated. Nekton-like scattering from 11/16 was significant over a range of spatial scales concentrated within the shelf region, but as the

front moved offshore, significant spatial scales of nekton-like scattering over the shelf moved closer to the shelf break and increased in scale off the shelf break from 2 – 4 km to 2 – 8 km. This could indicate that nekton-like scatterers are entrained in the physical cross-shelf flow as the front moves offshore, or these organisms are filling a spatial scale previously occupied by fish-like scatterers.

The analysis presented in this chapter provides an initial assessment of the distribution of categorized acoustic scattering regions within the shelf break region of the Mid-Atlantic Bight using opportunistically collected active acoustic data. The dynamic nature and high productivity of this region require synoptic, fine-scale sampling available from the EK60 data to elucidate the mechanistic processes that drive fish and zooplankton distributions.

4. Fine-scale Distribution of Three Cetacean Species within the Mid-Atlantic Bight Shelf Break Region

4.1 Introduction

Marine organisms function and interact at a variety of temporal and spatial scales that mirror their trophic levels. For instance, small plankton have life spans of several months and travel relatively short distances, whereas large marine predators, such as cetaceans, have life spans of decades and travel vast distances. However, even large marine predators tend to concentrate certain activities over localized regions and for short periods of time. For example, many marine mammals undertake long annual migrations, but return seasonally to confined foraging areas (Mate et al. 1995, Read and Westgate 1997, Baumgartner et al. 2003, Risch et al. 2014). Albatrosses range over ocean basins, but forage in comparatively small areas for extended periods of time (Hyrenbach et al. 2002). Usually interpreted as the result of foraging decisions made at meso- (10s to 100s km) and fine-scales (10s m to 10 km), we assume that these distribution patterns occur because highly mobile animals remain near a prey patch until the patch is no longer energetically beneficial to the animal (Stephens and Krebs 1986).

Many cetacean species aggregate along frontal systems, at bathymetric gradients, in upwelling areas, and at the edges of eddies on broad spatial scales (Waring et al. 1993,

2001, Hastie et al. 2004, 2005, Ferguson et al. 2005, Forney et al. 2012, Roberts et al. 2016). The Mid-Atlantic Bight shelf break region is a highly dynamic and productive area that provides a wide range of habitat to many marine species over every trophic level, and is a known area of high cetacean diversity and density (CeTAP 1982, Hain et al. 1985, 1992c, Kenney and Winn 1986, Selzer and Payne 1988, Roberts et al. 2016). At least 23 species of cetaceans have been sighted in this region. The prominent bathymetric feature is the shelf break and the prominent hydrographic feature is the shelf break front, a persistent thermohaline front with a jet that flows equatorward along the shelf break from Georges Bank to Cape Hatteras, NC (Chapman 1986, Chapman and Beardsley 1989, Gawarkiewicz and Chapman 1992, Linder and Gawarkiewicz 1998, Houghton et al. 2006, 2009, Gawarkiewicz et al. 2008). The shelf break system is also influenced by onshore intrusions of limbs from anticyclonic warm-core rings (Zhang and Gawarkiewicz 2015).

Although cetaceans are known to aggregate at the shelf break in the Mid-Atlantic Bight, it is unlikely that the relationship between cetacean distribution and environmental factors is directly causal. The influence of hydrographic systems on cetacean distributions is most likely the aggregation of prey species (Baumgartner 1997, Davis et al. 2000). Several studies in the Gulf of Mexico (Baumgartner 1997, Davis et al. 2000, Mullin and Fulling 2004) and North Atlantic (Kenney and Winn 1987, Waring et al.

1993, Hooker et al. 1999, Johnston et al. 2005) defined cetacean distributions in terms of physiography. For cetaceans who are benthic or demersal feeders, physiography is a direct factor limiting cetacean distribution; however, for cetaceans that prey on pelagic fish or cephalopods, physiography most likely plays an indirect role through forcing mechanisms such as topographically induced up-welling which increases primary production and aggregations of zooplankton (Haury and Wiebe 1982, Wiebe et al. 1996, Gawarkiewicz et al. 2004).

Cetacean distributions in the Mid-Atlantic Bight have been studied for several decades now through line transect surveys (CeTAP 1982, Geo-Marine Inc. (GMI) 2010b, Palka 2012, Roberts et al. 2016), acoustic studies (Clark 1995, Risch et al. 2013, 2014), and photo-identifications studies (Clapham and Seipt 1991, Read et al. 2003). However, these studies are at regional scales (line transect) or at home range or species specific ranges (photo-id) and are unable to address questions pertaining to fine scale distributions. This study characterizes the fine scale spatial distributions of common dolphins (*Delphinus delphis*), Risso's dolphins (*Grampus griseus*), and sperm whales (*Physeter macrocephalus*) through multidimensional scaling, classification tree analysis and random forest analysis of marine mammal line-transect survey data, multi-frequency active acoustic data and fine-scale *in situ* hydrographic data. Multi-frequency active acoustic data were broadly classified into proxies of middle trophic level groups through frequency response

methods to serve as prey proxies. Additionally, to gain an understanding of the spatial relationship between cetaceans and proxies of their prey in the Mid-Atlantic Bight, I examined the distribution of distances between cetacean sightings and the closest point of the nearest categorized acoustic region.

4.2 Methods

4.2.1 Study Area

The study area encompasses the shelf break region of the Mid-Atlantic Bight from the northeast corner of Georges Bank to the shelf break region off the Delmarva Peninsula. Marine mammal sightings, hydrographic data and active acoustic data from 19 ship-based daytime cross-shelf transects were analyzed. Six transects were sampled twice at least 48 hours after the initial transect was completed. Five transects were located on the northeastern and southwestern edges of Georges Bank (one transect line duplicated) and the other 14 transects ranged from the shelf break off Cape Cod to the shelf break off the Delmarva Peninsula (Figure 50).

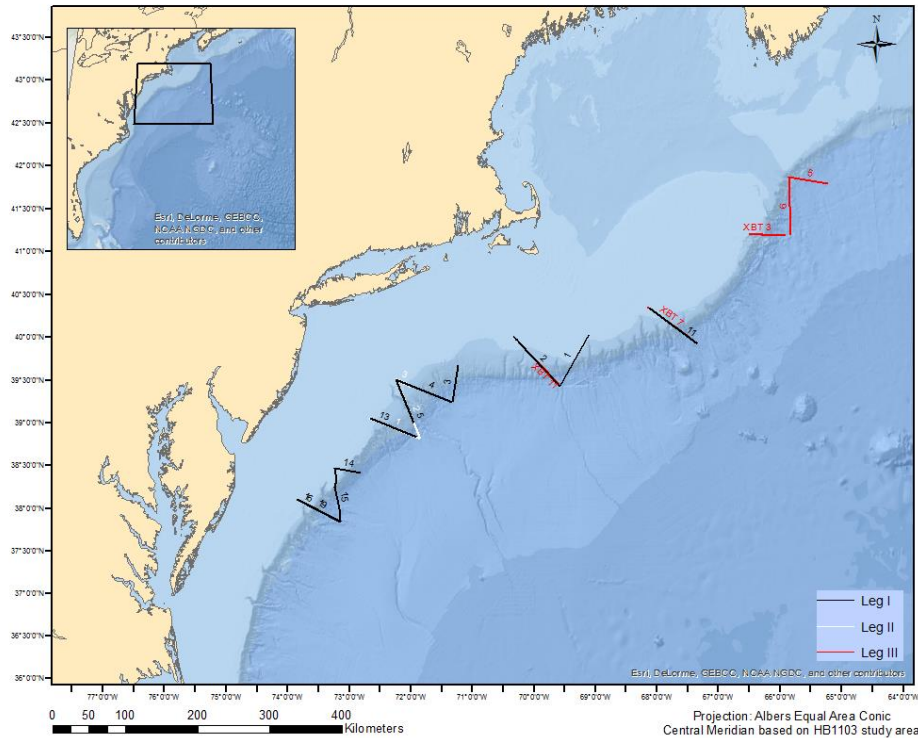


Figure 50: Labeled survey lines. Numbers are transect names (see Table 6). Black lines and numbers: Leg I. White lines and numbers: Leg II. Red lines and numbers: Leg III. Six tracklines were partially or completely sampled more than once.

4.2.2 Transect Region Classification

Each of the nineteen shelf break transects were divided into three regions: shelf (SH), shelf break (SB), and offshore of the shelf break (OSSB). Data were collected in all regions of 14 transects while the five remaining transects are missing data from either the SH or OSSB regions. Water depth along each cross shelf transect was determined using the bottom detection algorithm for the 18 kHz acoustic data described in Chapter

2 after all deviations from tracklines were removed. Deviations from tracklines occurred when the ship broke track to investigate marine mammal sightings or during CTD casts. Deviations from the trackline were marked in the 18 kHz data in Echoview 5.4 (Myriax 2013) and removed in MATLAB (The MathWorks Inc. 2009) during acoustic processing. Once the deviations were removed, linear distance along the trackline was calculated in MATLAB and converted to distance from the shelf break. The position of the shelf break for each transect was determined as the greatest bathymetric gradient from 149.0 to 151.0 meters depth. The shelf break front, a persistent and prominent hydrographic feature in the Mid-Atlantic Bight, has a spatial correction scale for the upper 60 m of the water column between 8 and 15 km (Gawarkiewicz et al. 2004). To encompass the horizontal scale of variability in water mass properties within the shelf break region, the shelf break region was defined as 15 km shoreward to 15 km offshore of the shelf break position (Todd et al. 2013). The shelf region was classified as the area along the transect shoreward of the shelf break region. The offshore shelf break region was classified as the area along the transect offshore of the shelf break region (Figure 51).

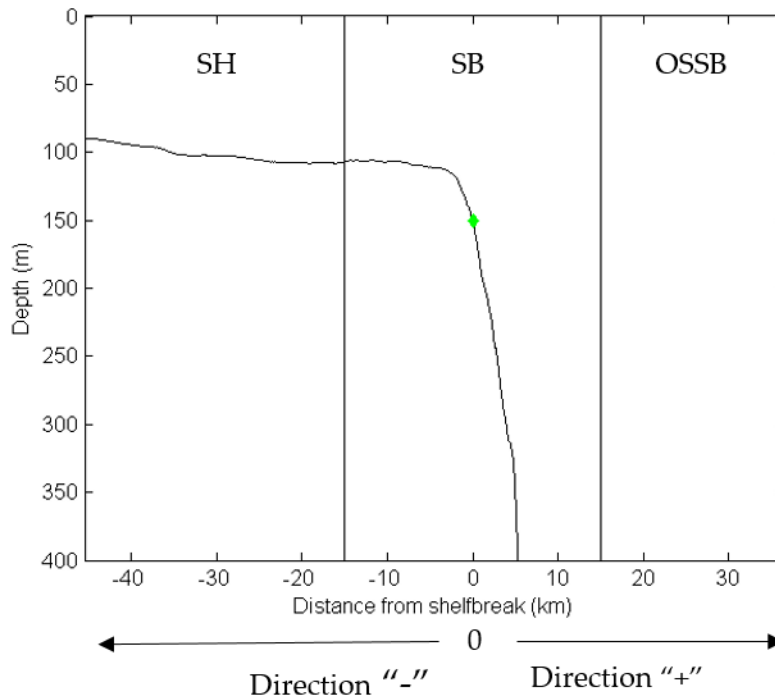


Figure 51: Regions of a shelf break transect. Green dot is the position of greatest bathymetric gradient between 149.0 and 151.0 meters depth. SH = shelf region, SB = shelfbreak region, OSSB = offshore shelfbreak region.

If the position of the shelf break could not be determined from the acoustic data (e.g. the shelf break was not crossed), the distance to the shelf break was calculated from the end of the transect to the 150 m isobath in ArcGIS 10.2 (ESRI 2013). All data in ArcGIS were projected in an Albers Equal Area Conic projection with a modified central meridian specific to the AMAPPS study area. Bathymetric contours were derived from an 88 m resolution bathymetric grid mosaicked from three data sources: Bathymetric

Terrain Model of the Atlantic Margin for Marine Geological Investigations (Andrews et al. 2013), National Geophysical Data Center 3-arc second coastal relief model (NGDC 2012), and the USGS 15 arc second Gulf of Maine gridded dataset (Signell and Roworth 2013).

4.2.3 Physical Environment

Surface water temperature and salinity were sampled every 2 seconds by a Sea Bird Electronics model 45 thermo-salinograph (TSG) during the entire cruise. Post cruise, surface temperature and salinity data were synchronized to the Simrad EK60 acoustic data and all deviations from the trackline were removed. For both temperature and salinity, outliers were determined by comparing the difference between a data point and its neighbors in MATLAB (The MathWorks Inc. 2009). If the difference was greater than a threshold of 0.02, the data were marked and removed. To reduce noise in the TSG data, I smoothed the temperature and salinity data sets with a median filter, window size of 29 (approximately 1 minute of sampling). Density of the near surface water was then calculated using the SEAWATERv3.3 routines (Morgan 1994). To determine the spatial variability in surface temperature, salinity, and density along each transect, a one dimensional gradient analysis of all variables was conducted on the smoothed data using the following equation:

$$\frac{\sum_{i=1}^N \left| \frac{\Delta y_i}{\Delta x_i} \right| \Delta x_i}{\sum_{i=1}^N \Delta x_i}$$

where N is the number of transect segments, Δx is the change in distance along the transect, and Δy is the change in the hydrographic variable of interest. To remove the weighting of the length of each segment, the denominator was added to the gradient analysis. The mean and standard deviation of temperature, salinity, and density for each section (SH, SB, OSSB) were calculated to examine their variability within each section. Distance from each gradient was calculated along each transect.

4.2.4 Active Acoustic Data

The EK60 system on the NOAA ship *Henry B. Bigelow* consists of 5 split-beam transducers operating at 18, 38, 70, 120 and 200 kHz, and are co-located on the ship's retractable centerboard. The beam widths are 7° for all transducers except the 18 kHz transducer, which has a beam width of 11°. Each frequency was transmitted simultaneously at a rate of one ping every two seconds when the vessel was in water depths less than 1000 meters, and one ping every five seconds when the vessel was in water depths greater than 1000 meters. Pulse duration for each frequency was 1.024 milliseconds. All five transducers in the EK60 system were successfully calibrated prior

to the survey using the standard target method (Foote et al. 1987). The ship's survey speed was approximately 5 m/sec (10 kts). Raw acoustic data were collected at 0.19 m vertical resolution, and approximately 10 m (ping every 2 seconds) and 25 m (ping every 5 seconds) horizontal resolution during survey effort. Volume backscatter (S_v) from the 18, 38, 70, 120, and 200 kHz echosounders were processed in Echoview 5.4 (Myriax 2013) to remove intermittent noise, background noise, ringdown effects and echoes from the seafloor. Volume backscattering strength is the summed backscatter of all animals present normalized to the sample volume.

Acoustic backscatter strength from plankton, nekton and fish is frequency-dependent (Stanton et al. 1994, 1996, 2004, Holliday and Pieper 1995, Korneliussen and Ona 2003, Warren et al. 2003, Lawson et al. 2006). To estimate species density, abundance, and biomass from acoustic data, net-tows or visual recorders are typically employed over targeted regions to ground-truth acoustic data (Benoit-Bird and Lawson 2016). However, this was not the case with this survey. Instead, I used multi-frequency analysis methods to classify active acoustic data into broad taxonomic groups without synoptic net-tow data based on the known frequency response of these groups. I follow the general process described in Trenkel and Berger (2013).

The ping rate and ping duration parameters, when at marine mammal survey speed, could not acoustically resolve individual targets. Instead, S_v was analyzed to

determine proxy regions of potential prey. I visually inspected each cross shelf echogram at each frequency to locate regions of intense scattering that could indicate aggregations of middle trophic level taxa as proxies of potential prey and categorized acoustic regions of interest based on the shape of an acoustic region's frequency response curve (e.g. Figure 1 in Lavery et al. 2007), into five groups: fish-like (with swim bladder), nekton-like, plankton-like, U-shaped, and other. Only fish-like, nekton-like, and plankton-like regions of acoustic scattering were used in the marine mammal habitat models.

All categorized scattering regions were determined through a two-step process:

1) a mask was set at a target frequency's echogram to eliminate scattering below a threshold, and 2) the shape of the slope of the frequency response curve within the region was compared to well-established models of fish, euphausiid, and copepod target strength over the frequency range (Stanton et al. 1994, 2004, Lawson et al. 2006, Lavery et al. 2007, Lee and Stanton 2014). For fish-like scattering regions, a -66 dB mask was applied to the 18 kHz S_v echogram (S_v less than -66 dB data were set to no-data). This scattering threshold was chosen based on visual inspection of the echograms and known target strength values of fish with swim-bladders in the Mid-Atlantic Bight (Jech and Michaels 2006). To determine nekton-like scattering, a -100 dB mask was applied to the 120 kHz S_v echogram and to determine plankton-like scattering, a -100 dB mask was

applied to the 200 kHz S_v echogram. Selected regions were exported to MATLAB and the shape and slope of the frequency response curves were compared to target strength models that represented the general taxa investigated (Figure 52). Once categorized, the presence or absence of an acoustic scattering type throughout the water column was tallied and exported to ArcGIS for sampling.

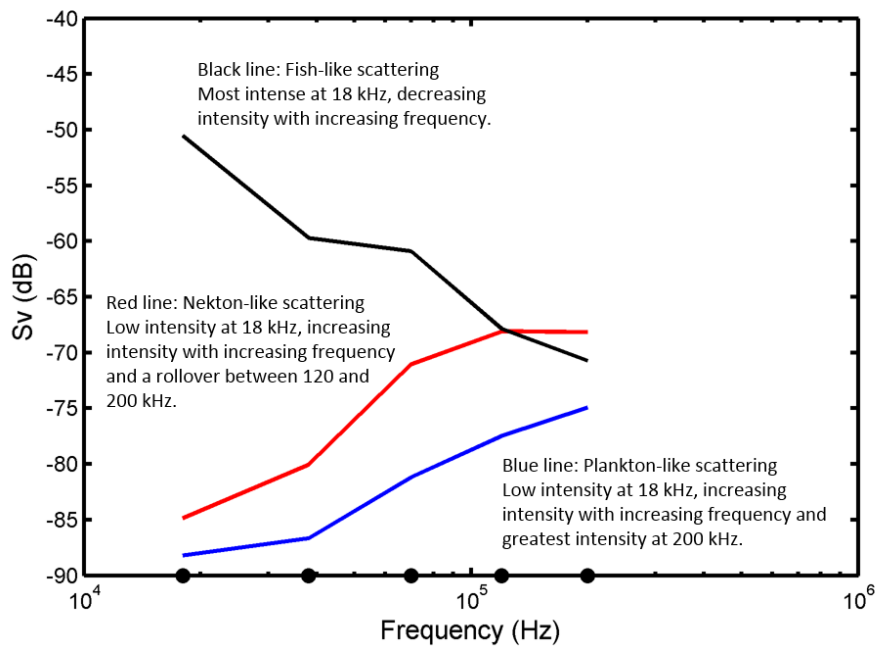


Figure 52: General shapes of frequency response curves used to categorize scattering regions for fish-like scattering (black line), nekton-like scattering (red line) and plankton-like scattering (blue line). Dots are the frequencies from the EK60 (18, 38, 70, 120, and 200 kHz).

4.2.5 Marine Mammal Sightings

Marine mammal sighting data were collected following standard ship-based line transect protocols for two independent teams (Palka 2000) from 0900h to 1800h local time while the ship was traveling at approximately 5 m/sec (10 kts.) in sea states less than Beaufort 5. All marine mammal sighting data were plotted in ArcGIS 10.2 (ESRI 2013) and projected in an Albers Equal Area Conic projection with a modified central meridian specific to the AMAPPS study area. If both observer teams had sightings of the same species in the same location, the marine mammal locations and time of sighting were inspected to determine if the sightings were duplicates. All duplicate sightings were removed and only marine mammal sightings on shelf break transects that coincided with EK60 data collection were analyzed. Marine mammal sightings not directly on the trackline, but within 1 km of the trackline, were relocated to the trackline via their perpendicular sighting distance for environmental, acoustic, and bathymetric sampling.

4.2.6 Presence/Pseudo-Absence Points

An issue with building any habitat model is appropriately sampling data where species are not found. Because the acoustic and hydrographic data were continuously sampled along all transects, allowing for ~10s meter sampling resolution, I created a

fine-scale sampling grid (500 m x 500 m) of polygons along all transects surveyed. Each polygon contained bathymetric, hydrographic, acoustic, and marine mammal attributes. If a sighting of a cetacean species occurred in a cell, it was marked as a presence cell for that species. If no cetacean sighting fell within a cell, it was marked as a pseudo-absence cell. The number of pseudo-absence cells for a species per transect used depended on the number of sightings of that species on that specific transect. For example, if a transect had six cells with common dolphin sightings, six pseudo-absence cells for that transect were randomly selected from the pseudo-absence cells and added to the common dolphin data set.

4.2.7 Analysis Methods

As a preliminary assessment of the fine-scale distribution of cetaceans in the shelf break region of the Mid-Atlantic Bight, the number of sightings for each species in each region of the shelf break transects (SH = shelf, SB = shelf break, OSSB = offshore of the shelf break) was corrected by kilometer of transect surveyed in that region. To test whether cetaceans showed a spatial preference for different acoustic scattering regions, I calculated the shortest distance to from each cetacean sighting to each categorized acoustic region within a transect and visualized the distribution of distances in boxplots. Only distances less than 2.1 km were included based on the assumption that cetaceans

respond to the presence or absence of acoustic scattering regions within their immediate vicinity.

Ecological data are often highly dimensional with nonlinear and complex interactions among variables. Linear statistical methods, such as often-used generalized linear models (GLMs), may be inadequate to discover complex patterns and relationships (De'ath and Fabricius 2000). Classification procedures are now widely used in ecology because of their ability to characterize complex interactions among variables, high classification accuracy, and simple interpretation (Cutler et al. 2007). In this chapter I use two classification procedures, classification trees (Breiman et al. 1984) and random forests (Breiman 2001, Cutler et al. 2007) to explore the relationships between cetaceans and their environment, and delineate habitat areas for common dolphins, Risso's dolphins, and sperm whales. Multidimensional scaling was used to illustrate the environmental separation among common dolphins, Risso's dolphins, and sperm whales.

Classification tree and random forest analyses are flexible, nonparametric approaches to distinguish differences between groups. In this study, both procedures were used to predict the membership of a categorical variable: habitat or not habitat. A classification tree is created by recursively partitioning the data, defined by a rule, based on a single explanatory variable. At each node, a single best predictor is selected to

bifurcate the data (branch the tree) through an optimization that results in the most homogenous subgroup, and the splitting continues until further divisions are no longer optimized (Breiman et al. 1984, De'ath and Fabricius 2000, Cutler et al. 2007). The result is a tree-like structure that traces the conditions that lead to group membership, and is considered "fully grown" (Breiman et al. 1984); however, fully grown trees are over-fitted due to the nature of the model optimization. To correct for over-fitting, trees were "pruned" by removing the low-level splits based on the cost complexity criterion, c_p . The level of pruning was chosen as the largest value of c_p such that the estimate of the 10-fold cross-validation error was less than the minimum cross-validation error plus one standard deviation.

Random forest models fit many classification trees to a data set and then combine the predictions from all the trees (Cutler et al. 2007). Random forest analysis provides an avenue for error estimation on small data sets, such as this one where independent model validation is not available. Random forests also provide measures of variable importance and measures of similarity of point data that can be used for multidimensional scaling (Cutler et al. 2007). Partial dependence plots (Hastie et al. 2009) are used to graphically characterize relationships between predictor variables and predictions of habitat classification obtained from the random forest. For a binary classification, partial dependence plots are on the logic scale (Cutler et al. 2007,

Appendix C). For error estimation, the random forest algorithm first selects bootstrap samples from the data. Observations in the original data set that do not occur in a bootstrap sample are called out-of-bag observations (OOB). A classification tree is fit to each bootstrap sample, but at each node, only a small number of randomly selected variables are entered into the model for binary partitioning. Trees are fully grown and each tree is used to predict the OOB observations. The predicted class of an observation is determined by majority vote of the OOB predictions for that observation. Accuracies and error rates are computed for each observation using the OOB predictions and then averaged over all observations. OOB estimates are essentially cross-validated accuracy estimates because the OOB observations are not used in the fitting of the trees.

Probabilities of membership in the different classes are estimated by the proportions of OOB in each class (Strobl et al. 2007, Cutler et al. 2007, Opper and Huettmann 2010).

Classification tree and random forest analyses were performed on presence/absence data for common dolphins (57 presence cells/57 pseudo-absence cells), Risso's dolphins (55 presence cells/55 pseudo-absence cells) and sperm whales (23 presence cells /23 pseudo-absence cells). Potential habitat variables included six environmental variables (temperature, salinity, density, directional distance from the shelf break, directional distance from the thermal gradient, and directional distance from the density gradient), two bathymetric variables (water depth and bathymetric slope),

two geographic variables (area location and transect region), and three acoustic proxies for biological variables (presence/absence of fish-like backscatter, presence/absence of nekton-like acoustic backscatter, presence/absence of plankton-like backscatter) (Table 4).

Table 4: Predictors variables for classification tree and random forest models.
^oC = degree Celsius. PSU = practical salinity units. P/A = presence/absence.

Predictor		Data Type	Unit
Environmental	Temperature	Continuous	^o C
	Salinity	Continuous	PSU
	Density	Continuous	kg m ⁻³
	Direction/Distance from temperature front	Continuous	+/- km
	Direction/Distance from density front	Continuous	+/- km
	Direction/Distance from shelf break	Continuous	+/- km
Bathymetric	Water depth	Continuous	m
	Bathymetric slope	Continuous	Degrees
Geographic	Area location	Categorical	MAB or GB
	Transect region	Categorical	SH/SB/OSSB
Acoustic	Presence/Absence of fish-like backscatter	Categorical	P / A
	Presence/Absence of nekton-like backscatter	Categorical	P / A
	Presence/Absence of plankton-like backscatter	Categorical	P / A

All statistical analyses were performed in R (R Core Team 2014) with the addition of the package 'rpart' (Therneau et al. 1997) to perform the classification tree analysis and 'randomForest' (Liaw and Wiener 2002) to perform random forest analysis.

4.3 Results

4.3.1 Cetacean Sightings

During the 2011 summer Atlantic Marine Assessment Program for Protected Species (AMAPPS) ship-based survey in the Mid-Atlantic Bight, 23 species of cetaceans and one guild (*Globicephala* sp.) were sighted within the entire AMAPPS study area (Figure 53, Table 5). Harbor porpoise (*Phocoena phocoena*) were only sighted over the continental shelf. Pantropical spotted dolphin (*Stenella attenuata*) and white-sided dolphin (*Lagenorhynchus acutus*) were only sighted on the shelf break transects. Clymene dolphin (*Stenella clymene*), rough-toothed dolphin (*Steno bredanensis*), killer whale (*Orcinus orca*), short-finned pilot whale (*Globicephala macrorhynchus*), dwarf sperm whale (*Kogia sima*), and Gervais beaked whale (*Mesoplodon europaeus*) were only sighted on the offshore transects. Only cetacean species sighted on shelf break transects were analyzed in this chapter.

Sixteen species of cetaceans were sighted on the shelf break transects. Of the 16 species, 9 species had an adequate amount of sightings, or could be put into a guild to pool sighting data, for further analysis (Figure 54, Table 6).

Table 5: All cetacean species sighted during the 2011 summer AMAPPS ship-based survey in the Mid-Atlantic Bight.

Scientific name	Common Name	# sightings on shelf transects	# sightings on shelf break transects	# sightings on off-shore transects	Total
<i>Phocoena phocoena</i>	Harbor porpoise	4			4
<i>Stenella frontalis</i>	Atlantic spotted dolphin		6	28	34
<i>Stenella attenuata</i>	Pantropical spotted dolphin		1		1
<i>Stenella coeruleoalba</i>	Striped dolphin		35	58	93
<i>Delphinus delphis</i>	Common dolphin	32	185	14	231
<i>Stenella clymene</i>	Clymene dolphin			1	1
<i>Lagenorhynchus acutus</i>	White-sided dolphin		1		1
<i>Tursiops truncatus</i>	Bottlenose dolphin	18	101	24	143
<i>Grampus griseus</i>	Risso's dolphin		134	49	183
<i>Steno bredanensis</i>	Rough-toothed dolphin			4	4
<i>Orcinus orca</i>	Killer whale			1	1
<i>Globicephala melas</i>	Long-finned pilot whale		1		1
<i>Globicephala macrorhynchus</i>	Short-finned pilot whale			3	3
<i>Globicephala sp.</i>	Pilot whales		62	8	70
<i>Kogia sima</i>	Dwarf sperm whale			13	13
<i>Kogia breviceps</i>	Pygmy sperm whale		4	8	12
<i>Physeter macrocephalus</i>	Sperm whale		37	53	90
<i>Ziphius cavirostris</i>	Cuvier's beaked whale		18	29	47
<i>Mesoplodon europaeus</i>	Gervais beaked whale			5	5
<i>Mesoplodon bidens</i>	Sowerby's beaked whale		14	2	16
<i>Balaenoptera physalus</i>	Fin whale		64	1	65
<i>Balaenoptera borealis</i>	Sei whale		10		10
<i>Balaenoptera acutorostrata</i>	Minke whale	16	6		22
<i>Megaptera novaeangliae</i>	Humpback whale	1	23	2	26

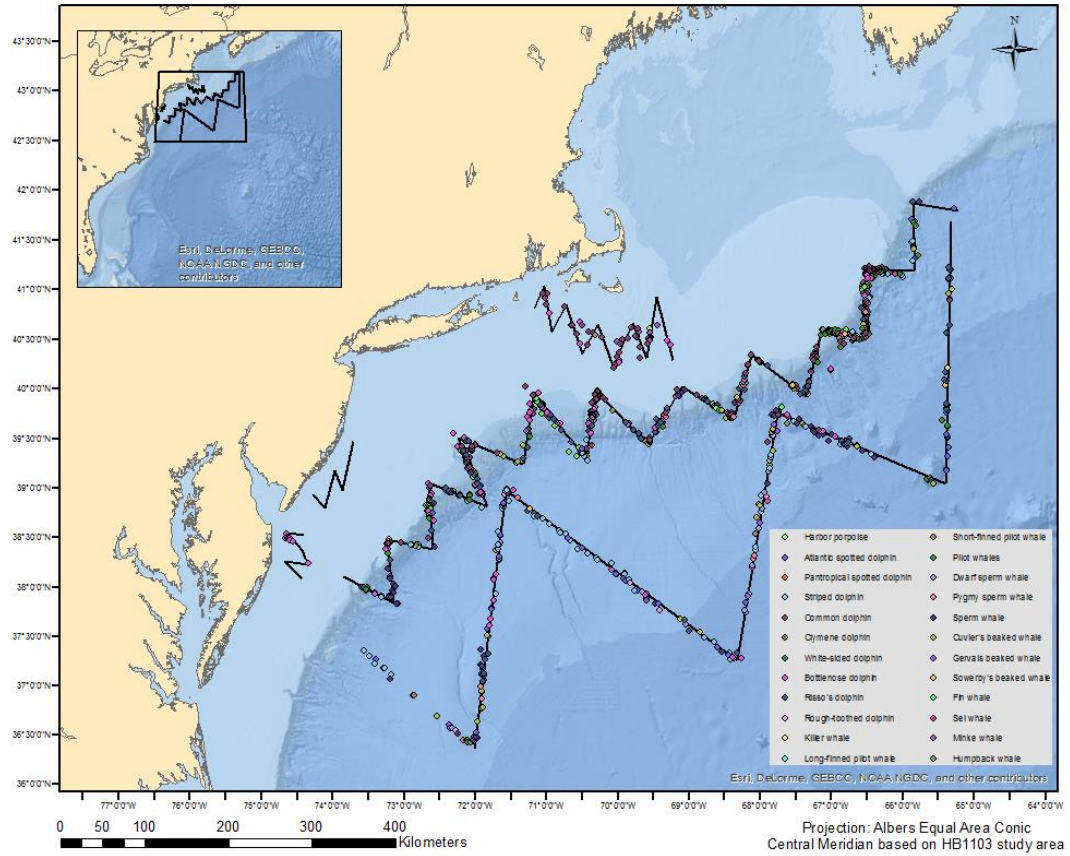


Figure 53: Geographic locations of all cetacean sightings during the 2011 summer, ship-based AMAPPS survey

Table 6: Cetacean species sighted on shelf break transects during the 2011 summer AMAPPS ship-based survey in the Mid-Atlantic Bight

Transects (coincident transects grouped)	Location	Striped dolphin	Common dolphin	Bottle-nose dolphin	Risso's dolphin	Pilot whale	Sperm whale	Cuvier's beaked whale	Sowerby's beaked whale	Fin whale	Total by trackline
lg1Acln01	MAB			10	7	1	3				21
lg1Acln02	MAB		9	3	5			1			18
lg3AclnXBT11	MAB				3						3
lg1Acln03	MAB				3	1		1		1	6
lg1Acln04	MAB	1	2		1			3			7
lg2Acln03	MAB		4	1	4						9
lg1Acln05	MAB		2	8	12	1	1	1		9	34
lg2Acln02	MAB		4	7	10		1				22
lg1Acln11	GB		1								1
lg3AclnXBT07	GB		9								9
lg1Acln13	MAB	1		2	8	1	1		1	1	15
lg2Acln01	MAB	1	1			1					3
lg1Acln14	MAB	4	1	2	1			2	1		11
lg1Acln15	MAB		5	2	1	1	7				16
lg1Acln16	MAB			3	2	2	7		2		16
lg1Acln19	MAB	1			2	1	3				7
lg3Acln05	GB				1		1				2
lg3Acln06	GB	3	2		1	7		1			14
lg3AclnXBT03	GB	9	34			9	1			1	54
Total by species		20	74	38	61	25	25	9	4	12	268

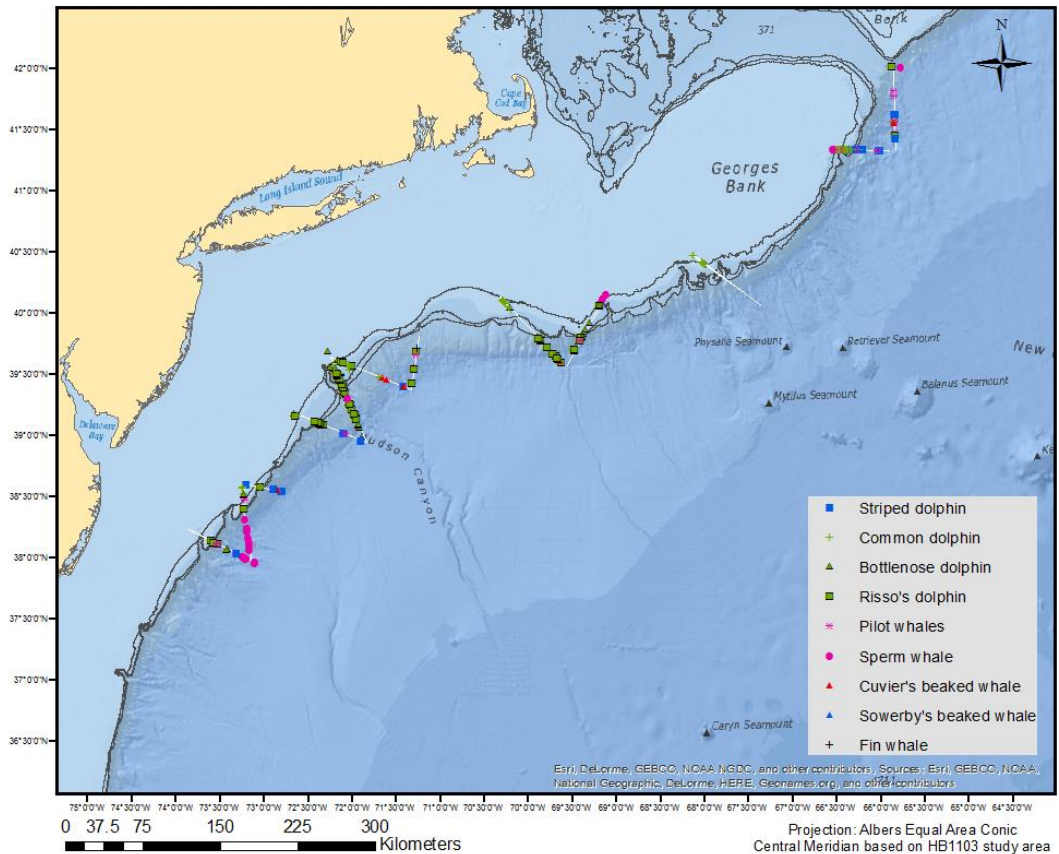


Figure 54: Geographic locations of cetacean sightings along shelf break transects during the 2011 summer ship-based AMAPPS survey. Only shelf break transects with concurrent EK60 data were analyzed.

As a preliminary step in examining the distribution of cetaceans within the shelf break region of the Mid-Atlantic Bight, the number of cetacean sightings was corrected by kilometer of trackline surveyed for all transects, and by kilometer of trackline surveyed in each region of a transect (SH = shelf, SB = shelf break, OSSB = offshore of the shelf break). Common dolphins were the most sighted cetacean species among all

transects and the most sighted species within shelf and shelf break regions. Risso's dolphins were the second most sighted cetacean species with the greatest concentration of sightings within the shelf break region. Bottlenose dolphins were the third most sighted cetacean species and were mostly sighted over the shelf and within the shelf break region. Sperm whales and pilot whales were the fourth most sighted cetacean species, with pilot whale sightings equally concentrated within the shelf break and offshore regions while sperm whale sightings were concentrated in the offshore regions (Figure 55). Habitat models were built for common dolphins, Risso's dolphins, sperm whale, bottlenose dolphins, and pilot whales. However, the bottlenose dolphin and pilot whale error rates were over 50% and are not reported here.

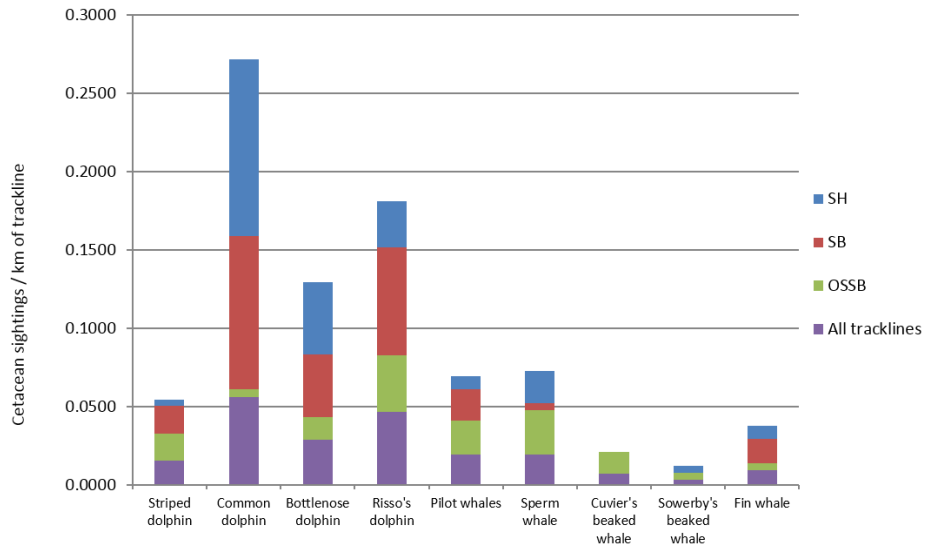


Figure 55: Cetacean sightings per km of trackline. SH shelf region. SB - shelf break region. OSSB – offshore of the shelf break region.

4.3.2 Distribution of Distances from Cetacean Sightings to Categorized Acoustic Regions

The range of distances between cetacean species sightings and categorized acoustic regions was 0.1 km to 2.1 km (the cut off value). Boxplots created to visualize the straight-line distance between cetacean sightings and closest point to a categorized acoustic region. No significant pattern of distances between cetacean sightings and acoustic regions was apparent (Figure 56).

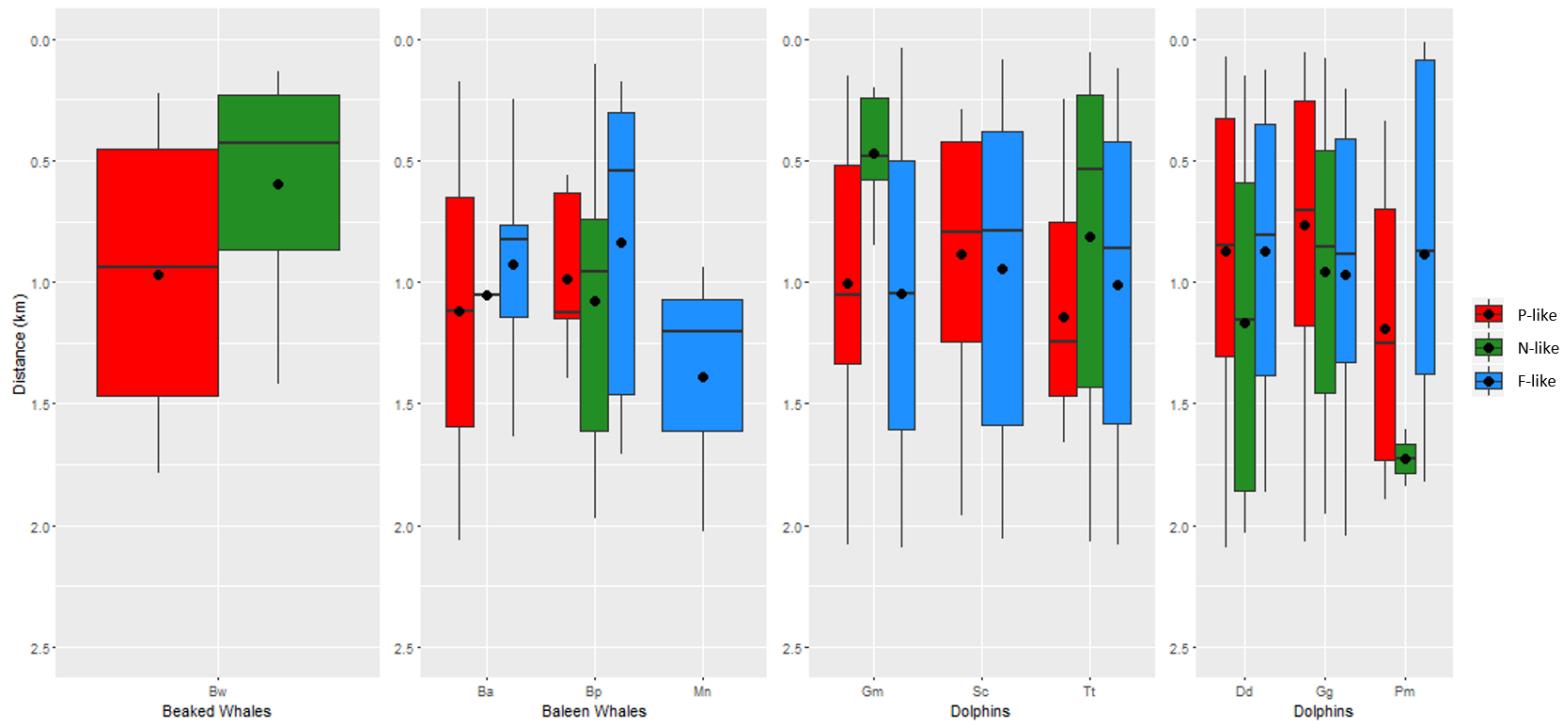


Figure 56: Boxplots of closest distance (km) between marine mammal sightings and categorized acoustic regions. Red = plankton-like scattering regions ("P-like"). Green = nekton-like scattering regions ("N-like"). Blue = fish-like scattering regions ("F-like"). Bw = beaked whale (*Mesoplodon* sp. and *Ziphius*). Ba = minke whale, Bp = fin whale, Mn = humpback whale, Gm = pilot whale, Sc = striped dolphin, Tt = bottlenose dolphin, Dd = common dolphin, Gg = Risso's dolphin, Pm = sperm whale. Y-axis, distance in kilometers with 0 at top of the panels. Horizontal lines within boxes are the medians. Dots are the means.

4.3.3 Multidimensional scaling, Classification Trees and Random Forests

The multidimensional scaling plot (Figure 57) indicates environmental separation among common dolphins, Risso's dolphins, and sperm whales. There are areas of overlap between common dolphins and Risso's dolphins. Sperm whales cluster in two regions, overlapping with both common dolphins and Risso's dolphins (Figure 57). The areas of overlap most likely occur because all three species were sighted at the head of canyons, which is indirectly accounted for in all of the variables, but not directly included in the models.

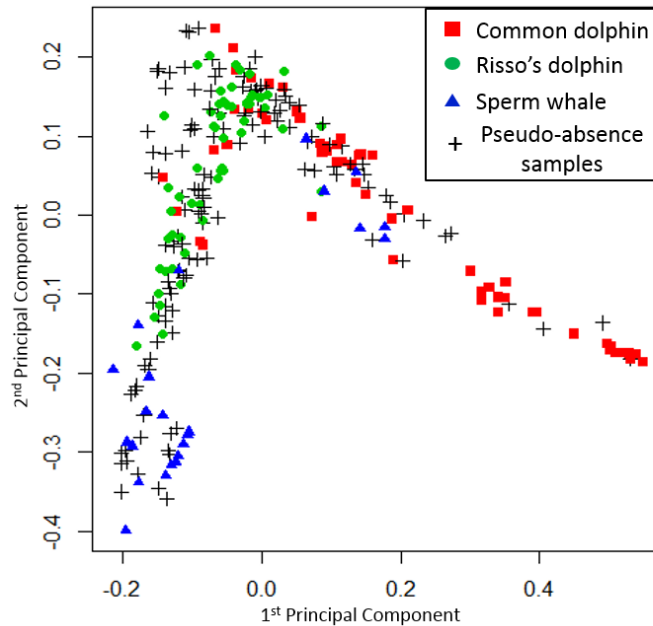


Figure 57: Multidimensional scaling plot of model variables at cetacean sighting locations and at pseudo-absense locations.

Habitat classification from the classification tree model and the random forest model suggests habitat partitioning among common dolphins, Risso's dolphins, and sperm whales within the shelf break region of the Mid-Atlantic Bight. The habitat model results for each species are presented in the following sections. For each classification tree, pink terminal nodes indicate non-habitat and blue terminal nodes indicate habitat. In each terminal node, the top line is the node's classification (not habitat or habitat), the middle line contains the probability of both not-habitat and habitat, and the bottom line

indicates the amount of data used (see Node Classification in Figure 58). Variable importance plots from the random forest outputs provide the mean decrease in the percentage of observations that are correctly classified; variables with the greatest mean decrease in accuracy are more important habitat classifiers. For common dolphins (Figures 58 and 59) and Risso's dolphins (Figures 62 and 63), the primary and secondary bifurcations in the classification tree agree with the first two important variables given in the random forest output. The sperm whale classification model and random forest model were based on distance from temperature fronts (Figures 66 and 67). OOB error estimates are the proportion of time a data point is misclassified during bootstrapping. The sperm whale habitat model misclassified habitat data 30% of the time (0.30). The common dolphin model misclassified habitat 36% of the time (0.36) and the Risso's dolphin model misclassified habitat 37% of the time (0.37) (Table 7).

Table 7: Combined confusion matrix based on random forest out-of-bag classification error for each model.

Species	Classification	Not Habitat	Habitat	Class Error
Common dolphin	Not Habitat	40	17	0.30
	Habitat	21	36	0.36
Risso's dolphin	Not Habitat	31	24	0.43
	Habitat	21	35	0.37
Sperm whale	Not Habitat	15	8	0.35
	Habitat	7	16	0.30

4.3.3.1 Common dolphin results

The largest value of c_p where the estimate of the 10-fold cross-validation error was less than the minimum cross-validation error plus one standard deviation for the common dolphin habitat model was 0.039, resulting in three classification tree branches with two terminal nodes classified as habitat (Figure 58). Water depth less than 148 m was the primary variable selected by the classification tree to describe common dolphin habitat. The second split, leading to the first terminal node, was water depth greater than and equal to 98 m. The first habitat classification node classified 45% of the data, with an 80% probability of habitat classification. The second habitat node included

temperature greater than or equal to 22 °C with 100% probability of habitat classification using 4% of the data. Following the tree's classification scheme, common dolphin habitat is between 98 and 148 m water depth and in temperatures greater than 22 °C in water depths less than 98 m.

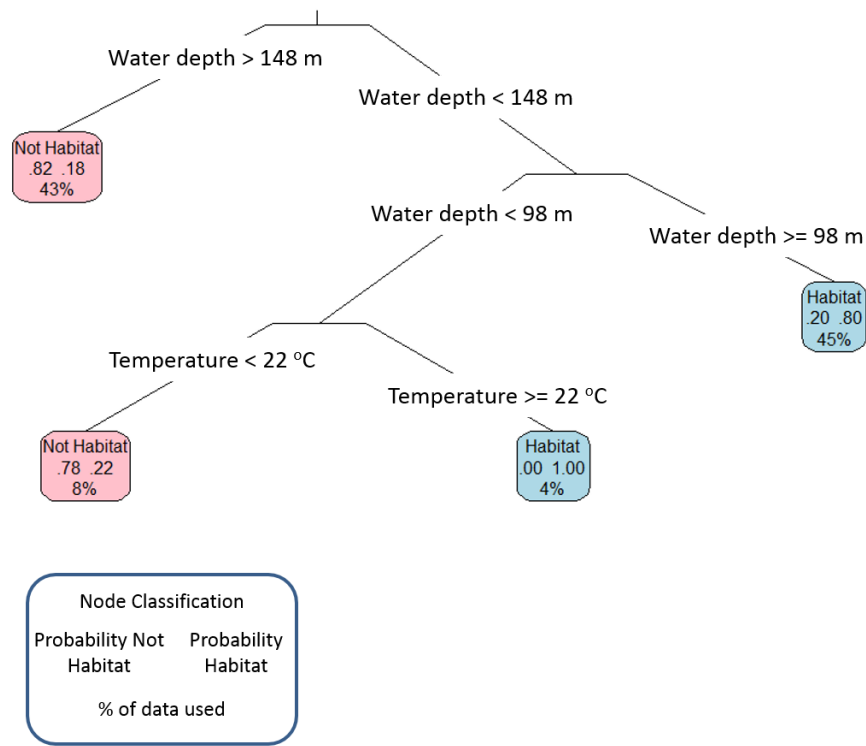


Figure 58: Classification tree output for common dolphin habitat. Pink nodes = not habitat. Blue nodes = habitat. The decimals (middle line in pink and blue nodes) are the probability of 'not habitat' and probability of 'habitat'. The bottom number is the percentage of data classified at that node.

According to the random forest variable importance metric, distance from shelf break and water depth were the two most important variables for common dolphins (Figure 59).

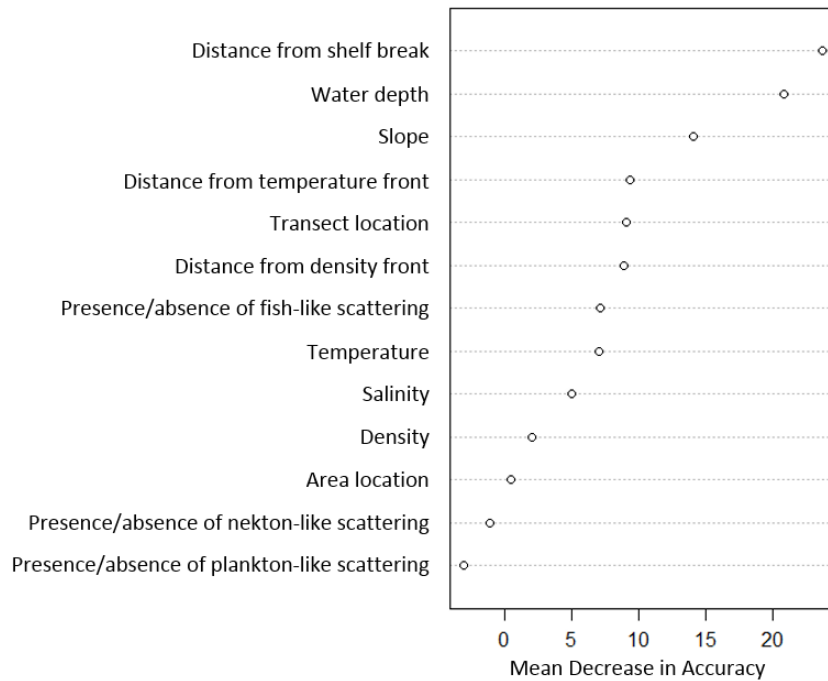


Figure 59: Random forest variable importance for common dolphin habitat.

Partial plots (Figure 60) of these two variables are interesting because the plots are nonlinear. Within the shelf break region, the probability of common dolphin habitat is greater over shelf-side distances to the shelf break, drops rapidly near the shelf break and remains low offshore of the shelf break. For water depth, the greatest probability of

habitat is narrowly defined as shallow water (< 150 m) areas, similar to the classification tree results.

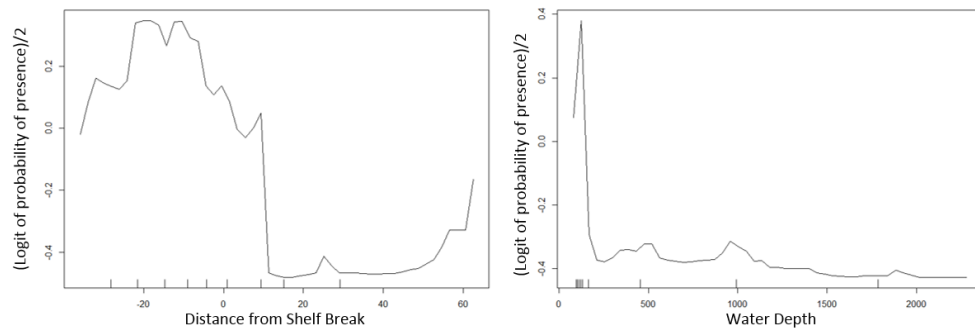


Figure 60: Partial dependence plots of random forest classification for common dolphin habitat. Partial dependence is the dependence of the probability of presence on one predictor variable after averaging out the effect of the other predictor variables in the model.

When mapped back into geographic space, common dolphin habitat mostly occupies the shelf region of the shelf break transects (Figure 61).

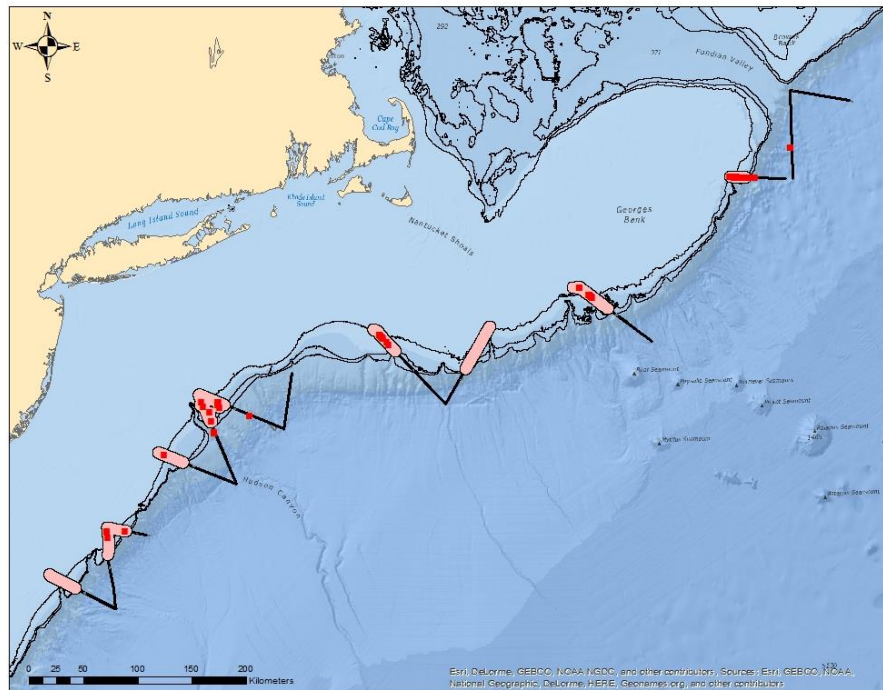


Figure 61: Common dolphin habitat (pink polygons) along transects with common dolphin sightings (red squares).

4.3.3.2 Risso's dolphin results

The c_p value for the Risso's dolphin classification model was 0.051, resulting in three classification tree branches with one terminal node classified as habitat (Figure 62). Distances less than 36 km on the offshore side of the surface density front was the primary variable selected by the classification tree to describe Risso's dolphin habitat. The second split was temperature greater than or equal to 19 °C, and the third split was

salinity less than 36 PSU (Figure 62). The habitat classification node classified 59% of the data, with a 72% probability of habitat classification. Following the tree's classification scheme, Risso's dolphin habitat is in waters less than 36 PSU, surface water temperatures greater than or equal to 19 °C, and within 36 km offshore of a density front.

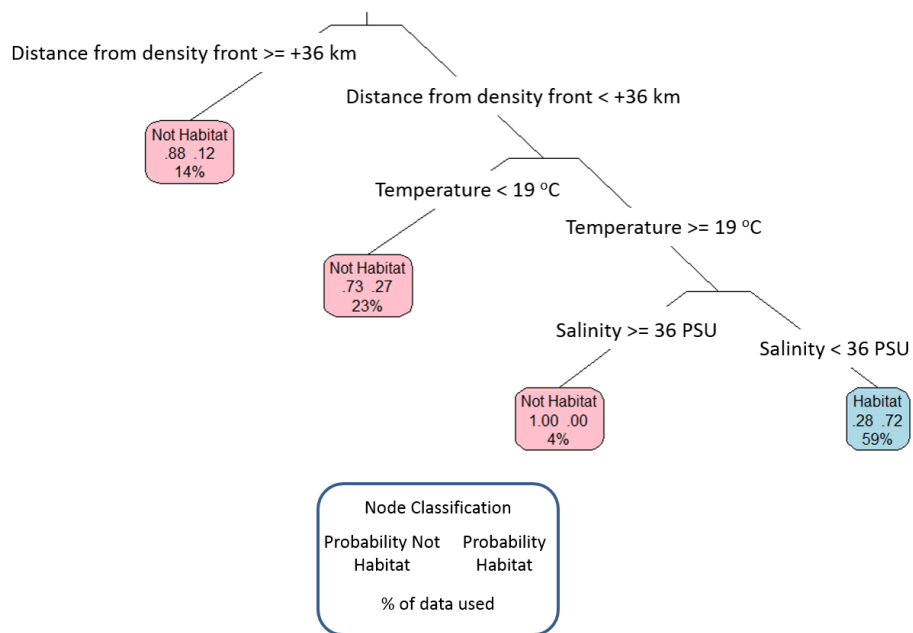


Figure 62: Classification tree output for Risso's dolphin habitat. Pink nodes = not habitat. Blue nodes = habitat. The decimals (middle line in pink and blue nodes) are the probability of 'not habitat' and probability of 'habitat'. The bottom number is the percentage of data classified at that node.

The random forest variable importance metric and classification tree both selected the same two variables, temperature and distance from density front, but in different order (Figure 63).

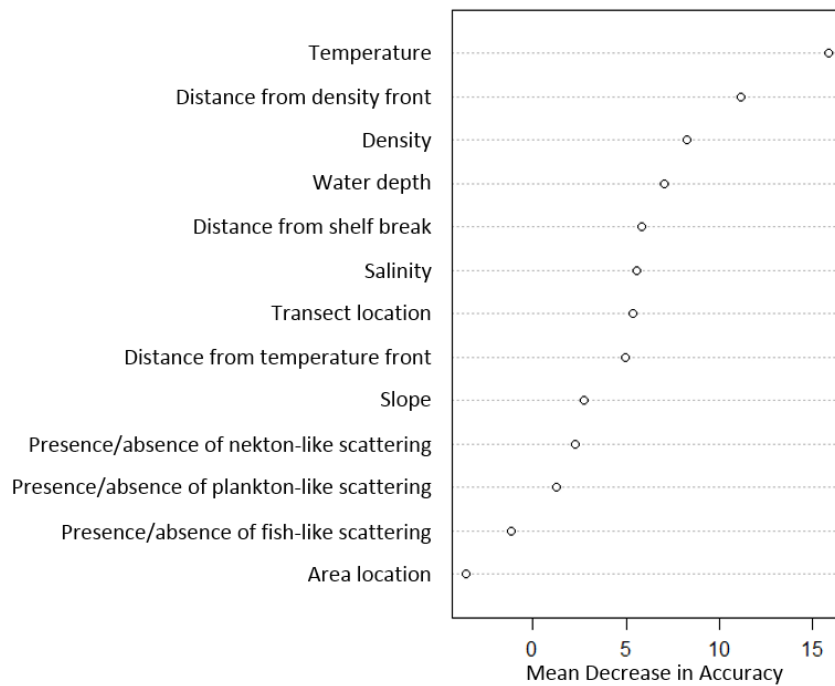


Figure 63: Random forest variable importance for Risso’s dolphin habitat.

The partial dependence plot of Risso’s dolphin habitat, with respect to temperature (Figure 64, left panel), indicates a linear but uninformative relationship at temperatures less than 19 °C, a sharp rise in predicted habitat above 19 °C, followed by a decline in predicted habitat that levels off at warmer temperatures. The shape of this

plot suggests that Risso's dolphin habitat is most likely in a surface water temperature range of 19 °C to 22 °C. The partial dependence plot of Risso's dolphin habitat with respect to distance from density front (Figure 64, right panel) indicates a more complex relationship. However, a decline in predicated habitat at distances greater than 20 km offshore of the density front is apparent.

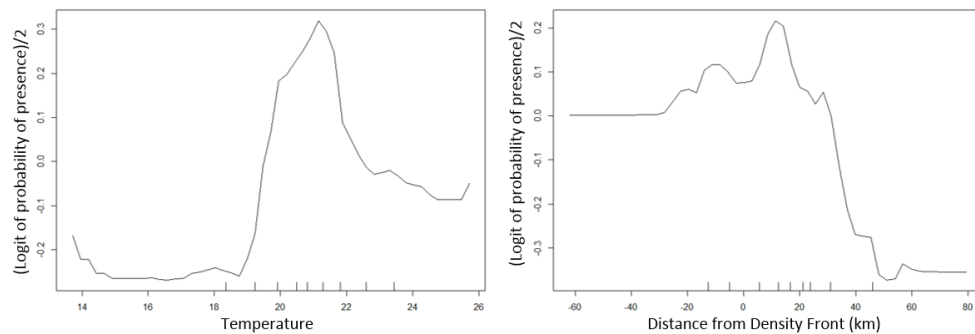


Figure 64: Partial dependence plots of random forest classification for Risso's dolphin habitat. Partial dependence is the dependence of the probability of presence on one predictor variable after averaging out the effect of the other predictor variables in the model.

When mapped back into geographic space, Risso's dolphin habitat mostly occupies the shelf break region and ranges offshore, but includes areas on the continental shelf at the head of canyons (Figure 65).

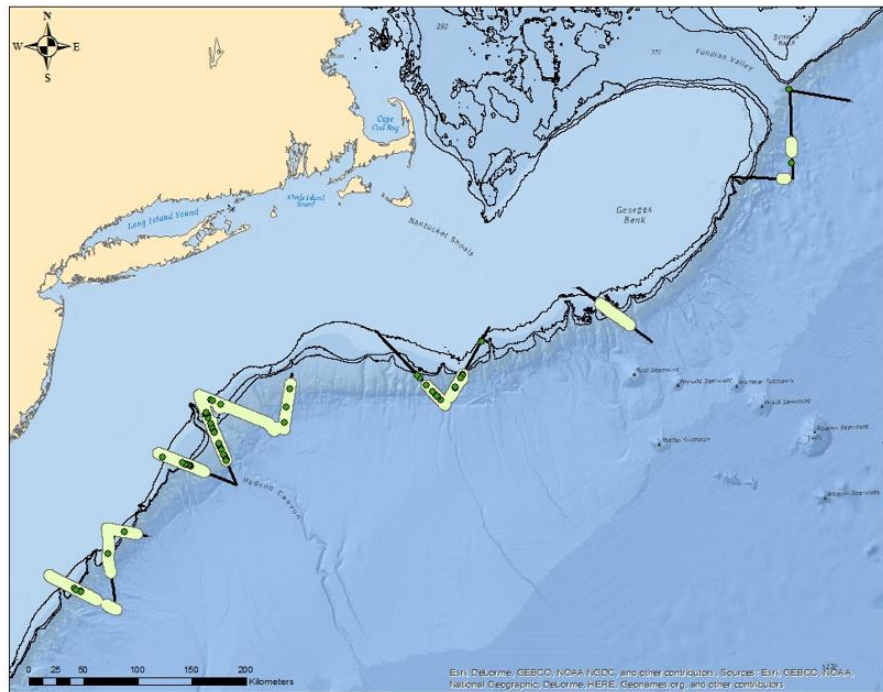


Figure 65: Risso's dolphin habitat (light green polygons) along transects with Risso's dolphin sightings (green circles).

4.3.3.3 Sperm whale results

The c_p value for the sperm whale classification model was 0.15, resulting in two classification tree branches with two terminal nodes classified as habitat (Figure 66). Distances greater than or equal to 29 km on the offshore side of the surface temperature front was the primary variable selected by the classification tree to describe sperm whale habitat. The second split was also distance from temperature front; however this split indicated directional distance towards shelf regions (Figure 66). The first habitat

classification node classified 24% of the data, with a 91% probability of habitat. The second habitat classification node classified 13% of the data with 100% probability of habitat. Following the tree's classification scheme, sperm whale habitat is in areas greater than 29 km offshore of surface temperature fronts, and in areas less than 34 km shoreward of temperature fronts.

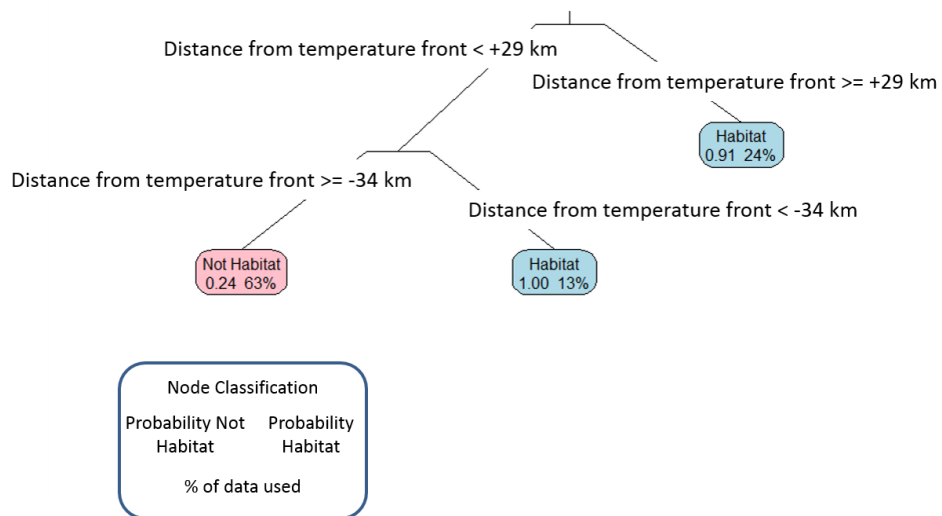


Figure 66: Classification tree output for sperm whale habitat. Pink nodes = not habitat. Blue nodes = habitat. The decimals (middle line in pink and blue nodes) are the probability of 'not habitat' and probability of 'habitat'. The bottom number is the percentage of data classified at that node.

The random forest model also selected distance from temperature front as the most important variable (Figure 67). Interestingly, there is a large gap in the variable importance metric between distance from temperature front and the second most important variable, density, indicating that sperm whale habitat is much more closely tied to temperature fronts than any of the other variables examined.

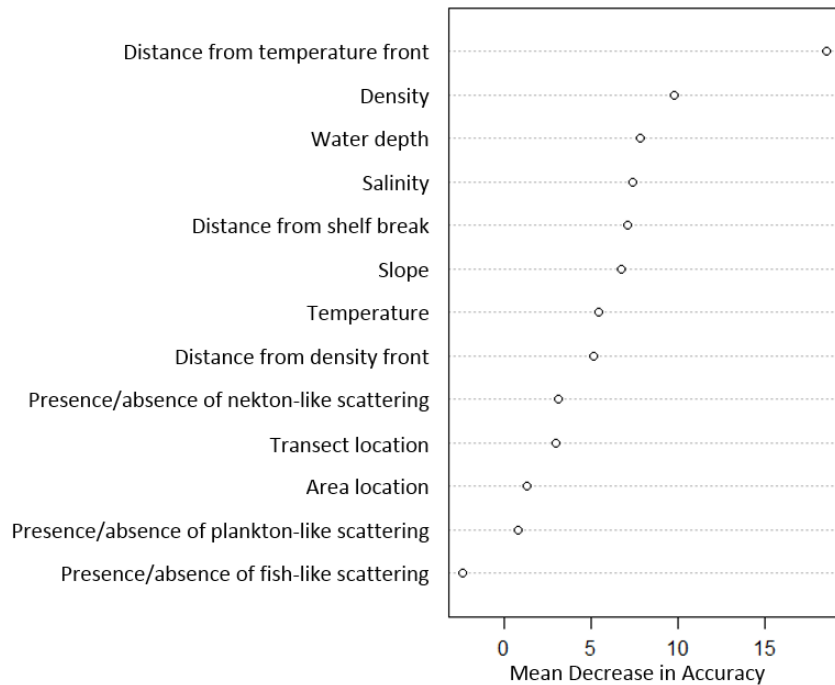


Figure 67: Random forest variable importance for sperm whale habitat.

The partial dependence plot of sperm whale habitat, with respect to distance from temperature fronts (Figure 68, left panel), shows a bimodal relationship that captures areas well offshore but also captures shallow water areas over the shelf. The partial dependence plot of sperm whale habitat, with respect to density (Figure 68, right panel) suggests a high probability of habitat in a narrow density range, approximately 24 to 24.5 kg m⁻³. Because water surface density is a function of water temperature and salinity at the surface, I also examined the distribution of water temperature and salinity values at sperm whale sightings to understand why there was a high probability of sperm whale habitat in narrow density range. Both surface temperature and salinity values at sperm whale sightings were centered on warmer, more saline values (25 °C, 36 PSU) with the tails of each distribution indicating cooler, less saline waters. If shelf areas are sperm whale habitat, as the distance from temperature front variable metric suggests, then shelf water temperatures and salinities should be apparent. Shelf water temperatures and salinities were not apparent.

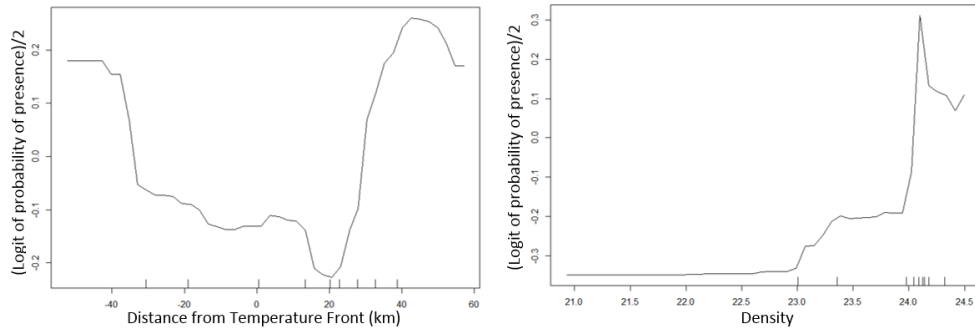


Figure 68: Partial dependence plots of random forest classification for sperm whale habitat. Partial dependence is the dependence of the probability of presence on one predictor variable after averaging out the effect of the other predictor variables in the mode

When mapped back in to geographic space, sperm whale habitat mostly occupies areas offshore in the Mid-Atlantic Bight shelf break region, but includes areas on the continental shelf at the head of canyons (Figure 69).

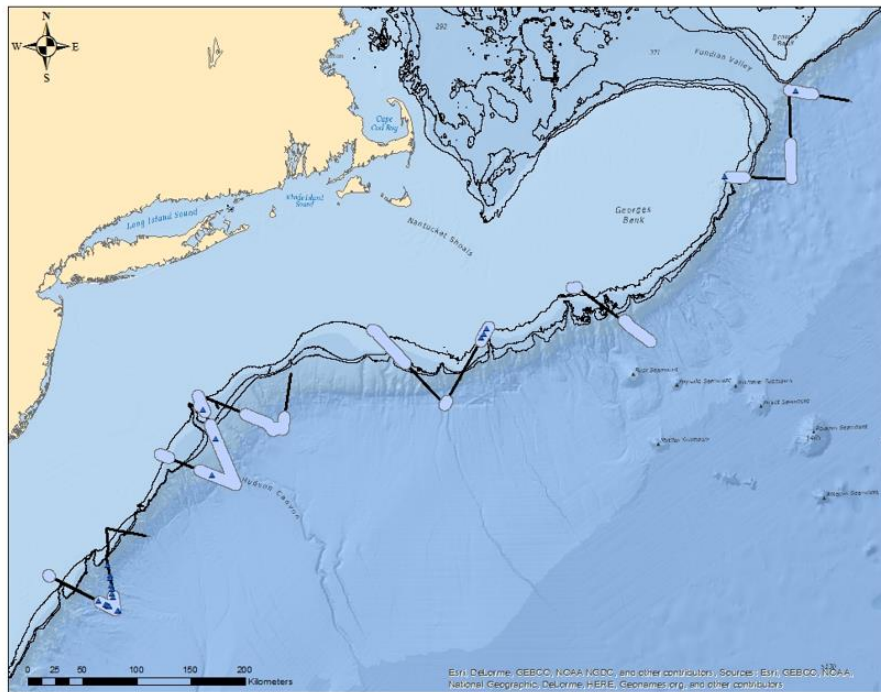


Figure 69: Sperm whale habitat (blue polygons) along transects with sperm whale sightings (blue triangles).

4.4 Discussion

This study of cetacean distribution within the shelf break system of the Mid-Atlantic Bight is the first to show fine-scale habitat delineations in a known regional cetacean hotspot. Within the shelf break system, common dolphin habitat is in shallow water over the shelf, Risso’s dolphin habitat is at the shelf break and slightly offshore of the shelf break, and sperm whale habitat is in the deeper, warmer, and more saline waters offshore as well as at the head of canyons. Although there is some spatial habitat

overlap among these species, especially at the head of canyons, their distributions encompass different regions of the shelf break area. It is possible that other cetacean species in the Mid-Atlantic Bight would show fine scale habitat preferences, but data were not sufficient to run tree models with classification errors below 0.5 for the other species. For example, there were more bottlenose dolphin sightings (38) than sperm whale sighting (25), but bottlenose dolphin classification tree and random forest models could not correctly classify a bottlenose dolphin data point more than 50% of the time. Bottlenose dolphins were sighted in all three regions of the transects, and they were sighted with equal frequency within the shelf and shelf break transect regions. Although there were enough data to build a bottlenose dolphin habitat model, the model could not find homogenous splits due the wide range of environmental variability across the bottlenose dolphin sightings.

Interestingly, the most important habitat classifiers for each species were different, lending more evidence to fine scale habitat delineation among common dolphins, Risso's dolphins, and sperm whales. The most important habitat classifiers also varied between static variables (depth for common dolphins) and dynamic variables (distances to density fronts for Risso's dolphins and distances to temperature fronts for sperm whales), suggesting that even within a hydrographically dynamic region where cross-shelf exchange is common, distribution of at least one species of

cetacean is described by a stationary descriptor. The results from the sperm whale habitat model were the most surprising considering the on-shore distance to temperature fronts. This seems counterintuitive considering sperm whales are well known to utilize the shelf edge and offshore waters (CeTAP 1982, Waring et al. 1993, 2014). After inspecting the sperm whale sighting data, I believe the predicted habitat over shelf areas is an artifact of the sperm whale sightings at the head of canyons. Because the nature of these data are linear (along transects), sightings at the head of canyons would appear as sightings in shallow water. I built models that incorporated distance from the head of canyons to try to capture this relationship, but adding that variable increased the misclassification rate to over 50%.

The presence or absence of categorized acoustic regions did not inform the habitat classification models. One possible reason for this is that acoustic regions were not correctly categorized. Every effort was made to categorize the acoustic scattering regions correctly within broad taxonomic categories but without trawl data to ground-truth the acoustic classifications, uncertainty around the acoustic classifications is high. All of the fish-like acoustic scattering regions presented a frequency response shape that matched generalized fish-like scattering models (most intense scattering at 18 kHz, decreasing in scattering intensity with increasing frequency), but in many cases, the slope of these frequency response curves was much greater than expected for fish with

swim bladders. These scattering regions could have been aggregations of squid (Benoit-Bird and Lawson 2016), possibly siphonophores (Warren et al. 2001), or mixed assemblages. Additionally acoustic and visual surveys were only conducted during daylight hours and these three species of cetacean are known to forage at night (Overholtz and Waring 1991, Shane 1995, Clarke 1996, Pusineri et al. 2007).

No obvious spatial patterns of the distance between cetaceans and acoustic regions of interest were apparent (Figure 56). However, this lack of patterns is interesting in itself. I expected that bottlenose dolphins, striped dolphins and common dolphins would be sighted significantly closer to regions of fish-like scattering than regions of nekton-like and plankton-like regions. I also expected that fin whales would be sighted closer to nekton-like scattering regions than fish-like scattering regions. The lack of a significant pattern between cetacean sightings and categorized acoustic regions is probably due, in part, to the generality of the acoustic categorizations and/or because data were daylight-biased. Because individual targets could not be resolved in the acoustic data, it is likely that the acoustic regions selected are probably mixed assemblages of middle trophic level prey species and non-prey species. Additionally, calculating the shortest distance between sightings and acoustic regions might not be ecologically relevant. Many of the acoustic regions span 10s of meters to kilometers horizontally and 10s of meters vertically, and the intensity of scattering is not uniformly

distributed through the region, suggesting differences in species assemblage or non-uniform density of animals. With the size of these regions and the fact that sightings were only recorded on the surface, it is possible that cetaceans are targeting other areas of the categorized acoustic regions.

Fish and plankton distributions in marine ecosystems are influenced by hydrologic features such as upwelling, thermal stratification, eddies and fronts (Olson and Backus 1985, Mann and Lazier 1991, Olson et al. 1994). As a result of these physical processes and animal behavior (Haury and Wiebe 1982, Mackas et al. 1985, Simard and Mackas 1989, Barange 1994), biological patchiness is considered a prominent feature of the marine environment (Steele and Henderson 1992) with the intensity of patchiness increasing in areas of upwelling, eddies and fronts (Owen 1981, Mackas et al. 1985, Olson and Backus 1985, Nash et al. 1989, Nero et al. 1990, Aoki and Inagaki 1992). This patchiness holds true for cetaceans as well. Patterns in species distributions can be overlooked if the scale at which the data are collected is too small, or patterns can be smoothed over if the scale is too large (Levin 1992). The shelf break in the Mid-Atlantic Bight is well known area of high cetacean density and diversity within the regional scale context of the U.S. Atlantic waters and even at the broader spatial scale of the North Atlantic. My research demonstrates that there are also fine scale components to cetacean distributions within this dynamic region that need to be studied further.

5. Summary and Future Directions

Effective conservation and management of top predators requires a comprehensive understanding of their distributions and of the underlying biological and physical processes that affect these distributions. The Mid-Atlantic Bight shelf break system is a dynamic and productive region where at least 32 species of cetaceans have been recorded through various systematic and opportunistic marine mammal surveys from the 1970s through 2012. My dissertation characterizes the spatial distribution and habitat of cetaceans in the Mid-Atlantic Bight shelf break system by utilizing marine mammal line-transect survey data, synoptic multi-frequency active acoustic data, and fine-scale hydrographic data collected during the 2011 summer Atlantic Marine Assessment Program for Protected Species (AMAPPS) survey. Although studies describing cetacean habitat and distributions have been previously conducted in the Mid-Atlantic Bight, my research specifically focuses on the shelf break region to elucidate both the physical and biological processes that influence cetacean distribution patterns within this cetacean hotspot.

In Chapter One I reviewed biologically important areas for cetaceans in the Atlantic waters of the United States. I described the study area, the shelf break region of the Mid-Atlantic Bight, in terms of the general oceanography, productivity and biodiversity. According to recent habitat-based cetacean density models, the shelf break

region is an area of high cetacean abundance and density, yet little research is directed at understanding the mechanisms that establish this region as a cetacean hotspot.

In Chapter Two I presented the basic physical principles of sound in water and described the methodology used to classify opportunistically collected, multi-frequency active acoustic data using a frequency responses technique and a presence/absence technique. Frequency response classification methods are usually employed in conjunction with net-tow data, but the logistics of the 2011 AMAPPS survey did not allow for appropriate net tow data to be collected. Biologically meaningful information can be extracted from acoustic scattering regions by comparing the frequency response curves of acoustic regions to theoretical curves of known scattering models. Using the five frequencies on the EK60 system (18, 38, 70, 120, and 200 kHz), I defined three categories of acoustic scatterers: fish-like (with swim bladder), nekton-like (e.g., euphausiids), and plankton-like (e.g., copepods). I also employed a multi-frequency acoustic categorization method using three frequencies (18, 38, and 120 kHz) that has been used in the Gulf of Maine and Georges Bank which is based the presence or absence of volume backscatter above a threshold. This method is more objective than the comparison of frequency response curves because it uses an established backscatter value for the threshold. By removing all data below the threshold, only strong scattering information is retained.

In Chapter Three I analyzed the distribution of the categorized acoustic regions of interest during the daytime cross shelf transects. Over all transects, plankton-like acoustic regions of interest were detected most frequently, followed by fish-like acoustic regions and then nekton-like acoustic regions. Plankton-like detections were the only significantly different acoustic detections per kilometer, although nekton-like detections were only slightly not significant. The threshold categorization method by Jech and Michaels (2006) provided a more conservative and discrete detection of acoustic scatterers and allowed me to use backscatter values areas that were classified into acoustic categories. This provided continuous data values that were integrated at discrete spatial increments for wavelet analysis. Wavelet analysis of duplicated transects indicate that small spatial scales (between one and eight kilometers) were significant for fish and nekton-like scattering among the transects analyzed.

In Chapter Four I analyzed the fine scale distribution of cetaceans in the shelf break system of the Mid-Atlantic Bight using corrected sightings per trackline region, classification trees, multidimensional scaling, and random forest analysis. I describe habitat for common dolphins, Risso's dolphins and sperm whales. From the distribution of cetacean sightings, patterns of habitat start to emerge: within the shelf break region of the Mid-Atlantic Bight, common dolphins were sighted more prevalently over the shelf while sperm whales were more frequently found in the deep waters offshore and Risso's

dolphins were most prevalent at the shelf break. Multidimensional scaling presented clear environmental separation among common dolphins and Risso's dolphins and sperm whales. The sperm whale random forest habitat model had the lowest misclassification error (0.30) and the Risso's dolphin random forest habitat model had the greatest misclassification error (0.37). Shallow water depth (less than 148 meters) was the primary variable selected in the classification model for common dolphin habitat. Distance to surface density fronts and surface temperature fronts were the primary variables selected in the classification models to describe Risso's dolphin habitat and sperm whale habitat respectively. When mapped back into geographic space, these three cetacean species occupy different fine-scale habitats within the dynamic Mid-Atlantic Bight shelf break system.

Taken together, the results of my dissertation demonstrate the use of opportunistically collected data in ecosystem studies, emphasize the need to incorporate middle trophic level data and oceanographic features into cetacean habitat models, and emphasize the importance of developing a more mechanistic understanding of dynamic ecosystems.

5.1 On-going research

Since the 2011 summer survey, the AMAPPS program has added various trawl data collection protocols to the surveys to address ecological questions in a more mechanistic manner. Of particular interest are the Multiple Opening and Closing Nets with an Environmental Sampling System (MOCNESS). Information from the MOCNESS trawls at the shelf break and canyon heads will help ground truth the EK60 and provide for a more robust categorization of the multi-frequency data. These data are currently being processed and should be available for analysis in summer 2016.

There are also data sets from the 2011 summer cruise that I processed but are not part of this dissertation. As previously mentioned, several of the transects were sampled twice, more than 24 hours after the initial survey of that transect. In a several of these pairs of transects the position of the shelf break front has moved either offshore or on-shore dramatically and the distribution of acoustic scatterers changes in accordance with the change with the surface position of the front. Although the surface temperature and salinity data do not provide information on the 2-dimensional structure of the front, CTD data from nighttime tow-yos in the vicinity should be able to resolve the structure and provide a more complete view of the shelf break ecosystem.

References

- Agler, B. A., R. L. Schooley, S. E. Frohock, S. K. Katona, and I. E. Seipt. 1993. Reproduction of Photographically Identified Fin Whales, *Balaenoptera physalus*, from the Gulf of Maine. *Journal of Mammalogy* 74:577–587.
- Andrews, B. D., J. D. Chaytor, U. S. ten Brink, D. S. Brothers, and J. V. Gardner. 2013. Bathymetric Terrain Model of the Atlantic Margin for Marine Geological Investigations. Open-File Report, U.S. Geological Survey.
- Aoki, I., and T. Inagaki. 1992. Acoustic observations of fish schools and scattering layers in a Kuroshio warm-core ring and its environs. *Fisheries Oceanography* 1:137–142.
- Backus, R. H., J. E. Craddock, R. L. Haedrich, D. L. Shores, J. M. Teal, A. S. Wing, G. W. Mead, and W. D. Clarke. 1968. *Ceratoscopelus maderensis*: Peculiar Sound-Scattering Layer Identified with This Myctophid Fish. *Science* 160:991–993.
- Badcock, J., and N. R. Merrett. 1976. Midwater fishes in the eastern North Atlantic—I. Vertical distribution and associated biology in 30°N, 23°W, with developmental notes on certain myctophids. *Progress in Oceanography* 7:3–58.
- Barange, M. 1994. Acoustic identification, classification and structure of biological patchiness on the edge of the Agulhas Bank and its relation to frontal features. *South African Journal of Marine Science* 14:333–347.
- Baumgartner, M. F. 1997. The distribution of Risso's dolphin (*Grampus griseus*) with respect to the physiography of the northern Gulf of Mexico. *Marine Mammal Science* 13:614–638.
- Baumgartner, M. F., T. V. Cole, R. G. Campbell, G. J. Teegarden, and E. G. Durbin. 2003. Associations between North Atlantic right whales and their prey, *Calanus finmarchicus*, over diel and tidal time scales. *Marine Ecology Progress Series* 264:155–166.

- Baumgartner, M. F., N. S. Lysiak, C. Schuman, J. Urban-Rich, and F. W. Wenzel. 2011. Diel vertical migration behavior of *Calanus finmarchicus* and its influence on right and sei whale occurrence. *Marine Ecology Progress Series* 423:167–184.
- Baumgartner, M. F., and B. R. Mate. 2003. Summertime foraging ecology of North Atlantic right whales. *Marine Ecology Progress Series* 264:123–135.
- Baumgartner, M. F., and B. R. Mate. 2005. Summer and fall habitat of North Atlantic right whales (*Eubalaena glacialis*) inferred from satellite telemetry. *Canadian Journal of Fisheries and Aquatic Sciences* 62:527–543.
- Beardsley, R. C., and C. N. Flagg. 1976. The water structure, mean currents, and shelf-water/slope-water front on the New England continental shelf. *Mem. Soc. Roy. Sci. Liege* 6:209–225.
- Becker, E. A., K. A. Forney, M. C. Ferguson, D. G. Foley, R. C. Smith, J. Barlow, and J. V. Redfern. 2010. Comparing California Current cetacean–habitat models developed using in situ and remotely sensed sea surface temperature data. *Mar Ecol Prog Ser* 413:163–183.
- Benoit-Bird, K. J., and W. W. Au. 2003. Prey dynamics affect foraging by a pelagic predator (*Stenella longirostris*) over a range of spatial and temporal scales. *Behavioral Ecology and Sociobiology* 53:364–373.
- Benoit-Bird, K. J., and G. L. Lawson. 2016. Ecological Insights from Pelagic Habitats Acquired Using Active Acoustic Techniques. *Annual Review of Marine Science* 8:463–490.
- Bergstad, O. A., T. Falkenhaug, O. S. Astthorsson, I. Byrkjedal, A. V. Gebruk, U. Piatkowski, I. G. Priede, R. S. Santos, M. Vecchione, P. Lorance, and J. D. M. Gordon. 2008. Towards improved understanding of the diversity and abundance patterns of the mid-ocean ridge macro- and megafauna. *Deep Sea Research Part II: Topical Studies in Oceanography* 55:1–5.
- Bergstad, O. A., G. M. M. Menezes, Å. S. Høines, J. D. M. Gordon, and J. K. Galbraith. 2012. Patterns of distribution of deepwater demersal fishes of the North Atlantic mid-ocean ridge, continental slopes, islands and seamounts. *Deep Sea Research Part I: Oceanographic Research Papers* 61:74–83.

- Best, P. B., J. L. Bannister, R. L. Brownell, and G. P. Donovan, editors. 2001. Right whales: worldwide status. *Journal of Cetacean Research and Management (Special Issue)* 2.
- Bigelow, H. B. 1933. Studies of the waters on the continental shelf, Cape Cod to Chesapeake Bay. I. The cycle of temperature. *Papers in Physical Oceanography and Meteorology* 2:1–135.
- Block, B. A., H. Dewar, S. B. Blackwell, T. D. Williams, E. D. Prince, C. J. Farwell, A. Boustany, S. L. H. Teo, A. Seitz, A. Walli, and D. Fudge. 2001. Migratory Movements, Depth Preferences, and Thermal Biology of Atlantic Bluefin Tuna. *Science* 293:1310–1314.
- Borcard, D., and P. Legendre. 2002. All-scale spatial analysis of ecological data by means of principal coordinates of neighbour matrices. *Ecological Modelling* 153:51–68.
- Bradshaw, G. A., and T. A. Spies. 1992. Characterizing Canopy Gap Structure in Forests Using Wavelet Analysis. *Journal of Ecology* 80:205–215.
- Breiman, L. 2001. Random Forests. *Machine Learning* 45:5–32.
- Breiman, L., J. Friedman, C. J. Stone, and R. A. Olshen. 1984. Classification and regression trees. CRC press.
- Brown, M. W., S. Brault, P. K. Hamilton, R. D. Kenney, A. R. Knowlton, M. K. Marx, C. A. Mayo, C. K. Slay, and S. D. Kraus. 2001. Sighting heterogeneity of right whales in the western North Atlantic: 1980–1992. *Journal of Cetacean Research and Management (Special Issue)* 2:245–250.
- Burgos, J. M., and J. K. Horne. 2007. Sensitivity analysis and parameter selection for detecting aggregations in acoustic data. *ICES Journal of Marine Science: Journal du Conseil* 64:160–168.
- Cazelles, B., K. Cazelles, and M. Chavez. 2014. Wavelet analysis in ecology and epidemiology: impact of statistical tests. *Journal of The Royal Society Interface* 11.

- Cazelles, B., M. Chavez, D. Berteaux, F. Ménard, J. O. Vik, S. Jenouvrier, and N. C. Stenseth. 2008. Wavelet analysis of ecological time series. *Oecologia* 156:287–304.
- CeTAP. 1982. A characterization of marine mammals and turtles in the mid-and north Atlantic areas of the US outer continental shelf.
- Chapman, D. C. 1986. A simple model of the formation and maintenance of the shelf/slope front in the Middle Atlantic Bight. *Journal of Physical Oceanography* 16:1273–1279.
- Chapman, D. C., and R. C. Beardsley. 1989. On the origin of shelf water in the Middle Atlantic Bight. *Journal of Physical Oceanography* 19:384–391.
- Chapman, D. C., and S. J. Lentz. 1994. Trapping of a coastal density front by the bottom boundary layer. *Journal of Physical Oceanography* 24:1464–1479.
- Chave, J. 2013. The problem of pattern and scale in ecology: what have we learned in 20 years? *Ecology Letters* 16:4–16.
- Churchill, J. H., and G. Gawarkiewicz. 2009. Shelfbreak frontal eddies over the continental slope north of Cape Hatteras. *Journal of Geophysical Research-Oceans* 114:C02017.
- Clapham, P. J., and I. E. Seipt. 1991. Resightings of Independent Fin Whales, *Balaenoptera physalus*, on Maternal Summer Ranges. *Journal of Mammalogy* 72:788–790.
- Clark, C. W. 1995. Application of US Navy underwater hydrophone arrays for scientific research on whales. *Rep. int. Whal. Commn* 45:210–212.
- Clarke, M. R. 1996. The Role of Cephalopods in the World's Oceans: An Introduction. *Philosophical Transactions: Biological Sciences* 351:979–983.
- Cole, T. V. N., P. Hamilton, A. G. Henry, P. Duley, R. M. P. III, B. N. White, and T. Frasier. 2013. Evidence of a North Atlantic right whale *Eubalaena glacialis* mating ground. *Endangered Species Research* 21:55–64.
- Cressie, N. A. 1993. *Statistics for spatial data*. Wiley New York.

- Csillag, F., and S. Kabos. 2002. Wavelets, boundaries, and the spatial analysis of landscape pattern. *Ecoscience*:177–190.
- Cutler, D. R., T. C. Edwards Jr., K. H. Beard, A. Cutler, K. T. Hess, J. Gibson, and J. J. Lawler. 2007. Random Forests for Classification in Ecology. *Ecology* 88:2783–2792.
- Dale, M. R. ., and M. Mah. 1998. The use of wavelets for spatial pattern analysis in ecology. *Journal of Vegetation Science* 9:805–814.
- Davis, R. W., W. E. Evans, and B. Wursig. 2000. Cetaceans, Sea Turtles and Seabirds in the Northern Gulf of Mexico: Distribution, Abundance and Habitat Associations. Volume I: Executive Summary. Prepared by Texas A&M University at Galveston and the National Marine Fisheries Service. US Department of the Interior, Geological Survey, Biological Resources Division. USGS/BRD/CR–1999-0006 and Minerals Management Service, Gulf of Mexico OCS Region, New Orleans, LA. OCS Study MMS 2000-002 27 pp. iii.
- Dayton, P. K., and M. J. Tegner. 1984. The importance of scale in community ecology: A kelp forest example with terrestrial analogs.
- De'ath, G., and K. E. Fabricius. 2000. Classification and Regression Trees: A Powerful Yet Simple Technique for Ecological Data Analysis. *Ecology* 81:3178–3192.
- De Robertis, A., and I. Higginbottom. 2007. A post-processing technique to estimate the signal-to-noise ratio and remove echosounder background noise. *ICES Journal of Marine Science* 64:1282 –1291.
- De Robertis, A., D. R. McKelvey, and P. H. Ressler. 2010. Development and application of an empirical multifrequency method for backscatter classification. *Canadian Journal of Fisheries and Aquatic Sciences* 67:1459–1474.
- Donovan, G. P. 1991. A review of IWC stock boundaries. Rept. Int. Whal. Commn., Special:39–68.

- Dragon, A. C., P. Monestiez, A. Bar-Hen, and C. Guinet. 2010. Linking foraging behaviour to physical oceanographic structures: Southern elephant seals and mesoscale eddies east of Kerguelen Islands. *Progress in Oceanography* 87:61–71.
- Dungan, J. L., J. N. Perry, M. R. T. Dale, P. Legendre, S. Citron-Pousty, M.-J. Fortin, A. Jakomulska, M. Miriti, and M. S. Rosenberg. 2002. A balanced view of scale in spatial statistical analysis. *Ecography* 25:626–640.
- ESRI. 2013. ArcGIS Desktop: Release 10.2. Environmental Systems Research Institute, Redlands, CA.
- Fauchald, P., and K. E. Erikstad. 2002. Scale-dependent predator-prey interactions: the aggregative response of seabirds to prey under variable prey abundance and patchiness. *Marine ecology progress series* 231:279–291.
- Fauchald, P., K. E. Erikstad, and H. Skarsfjord. 2000. Scale-dependent predator-prey interactions: the hierarchical spatial distribution of seabirds and prey. *Ecology* 81:773–783.
- Ferguson, M. C., J. Barlow, S. B. Reilly, and T. Gerrodette. 2005. Predicting Cuvier's (*Ziphius cavirostris*) and Mesoplodon beaked whale population density from habitat characteristics in the eastern tropical Pacific Ocean. *Journal of Cetacean Research and Management* 7:287.
- Ferguson, M. C., C. Curtice, J. Harrison, and S. M. Van Parijs. 2015. Biologically Important Areas for Cetaceans Within U.S. Waters - Overview and Rationale. *Aquatic Mammals* 41:2–16.
- Foley, H. J., R. C. Holt, R. E. Hardee, P. B. Nilsson, K. A. Jackson, A. J. Read, D. A. Pabst, and W. A. McLellan. 2011. Observations of a western North Atlantic right whale (*Eubalaena glacialis*) birth offshore of the protected southeast U.S. critical habitat. *Marine Mammal Science* 27:E234–E240.
- Foote, K. G., H. P. Knudsen, G. Vestnes, D. N. MacLennan, and E. J. Simmonds. 1987. Calibration of acoustic instruments for fish density estimation: a practical guide. *Int. Counc. Explor. Sea Coop. Res. Rep* 144.

- Forney, K. A., M. C. Ferguson, E. A. Becker, P. C. Fiedler, J. V. Redfern, J. Barlow, I. L. Vilchis, and L. T. Ballance. 2012. Habitat-based spatial models of cetacean density in the eastern Pacific Ocean. *Endangered Species Research* 16:113–133.
- Franks, P. J. S. 1992. Phytoplankton blooms at fronts: patterns, scales, and physical forcing mechanisms. *Rev Aquat Sci* 6:121–137.
- Fratantoni, P. S., and R. S. Pickart. 2007. The Western North Atlantic Shelfbreak Current System in Summer. *Journal of Physical Oceanography* 37:2509–2533.
- Fratantoni, P. S., R. S. Pickart, D. J. Torres, and A. Scotti. 2001. Mean structure and dynamics of the shelfbreak jet in the Middle Atlantic Bight during fall and winter. *Journal of Physical Oceanography* 31:2135–2156.
- Gawarkiewicz, G., K. H. Brink, F. Bahr, R. C. Beardsley, M. Caruso, J. F. Lynch, and C. S. Chiu. 2004. A large-amplitude meander of the shelfbreak front during summer south of New England: Observations from the Shelfbreak PRIMER experiment. *Journal of Geophysical Research-Oceans* 109:C03006.
- Gawarkiewicz, G., and D. C. Chapman. 1992. The role of stratification in the formation and maintenance of shelf-break fronts. *Journal of Physical Oceanography* 22:753–772.
- Gawarkiewicz, G., J. Churchill, F. Bahr, C. Linder, and C. Marquette. 2008. Shelfbreak frontal structure and processes north of Cape Hatteras in winter. *Journal of Marine Research* 66:775–799.
- Genin, A. 2004. Bio-physical coupling in the formation of zooplankton and fish aggregations over abrupt topographies. *Journal of Marine Systems* 50:3–20.
- Geo-Marine Inc. (GMI). 2010a. Ocean/wind power ecological baseline studies, January 2008 – December 2009. Final report. Department of Environmental Protection, Office of Science, Trenton, NJ.
- Geo-Marine Inc. (GMI). 2010b. Ocean/wind power ecological baseline studies, January 2008 – December 2009. Final report. Department of Environmental Protection, Office of Science, Trenton, NJ.

- Good, C. P. 2008. Spatial Ecology of the North Atlantic Right Whale (*Eubalaena Glacialis*). Duke University.
- Hain, J. H. ., M. A. . Hyman, R. D. Kenney, and H. E. Winn. 1985. The role of cetaceans in the shelf-edge region of the northeastern United States. *Marine Fisheries Review* 47:13–17.
- Hain, J. H. ., M. J. Ratnaswamy, R. D. Kenney, and H. E. Winn. 1992a. The fin whale, *Balaenoptera physalus*, in waters of the northeastern United States continental shelf. *Rep. int. Whal. Commn* 42:653–669.
- Halpern, B. S., S. Walbridge, K. A. Selkoe, C. V. Kappel, F. Micheli, C. D'Agrosa, J. F. Bruno, K. S. Casey, C. Ebert, H. E. Fox, R. Fujita, D. Heinemann, H. S. Lenihan, E. M. P. Madin, M. T. Perry, E. R. Selig, M. Spalding, R. Steneck, and R. Watson. 2008. A Global Map of Human Impact on Marine Ecosystems. *Science* 319:948–952.
- Hamilton, P. K., and C. A. Mayo. 1990. Population characteristics of right whales (*Eubalaena glacialis*) observed in Cape Cod and Massachusetts Bays, 1978-1986. *Rep. Int. Whal. Comm., Special*:203–208.
- Hastie, G. D., R. J. Swift, G. Slessor, P. M. Thompson, and W. R. Turrell. 2005. Environmental models for predicting oceanic dolphin habitat in the Northeast Atlantic. *ICES Journal of Marine Science* 62:760.
- Hastie, G. D., B. Wilson, L. J. Wilson, K. M. Parsons, and P. M. Thompson. 2004. Functional mechanisms underlying cetacean distribution patterns: hotspots for bottlenose dolphins are linked to foraging. *Marine Biology* 144:397–403.
- Hastie, T., J. H. Friedman, and R. Tibshirani. 2009. *The elements of statistical learning : data mining, inference, and prediction*. 2nd ed. Springer, New York.
- Haury, L. R., J. A. McGowan, and P. H. Wiebe. 1978. Patterns and processes in the time-space scales of plankton distributions. Pages 277–327 *in* J. H. Steele, editor. *Spatial Pattern in Plankton Communities*.

- Haury, L. R., and P. H. Wiebe. 1982. Fine-scale multi-species aggregations of oceanic zooplankton. *Deep Sea Research Part A. Oceanographic Research Papers* 29:915–921.
- Hazen, E. L., S. M. Maxwell, H. Bailey, S. J. Bograd, M. Hamann, P. Gaspar, B. J. Godley, and G. L. Shillinger. 2012. Ontogeny in marine tagging and tracking science: technologies and data gaps. *Marine Ecology Progress Series* 457:221–240.
- Hazen, E. L., R. M. Suryan, J. A. Santora, S. J. Bograd, Y. Watanuki, and R. P. Wilson. 2013. Scales and mechanisms of marine hotspot formation. *Marine ecology. Progress series* 487:177–183.
- Hewitt, R. P., and D. A. Demer. 2000. The use of acoustic sampling to estimate the dispersion and abundance of euphausiids, with an emphasis on Antarctic krill, *Euphausia superba*. *Fisheries Research* 47:215–229.
- Holliday, D. V., and R. E. Pieper. 1995. Bioacoustical oceanography at high frequencies. *ICES Journal of Marine Science: Journal du Conseil* 52:279.
- Holling, C. S. 1992. Cross-Scale Morphology, Geometry, and Dynamics of Ecosystems. *Ecological Monographs* 62:447–502.
- Hooker, S. K., and L. R. Gerber. 2004. Marine Reserves as a Tool for Ecosystem-Based Management: The Potential Importance of Megafauna. *BioScience* 54:27–39.
- Hooker, S. K., H. Whitehead, S. Gowans, S. K. Hooker, H. Whitehead, and S. Gowans. 1999. Marine Protected Area Design and the Spatial and Temporal Distribution of Cetaceans in a Submarine Canyon, *Marine Protected Area Design and the Spatial and Temporal Distribution of Cetaceans in a Submarine Canyon*. *Conservation Biology*, *Conservation Biology* 13, 13:592, 592–602, 602.
- Horne, J. K. 2000. Acoustic approaches to remote species identification: a review. *Fisheries oceanography* 9:356–371.
- Houghton, R. W., D. Hebert, and M. Prater. 2006. Circulation and mixing at the New England shelfbreak front: Results of purposeful tracer experiments. *Progress in Oceanography* 70:289–312.

- Houghton, R. W., and J. Marra. 1983. Physical/biological structure and exchange across the thermohaline shelf/slope front in the New York Bight. *Journal of Geophysical Research* 88:4467–4482.
- Houghton, R. W., R. Schlitz, R. C. Beardsley, B. Butman, and J. L. Chamberlin. 1982. The Middle Atlantic Bight cold pool: Evolution of the temperature structure during summer 1979. *Journal of Physical Oceanography* 12:1019–1029.
- Houghton, R. W., R. D. Vaillancourt, J. Marra, D. Hebert, and B. Hales. 2009. Cross-shelf circulation and phytoplankton distribution at the summertime New England shelfbreak front. *Journal of Marine Systems* 78:411–425.
- Hyrenbach, K. D., P. Fernández, and D. J. Anderson. 2002. Oceanographic habitats of two sympatric North Pacific albatrosses during the breeding season. *Marine Ecology Progress Series* 233:283–301.
- Jech, J. M., and J. K. Horne. 2002. Three-dimensional visualization of fish morphometry and acoustic backscatter. *Acoustics Research Letters Online* 3:35–40.
- Jech, J. M., and W. L. Michaels. 2006. A multifrequency method to classify and evaluate fisheries acoustics data. *Canadian Journal of Fisheries and Aquatic Sciences* 63:2225–2235.
- Johnston, D. W., A. J. Westgate, and A. J. Read. 2005. Effects of fine-scale oceanographic features on the distribution and movements of harbour porpoises *Phocoena phocoena* in the Bay of Fundy. *Marine Ecology Progress Series* 295:279–293.
- Jonsgard, A., and K. Darling. 1977. On the biology of the Eastern North Atlantic sei whale, *Balaenoptera borealis* Lesson 1:124–129.
- Kaschner, K., N. J. Quick, R. Jewell, R. Williams, and C. M. Harris. 2012. Global Coverage of Cetacean Line-Transect Surveys: Status Quo, Data Gaps and Future Challenges. *PLOS ONE* 7:e44075.
- Keitt, T. H. 2000. Spectral representation of neutral landscapes. *Landscape Ecology* 15:479–494.

- Keitt, T. H., and J. Fischer. 2006. Detection of Scale-Specific Community Dynamics Using Wavelets. *Ecology* 87:2895–2904.
- Keller, C. A., L. Garrison, R. Baumstark, L. I. Ward-Geiger, and E. Hines. 2012. Application of a habitat model to define calving habitat of the North Atlantic right whale in the southeastern United States. *Endangered Species Research* 18:73–87.
- Keller, C. A., L. I. Ward-Geiger, W. B. Brooks, C. K. Slay, C. R. Taylor, and B. J. Zoodsma. 2006. North Atlantic right whale distribution in relation to sea-surface temperature in the southeastern United States calving grounds. *Marine Mammal Science* 22:426–445.
- Kenney, R. D. 2001. Anomalous 1992 spring and summer right whale (*Eubalaena glacialis*) distributions in the Gulf of Maine. *Journal of Cetacean Research and Management (Special Issue 2)*:209–223.
- Kenney, R. D., C. A. Mayo, and H. E. Winn. 2001. Migration and foraging strategies at varying spatial scales in western North Atlantic right whales: a review of hypotheses. *Journal of Cetacean Research and Management* 2:251–260.
- Kenney, R. D., P. M. Payne, D. W. Heinemann, and H. E. Winn. 1996. Shifts in Northeast shelf cetacean distributions relative to trends in Gulf of Maine/Georges Bank finfish abundance. *The northeast shelf ecosystem: assessment, sustainability, and management*. Blackwell Science, Cambridge, MA 2142:169–196.
- Kenney, R. D., and H. E. Winn. 1986. Cetacean high-use habitats of the northeast United States continental shelf. *Fish. Bull.:(United States)* 84.
- Kenney, R. D., and H. E. Winn. 1987. Cetacean biomass densities near submarine canyons compared to adjacent shelf/slope areas. *Continental Shelf Research* 7:107–114.
- Kenney, R. D., H. E. Winn, and M. C. Macaulay. 1995. Cetaceans in the Great South Channel, 1979-1989: right whale (*Eubalaena glacialis*). *Continental Shelf Research* 15:385–414.

- Kimura, K. 1929. On the detection of fish-groups by an acoustic method. *Journal of the Imperial Fisheries Institute, Tokyo* 24:41–45.
- Kloser, R. J. 1996. Improved precision of acoustic surveys of benthopelagic fish by means of a deep-towed transducer. *ICES Journal of Marine Science* 53:407–413.
- Knowlton, A. R., S. D. Kraus, and R. D. Kenney. 1994. Reproduction in North Atlantic right whales (*Eubalaena glacialis*). *Canadian Journal of Zoology* 72:1297–1305.
- Knowlton, A. R., J. B. Ring, and B. Russell. 2002. Right whale sightings and survey effort in the Mid Atlantic Region: Migratory corridor, time frame, and proximity to port entrances. A report submitted to the NMFS Ship Strike Working Group.
- Korneliussen, R. J. 2000. Measurement and removal of echo integration noise. *ICES Journal of Marine Science: Journal du Conseil* 57:1204–1217.
- Korneliussen, R. J., and E. Ona. 2003. Synthetic echograms generated from the relative frequency response. *ICES Journal of Marine Science: Journal du Conseil* 60:636 – 640.
- Koslow, J. A. 2009. The role of acoustics in ecosystem-based fishery management. *ICES Journal of Marine Science*.
- Kot, C. Y., E. Fujioka, L. J. Hazen, B. D. Best, A. J. Read, and P. N. Halpin. 2010. Spatio-Temporal Gap Analysis of OBIS-SEAMAP Project Data: Assessment and Way Forward. *PLOS ONE* 5:e12990.
- LaBrecque, E., C. Curtice, J. Harrison, S. Van Parijs, and P. Halpin. 2015. Biologically Important Areas for Cetaceans Within U.S. Waters – East Coast Region. *Aquatic Mammals* 41:17–29.
- Lammers, M. O., R. E. Brainard, W. W. L. Au, T. A. Mooney, and K. B. Wong. 2008. An ecological acoustic recorder (EAR) for long-term monitoring of biological and anthropogenic sounds on coral reefs and other marine habitats. *The Journal of the Acoustical Society of America* 123:1720–1728.

- Lavery, A. C., P. H. Wiebe, T. K. Stanton, G. L. Lawson, M. C. Benfield, and N. Copley. 2007. Determining dominant scatterers of sound in mixed zooplankton populations. *The Journal of the Acoustical Society of America* 122:3304–3326.
- Lawson, G. L., P. H. Wiebe, C. J. Ashjian, D. Chu, and T. K. Stanton. 2006. Improved parametrization of Antarctic krill target strength models. *The Journal of the Acoustical Society of America* 119:232–242.
- Lawson, G. L., P. H. Wiebe, C. J. Ashjian, S. M. Gallager, C. S. Davis, and J. D. Warren. 2004. Acoustically-inferred zooplankton distribution in relation to hydrography west of the Antarctic Peninsula. *Deep-Sea Research Part II* 51:2041–2072.
- Lee, W.-J. 2013. Broadband and statistical characterization of echoes from random scatterers: application to acoustic scattering by marine organisms. Massachusetts Institute of Technology, Boston, MA.
- Lee, W.-J., and T. K. Stanton. 2014. Statistics of Echoes From Mixed Assemblages of Scatterers With Different Scattering Amplitudes and Numerical Densities. *IEEE Journal of Oceanic Engineering* 39:740–754.
- Legendre, L., and S. Demers. 1984. Towards dynamic biological oceanography and limnology. *Canadian Journal of Fisheries and Aquatic Sciences* 41:2–19.
- Levin, S. A. 1992. The problem of pattern and scale in ecology: the Robert H. MacArthur award lecture. *Ecology* 73:1943–1967.
- Levin, S. A. 2000. Multiple Scales and the Maintenance of Biodiversity. *Ecosystems* 3:498–506.
- Liaw, A., and M. Wiener. 2002. Classification and Regression by randomForest. *R News* 2:18–22.
- Linder, C. A., and G. Gawarkiewicz. 1998. A climatology of the shelfbreak front in the Middle Atlantic Bight. *Journal of Geophysical Research* 103:18–405.
- Longhurst, A. R. 2007. *Ecological geography of the sea*. Academic Pr.

- Lozier, M. S., and G. Gawarkiewicz. 2001. Cross-frontal exchange in the Middle Atlantic Bight as evidenced by surface drifters. *Journal of Physical Oceanography* 31:2498–2510.
- Mackas, D. L., K. L. Denman, and M. R. Abbott. 1985. Plankton patchiness: biology in the physical vernacular. *Bulletin of Marine Science* 37:652–674.
- MacLennan, D. N. 1986. Time varied gain functions for pulsed sonars. *Journal of Sound and Vibration* 110:511–522.
- MacLennan, D. N., and D. V. Holliday. 1996. Fisheries and plankton acoustics: past, present, and future. *ICES Journal of Marine Science* 53:513–516.
- Malik, S., M. W. Brown, S. D. Kraus, A. R. Knowlton, P. K. Hamilton, and B. N. White. 1999. Assessment of mitochondrial DNA structuring and nursery use in the North Atlantic right whale (*Eubalaena glacialis*). *Canadian Journal of Zoology* 77:1217–1222.
- Malone, T. C., T. S. Hopkins, P. G. Falkowski, and T. E. Whittedge. 1983. Production and transport of phytoplankton biomass over the continental shelf of the new york bight. *Continental Shelf Research* 1:305–337.
- Mann, K. H., and J. R. N. Lazier. 1991. *Dynamics of marine ecosystems: biological-physical interactions in the oceans*. Blackwell Pub.
- Marra, J., R. W. Houghton, D. C. Boardman, and P. J. Neale. 1982. Variability in surface chlorophyll-a at a shelf-break front. *Journal of Marine Research* 40:575–591.
- Marra, J., R. W. Houghton, and C. Garside. 1990. Phytoplankton growth at the shelf-break front in the Middle Atlantic Bight. *Journal of Marine Research* 48:851–868.
- Mate, B. R., K. A. Rossbach, S. L. Nieuwkerk, R. S. Wells, A. Blair Irvine, M. D. Scott, and A. J. Read. 1995. Satellite-monitored movements and dive behavior of a bottlenose dolphin (*Tursiops truncatus*) in Tampa Bay, FL. *Marine Mammal Science* 11:452–463.
- Mate, B. R., Sharon L. Nieuwkerk, and S. D. Kraus. 1997. Satellite-Monitored Movements of the Northern Right Whale. *The Journal of Wildlife Management* 61:1393–1405.

- McClatchie, S., R. E. Thorne, P. Grimes, and S. Hanchet. 2000. Ground truth and target identification for fisheries acoustics. *Fisheries Research* 47:173–191.
- McLellan, W. A. 2004. Winter right whale sightings from aerial surveys of the coastal waters of the US mid-Atlantic.
- Mead, J. G. 1977. Records of sei and Bryde's whales from the Atlantic coast of the United States, the Gulf of Mexico, and the Caribbean. *Rep. Int. Whal. Comm.(Special Issue)* 1:113–116.
- Mitchell, E. 1975. Preliminary report on Nova Scotia fishery for sei whales (*Balaenoptera borealis*). *Rep. int. Whal. Commn* 25:218–225.
- Mitchell, E. D. 1991. Winter records of the minke whale (*Balaenoptera acutorostrata* Lacepede 1804) in the southern North Atlantic. *Rep. int Whal. Commn* 41:455–457.
- Mi, X., H. Ren, Z. Ouyang, W. Wei, and K. Ma. 2005. The Use of the Mexican Hat and the Morlet Wavelets for Detection of Ecological Patterns. *Plant Ecology* 179:1–19.
- Mizroch, S. A., D. W. Rice, and J. M. Breiwick. 1984a. The sei whale, *Balaenoptera borealis*. *Marine Fisheries Review* 46:25–29.
- Mizroch, S. A., D. W. Rice, and J. M. Breiwick. 1984b. The fin whale, *Balaenoptera physalus*. *Marine Fisheries Review* 46:20–24.
- Morano, J. L., A. N. Rice, J. T. Tielens, B. J. Estabrook, A. Murray, B. L. Roberts, and C. W. Clark. 2012. Acoustically Detected Year-Round Presence of Right Whales in an Urbanized Migration Corridor. *Conservation Biology* 26:698–707.
- Morgan, P. 1994. SEAWATER: A Library of MATLAB. Computational Routines for the Properties of Sea Water. CSIRO Division of Oceanography, Tasmania, Australia.
- Morris, D. W. 2003. Toward an ecological synthesis: a case for habitat selection. *Oecologia* 136:1–13.
- Mullin, K. D., and G. L. Fulling. 2004. Abundance of cetaceans in the oceanic northern Gulf of Mexico, 1996–2001. *Marine Mammal Science* 20:787–807.

- Murphy, M. A. 1995. Occurrence and group characteristics of minke whales, *Balaenoptera acutorostrata*, in Massachusetts Bay and Cape Cod Bay. *Fisheries Bulletin* 93:577–585.
- Myers, N. 1988. Threatened biotas: “Hot spots” in tropical forests. *Environmentalist* 8:187–208.
- Myers, N., R. A. Mittermeier, C. G. Mittermeier, G. A. B. da Fonseca, and J. Kent. 2000. Biodiversity hotspots for conservation priorities. *Nature* 403:853+.
- Myriax. 2013. Echoview.
- Nash, R. D. ., J. J. Magnuson, C. S. Clay, and T. K. Stanton. 1987. A Synoptic View of the Gulf Stream Front with 70-kHz Sonar: Taking Advantage of a Closer Look. *Canadian Journal of Fisheries and Aquatic Sciences* 44:2022–2024.
- Nash, R. D. ., J. J. Magnuson, T. K. Stanton, and C. S. Clay. 1989. Distribution of peaks of 70 kHz acoustic scattering in relation to depth and temperature during day and night at the edge of the Gulf Stream–EchoFront 83. *Deep Sea Research Part A. Oceanographic Research Papers* 36:587–596.
- Nero, R. W., J. J. Magnuson, S. B. Brandt, T. K. Stanton, and J. M. Jech. 1990. Finescale biological patchiness of 70 kHz acoustic scattering at the edge of the Gulf Stream–EchoFront 85. *DEEP-SEA RES.(A OCEANOGR. RES. PAP.)*. 37:999–1016.
- Newhall, A. E., Y.-T. Lin, J. F. Lynch, M. F. Baumgartner, and G. G. Gawarkiewicz. 2012a. Long distance passive localization of vocalizing sei whales using an acoustic normal mode approach. *The Journal of the Acoustical Society of America* 131:1814–1825.
- Newhall, A. E., Y.-T. Lin, J. F. Lynch, M. F. Baumgartner, and G. G. Gawarkiewicz. 2012b. Long distance passive localization of vocalizing sei whales using an acoustic normal mode approach. *The Journal of the Acoustical Society of America* 131:1814–1825.
- NGDC. 2012. NOAA National Geophysical Data Center, U.S. Coastal Relief Model.

- Nilsson, P., E. Cummings, H. Foley, R. Hardee, R. McAlarney, W. A. McLellan, D. A. Pabst, and A. J. Read. 2011. Recent winter sightings of minke whales (*Balaenoptera acutorostrata*) in the South Atlantic Bight. Tampa, FL.
- Nowacek, D. P., C. W. Clark, D. Mann, P. J. Miller, H. C. Rosenbaum, J. S. Golden, M. Jasny, J. Kraska, and B. L. Southall. 2015. Marine seismic surveys and ocean noise: time for coordinated and prudent planning. *Frontiers in Ecology and the Environment* 13:378–386.
- Olson, D. B., and R. H. Backus. 1985. The concentrating of organisms at fronts: a cold-water fish and a warm-core Gulf Stream ring. *Journal of Marine Research* 43:113–137.
- Olson, D. B., G. L. Hitchcock, A. J. Mariano, C. J. Ashjian, G. Peng, R. W. Nero, and G. P. Podesta. 1994. Life on the edge: marine life and fronts. *Oceanography* 7:52–60.
- Oppel, S., and F. Huettmann. 2010. Using a Random Forest Model and Public Data to Predict the Distribution of Prey for Marine Wildlife Management. *Spatial Complexity, Informatics, and Wildlife Conservation* 151:163.
- Overholtz, W. J., and G. T. Waring. 1991. Diet composition of Pilot Whales *Globicephala* sp. and Common Dolphins *Delphinus delphis* in the Mid-Atlantic Bight during Spring 1989. *Fishery Bulletin* 89:723–728.
- Owen, R. W. 1981. Fronts and Eddies in the Sea: Mechanisms, Interactions and Biological Effects. *Analysis of marine ecosystems*:197.
- Palacios, D. M., S. J. Bograd, D. G. Foley, and F. B. Schwing. 2006. Oceanographic characteristics of biological hot spots in the North Pacific: a remote sensing perspective. *Deep-Sea Research Part II* 53:250–269.
- Palka, D. 2000. Abundance of the Gulf of Maine/Bay of Fundy Harbor Porpoise Based on Shipboard and Aerial Surveys during 1999. Northeast Fish Sci Cent Ref Doc. 00-7.
- Palka, D. 2012. A comprehensive assessment of marine mammal, marine turtle, and seabird abundance and spatial distribution in U.S. waters of the western North

Atlantic Ocean. 2011 Annual Report to the Inter-agency Agreement
M10PG00075/0001.

- Pauly, D., A. W. Trites, E. Capuli, and V. Christensen. 1998. Diet composition and trophic levels of marine mammals. *ICES Journal of Marine Science: Journal du Conseil* 55:467–481.
- Payne, P. M., D. N. Wiley, S. B. Young, S. Pittman, P. J. Clapham, and J. W. Jossi. 1990. Recent fluctuations in the abundance of baleen whales in the southern Gulf of Maine in relation to changes in selected prey. *Fishery Bulletin* 88:687–696.
- Perry, S. L., D. P. DeMaster, and G. K. Silber. 1999. The fin whale. *Marine Fisheries Review* 61:44–51.
- Pittman, S., B. Costa, C. Kot, D. Wiley, and R. D. Kenney. 2006. Cetacean distribution and diversity. An Ecological Characterization of the Stellwagen Bank National Marine Sanctuary Region: Oceanographic, Biogeographic, and Contaminants Assessment. NOAA Technical Memorandum NCCOS 45:265–326.
- Plotnick, R. E., R. H. Gardner, W. W. Hargrove, K. Prestegard, and M. Perlmutter. 1996. Lacunarity analysis: A general technique for the analysis of spatial patterns. *Physical Review E* 53:5461–5468.
- Pusineri, C., V. Magnin, L. Meynier, J. Spitz, S. Hassani, and V. Ridoux. 2007. Food and Feeding Ecology of the Common Dolphin (*delphinus Delphis*) in the Oceanic Northeast Atlantic and Comparison with Its Diet in Neritic Areas. *Marine Mammal Science* 23:30–47.
- R Core Team. 2014. R: A language and environment for statistical computing. R Foundation for Statistical Computing, Vienna, Austria.
- Read, A. J., K. W. Urian, B. Wilson, and D. M. Waples. 2003. Abundance of bottlenose dolphins in the bays, sounds, and estuaries of North Carolina. *Marine Mammal Science* 19:59–073.
- Read, A. J., and A. J. Westgate. 1997. Monitoring the movements of harbour porpoises (*Phocoena phocoena*) with satellite telemetry. *Marine Biology* 130:315–322.

- Redfern, J. V., J. Barlow, L. T. Ballance, T. Gerrodette, and E. A. Becker. 2008. Absence of scale dependence in dolphin-habitat models for the eastern tropical Pacific Ocean. *Marine Ecology Progress Series* 363:1–14.
- Risch, D., M. Castellote, C. W. Clark, G. E. Davis, P. J. Dugan, L. E. Hodge, A. Kumar, K. Lucke, D. K. Mellinger, S. L. Nieukirk, C. M. Popescu, C. Ramp, A. J. Read, A. N. Rice, M. A. Silva, U. Siebert, K. M. Stafford, H. Verdaat, and S. M. V. Parijs. 2014. Seasonal migrations of North Atlantic minke whales: novel insights from large-scale passive acoustic monitoring networks. *Movement Ecology* 2:17.
- Risch, D., C. W. Clark, P. J. Dugan, M. Popescu, U. Siebert, and S. M. Van Parijs. 2013. Minke whale acoustic behavior and multi-year seasonal and diel vocalization patterns in Massachusetts Bay, USA. *Marine Ecology Progress Series* 489:279–295.
- Roberts, J. J., B. D. Best, L. Mannocci, E. Fujioka, P. N. Halpin, D. L. Palka, L. P. Garrison, K. D. Mullin, T. V. N. Cole, C. B. Khan, W. A. McLellan, D. A. Pabst, and G. G. Lockhart. 2016. Habitat-based cetacean density models for the U.S. Atlantic and Gulf of Mexico. *Scientific Reports* 6:22615.
- Santora, J. A., W. J. Sydeman, I. D. Schroeder, B. K. Wells, and J. C. Field. 2011. Mesoscale structure and oceanographic determinants of krill hotspots in the California Current: Implications for trophic transfer and conservation. *Progress In Oceanography* 91:397–409.
- Saunders, S. C., J. Chen, T. D. Drummer, T. R. Crow, K. D. Brosofske, and E. J. Gustafson. 2002. The patch mosaic and ecological decomposition across spatial scales in a managed landscape of northern Wisconsin, USA. *Basic and Applied Ecology* 3:49–64.
- Savidge, D. K., and J. A. Austin. 2007. The Hatteras Front: August 2004 velocity and density structure. *J. Geophys. Res.* 112.
- Scales, K. L., P. I. Miller, L. A. Hawkes, S. N. Ingram, D. W. Sims, and S. C. Votier. 2014. On the Front Line: frontal zones as priority at-sea conservation areas for mobile marine vertebrates. *Journal of Applied Ecology*

- Schaeff, C. M., S. D. Kraus, M. W. Brown, and B. N. White. 1993. Assessment of the population structure of western North Atlantic right whales (*Eubalaena glacialis*) based on sighting and mtDNA data. *Canadian Journal of Zoology* 71:339–339.
- Schick, R. S., P. N. Halpin, A. J. Read, C. K. Slay, S. D. Kraus, B. R. Mate, M. F. Baumgartner, J. J. Roberts, B. D. Best, C. P. Good, S. R. Loarie, and J. S. Clark. 2009. Striking the right balance in right whale conservation. *Canadian Journal of Fisheries and Aquatic Sciences* 66:1399–1403.
- Schick, R. S., S. R. Loarie, F. Colchero, B. D. Best, A. Boustany, D. A. Conde, P. N. Halpin, L. N. Joppa, C. M. McClellan, and J. S. Clark. 2008. Understanding movement data and movement processes: current and emerging directions. *Ecology Letters* 11:1338–1350.
- Schilling, M. R., I. Seipt, M. T. Weinrich, S. E. Frohock, A. E. Kuhlberg, and P. J. Clapham. 1992. Behavior of individually-identified sei whales *Balaenoptera borealis* during an episodic influx into the southern Gulf of Maine in 1986. *Fisheries Bulletin* 90:749–749.
- Schulte, D., and C. R. Taylor. 2012. Documenting Spatial and Temporal Distribution of North Atlantic Right Whales off South Carolina and Northern Georgia 2011 – 2012. Page 26. Final Report to National Oceanic and Atmospheric Administration (NOAA), Contract No. WC113F-11-CN-0144.
- Seipt, I. E., P. J. Clapham, C. A. Mayo, and M. P. Hawvermale. 1990. Population characteristics of individually identified fin whales *Balaenoptera physalus* in Massachusetts Bay. *Fishery Bulletin* 88:271–278.
- Selzer, L. A., and P. M. Payne. 1988. The distribution of white-sided (*Lagenorhynchus acutus*) and common dolphins (*Delphinus delphis*) vs. environmental features of the continental shelf of the Northeastern United States. *Marine Mammal Science* 4:141–153.
- Shane, S. H. 1995. Relationship between pilot whales and Risso's dolphins at Santa Catalina Island, California, USA. *Marine Ecology Progress Series* 123:5–11.
- Sigler, M. F., K. J. Kuletz, P. H. Ressler, N. A. Friday, C. D. Wilson, and A. N. Zerbini.

2012. Marine predators and persistent prey in the southeast Bering Sea. *Deep Sea Research Part II: Topical Studies in Oceanography* 65–70:292–303.
- Signell, R., and E. Roworth. 2013. *Digital Bathymetry for the Gulf of Maine*. U.S. Geological Society.
- Simard, Y., and D. L. Mackas. 1989. Mesoscale Aggregations of Euphausiid Sound Scattering Layers on the Continental Shelf of Vancouver Island. *Canadian Journal of Fisheries and Aquatic Sciences* 46:1238–1249.
- Simmonds, E. J., and D. N. MacLennan. 2005. *Fisheries acoustics: theory and practice*. Blackwell Pub.
- Stanton, T. K., and D. Chu. 2000. Review and recommendations for the modelling of acoustic scattering by fluid-like elongated zooplankton: euphausiids and copepods. *ICES Journal of Marine Science: Journal du Conseil* 57:793–807.
- Stanton, T. K., D. Chu, and D. B. Reeder. 2004. Non-Rayleigh acoustic scattering characteristics of individual fish and zooplankton. *IEEE Journal of Oceanic Engineering* 29:260–268.
- Stanton, T. K., D. Chu, and P. H. Wiebe. 1996. Acoustic scattering characteristics of several zooplankton groups. *ICES Journal of Marine Science: Journal du Conseil* 53:289–295.
- Stanton, T. K., D. Chu, and P. H. Wiebe. 1998a. Sound scattering by several zooplankton groups. II. Scattering models. *The Journal of the Acoustical Society of America* 103:236–253.
- Stanton, T. K., D. Chu, P. H. Wiebe, L. V. Martin, and R. L. Eastwood. 1998b. Sound scattering by several zooplankton groups. I. Experimental determination of dominant scattering mechanisms. *The Journal of the Acoustical Society of America* 103:225–235.
- Stanton, T. K., P. H. Wiebe, D. Chu, and L. Goodman. 1994. Acoustic characterization and discrimination of marine zooplankton and turbulence. *ICES Journal of Marine Science: Journal du Conseil* 51:469–479.

- Stanton, T., R. Nash, R. Eastwood, and R. Nero. 1987. A field examination of acoustical scattering from marine organisms at 70 kHz. *IEEE Journal of Oceanic Engineering* 12:339–348.
- Steele, J. H. 1978. Some Comments on Plankton Patches. In: *Spatial Pattern in Plankton Communities*. (J. H. Steele, Ed.). Plenum Press, New York.
- Steele, J. H., and E. W. Henderson. 1992. A simple model for plankton patchiness. *J. Plankton Res.* 14:1397–1403.
- Stefansson, U., L. P. Atkinson, and D. F. Bumpus. 1971. Hydrographic properties and circulation of the North Carolina shelf and slope waters. *Deep-Sea Res* 18:383-420.
- Stephens, D. W., and J. R. Krebs. 1986. *Foraging theory*. Princeton University Press.
- Stokesbury, M. J. W., S. L. H. Teo, A. Seitz, R. K. O’Dor, and B. A. Block. 2004. Movement of Atlantic bluefin tuna (*Thunnus thynnus*) as determined by satellite tagging experiments initiated off New England. *Canadian Journal of Fisheries and Aquatic Sciences* 61:1976–1987.
- Stommel, H. 1963. Varieties of oceanographic experience. *Science* 139:373.
- Strobl, C., A.-L. Boulesteix, A. Zeileis, and T. Hothorn. 2007. Bias in random forest variable importance measures: Illustrations, sources and a solution. *BMC Bioinformatics* 8:25.
- von Szalay, P. G., D. A. Somerton, and S. Kotwicki. 2007. Correlating trawl and acoustic data in the eastern Bering Sea: A first step toward improving biomass estimates of walleye pollock (*Theragra chalcogramma*) and Pacific cod (*Gadus macrocephalus*)? *Fisheries Research* 86:77–83.
- Takao, Y., and M. Furusawa. 1995. Noise measurement by echo integrator. *Fisheries Science* 61:637–640.
- The MathWorks Inc. 2009. *MATLAB*. Natick, Massachusetts, United States.
- Therneau, T. M., E. J. Atkinson, and others. 1997. An introduction to recursive partitioning using the RPART routines.

- Todd, R. E., G. G. Gawarkiewicz, and W. B. Owens. 2013. Horizontal scales of variability over the Middle Atlantic Bight shelf break and continental rise from finescale observations.
- Torrence, C., and G. P. Compo. 1998. A practical guide to wavelet analysis. *Bulletin of the American Meteorological Society* 79:61–78.
- Torres, L. G., A. J. Read, and P. Halpin. 2008. Fine-scale habitat modeling of a top marine predator: Do prey data improve predictive capacity? *Ecological Applications* 18:1702–1717.
- Trenkel, V. M., and L. Berger. 2013. A fisheries acoustic multi-frequency indicator to inform on large scale spatial patterns of aquatic pelagic ecosystems. *Ecological Indicators* 30:72–79.
- Turner, M. G., W. H. Romme, R. H. Gardner, R. V. O'Neill, and T. K. Kratz. 1993. A revised concept of landscape equilibrium: Disturbance and stability on scaled landscapes. *Landscape Ecology* 8:213–227.
- Urban, D. L., R. V. O'Neill, and H. H. Shugart Jr. 1987. Landscape Ecology: A hierarchical perspective can help scientists understand spatial patterns. *BioScience* 37:119–127.
- Urick, R. J. 1983. *Principles of underwater sound*. 1983. Third edition. Peninsula Publishing, Los Altos California.
- Waring, G. T., C. P. Fairfield, C. M. Ruhsam, and M. Sano. 1993. Sperm whales associated with Gulf Stream features off the north-eastern USA shelf. *Fisheries Oceanography* 2:101–105.
- Waring, G. T., T. Hamazaki, D. Sheehan, G. Wood, and S. Baker. 2001. Characterization of beaked whale (*Ziphiidae*) and sperm whale (*Physeter macrocephalus*) summer habitat in the shelf-edge and deeper waters off the Northeast U.S. *Marine Mammal Science* 17:703–717.

- Waring, G. T., E. Josephson, K. Maze-Foley, and P. E. Rosel. 2013. U.S. Atlantic and Gulf of Mexico Marine Mammal Stock Assessments - 2012. Page 425. SAR, Northeast Fisheries Science Center, Woods Hole, MA.
- Waring, G. T., E. Josephson, K. Maze-Foley, and P. E. Rosel. 2014. U.S. Atlantic and Gulf of Mexico Marine Mammal Stock Assessments - 2013. Page 464. SAR, Northeast Fisheries Science Center, Woods Hole, MA.
- Warren, J. D., T. K. Stanton, M. C. Benfield, P. H. Wiebe, D. Chu, and M. Sutor. 2001. In situ measurements of acoustic target strengths of gas-bearing siphonophores. *ICES Journal of Marine Science: Journal du Conseil* 58:740–749.
- Warren, J. D., T. K. Stanton, P. H. Wiebe, and H. E. Seim. 2003. Inference of biological and physical parameters in an internal wave using multiple-frequency, acoustic-scattering data. *ICES Journal of Marine Science: Journal du Conseil* 60:1033–1046.
- Weinrich, M. T., R. D. Kenney, and P. K. Hamilton. 2000. Right whales (*Eubalaena glacialis*) on Jeffreys Ledge: A habitat of unrecognized importance? *Marine mammal science* 16:326–337.
- Whitt, A. D., K. Dudzinski, and J. R. Lalibert. 2013. North Atlantic right whale distribution and seasonal occurrence in nearshore waters off New Jersey, USA, and implications for management. *Endangered Species Research* 20:59–69.
- Wiebe, P. H., D. G. Mountain, T. K. Stanton, C. H. Greene, G. Lough, S. Kaartvedt, J. Dawson, and N. Copley. 1996. Acoustical study of the spatial distribution of plankton on Georges Bank and the relationship between volume backscattering strength and the taxonomic composition of the plankton. *Deep Sea Research Part II: Topical Studies in Oceanography* 43:1971–2001.
- Wiens, J. A. 1989. Spatial Scaling in Ecology. *Functional Ecology* 3:385–397.
- Xu, Y., R. Chant, D. Gong, R. Castelao, S. Glenn, and O. Schofield. 2011. Seasonal variability of chlorophyll a in the Mid-Atlantic Bight. *Continental Shelf Research* 31:1640–1650.

- Zamon, J. E., C. H. Greene, E. Meir, D. A. Demer, R. P. Hewitt, and S. Sexton. 1996. Acoustic characterization of the three-dimensional prey field of foraging chinstrap penguins. *Mar Ecol Prog Ser* 131:1–10.
- Zani, M. A., J. K. D. Taylor, and S. D. Kraus. 2008. Observation of a Right Whale (*Eubalaena glacialis*) Birth in the Coastal Waters of the Southeast United States. *Aquatic Mammals* 34:21–24.
- Zar, J. H. 1999. *Biostatistical analysis*. 4th ed. Prentice Hall, Upper Saddle River, N.J.
- Zhang, W. G., and G. G. Gawarkiewicz. 2015. Dynamics of the direct intrusion of Gulf Stream ring water onto the Mid-Atlantic Bight shelf. *Geophysical Research Letters* 42:2015GL065530.
- Zhang, W. G., D. J. McGillicuddy, and G. G. Gawarkiewicz. 2013. Is biological productivity enhanced at the New England shelfbreak front? *Journal of Geophysical Research: Oceans* 118:517–535.

Biography

Erin Ann LaBrecque
Born: January 28, 1976
Littleton, New Hampshire, USA

Education

2016 PhD, Marine Science and Conservation, Duke University
2006 MEM Costal Environmental Management, Duke University
2006 Geospatial Certificate, Duke University
1998 BSc Biology, Honors Program, University of Maryland Eastern Shore

Publications

LaBrecque, E., Curtice, C., Harrison, J., Van Parijs, S. M., & Halpin, P. N. (2015). 2. Biologically Important Areas for cetaceans within U.S. waters – East coast region. In S. M. Van Parijs, C. Curtice, & M. C. Ferguson (Eds.), *Biologically Important Areas for cetaceans within U.S. waters* (pp. 17-29). *Aquatic Mammals* (Special Issue), 41(1). 128 pp.

LaBrecque, E., Curtice, C., Harrison, J., Van Parijs, S. M., & Halpin, P. N. (2015). 3. Biologically Important Areas for cetaceans within U.S. waters – Gulf of Mexico region. In S. M. Van Parijs, C. Curtice, & M. C. Ferguson (Eds.), *Biologically Important Areas for cetaceans within U.S. waters* (pp. 30-38). *Aquatic Mammals* (Special Issue), 41(1). 128 pp.

Best, B., P. N. Halpin, A. J. Read, E. Fujioka, C. P. Good, **E. LaBrecque**, R.S. Schick, et al. 2012. Online Cetacean Habitat Modeling System for the US East Coast and Gulf of Mexico. *Endangered Species Research* 18 (1): 1–15.

Schick, R. S., P. N. Halpin, A. J. Read, D. L. Urban, B. D. Best, C. P. Good, J. J. Roberts, **E. A. LaBrecque**, C. Dunn, L. P. Garrison, K. D. Hyrenbach, W. A. McLellan, D. A. Pabst, D. L. Palka, and P. Stevick. 2011. Community Structure in Pelagic Marine Mammals at Large Spatial Scales. *Marine Ecology Progress Series* 434:165–181. doi: 10.3354/meps09183.

Halpin, P. N, A. J. Read, E. Fujioka, B. D. Best, B. Donnelly, L. J. Hazen, C. Kot, K. Urian, **E. LaBrecque**, A. Dimatteo, J. Cleary, C. Good, L. Crowder, and K. D. Hyrenbach. 2009. OBIS-SEAMAP: The World Data Center for Marine Mammal, Sea Bird, and Sea Turtle Distributions. *Oceanography* 22, no. 2: 96-107.

LaBrecque, E., C. Fritz, J. Tober, P. J. Behr, and I. Valiela. 1996. Abundance and Age-Specific Growth Rates in Relation to Population Densities of *Fundulus heteroclitus* in Waquoit Bay Estuaries Subject to Different Nitrogen Loads. *Biological Bulletin* (191):319-320.

Fritz, C., **E. LaBrecque**, J. Tober, P. J. Behr, and I. Valiela. 1996. Shrimp in Waquoit Bay: Effects of Nitrogen Loading on Size and Abundance. *Biological Bulletin* (191):326-327.

Tober, J., C. Fritz, **E. LaBrecque**, P. J. Behr, and I. Valiela. 1996. Abundance, Biomass, and Species Richness of Fish Communities in Relation to Nitrogen-Loading Rates of Waquoit Bay Estuaries. *Biological Bulletin* (191):321-322.

Awards and Scholarships

Nancy Foster Scholarship
Duke University Marine Lab Writing Fellowship
WHOI-Duke University Fellowship in Marine Conservation
Best Oral Presentation – DUML Graduate Student Symposium
Duke University, Nicholas School Academic Scholarship

Professional Affiliations

American Association for the Advancement of Science
American Geophysical Union
Acoustical Society of America
Association for Women in Science
Society for Conservation Biology
Society for Marine Mammalogy